
University of Crete
FACULTY OF MEDICINE


http://inflacare.imbb.forth.gr

PhD Thesis

Study of the role and regulation of Tpl2 /COT (MAP3K8) in lung carcinogenesis: a proto-oncogene with a tumor suppressive function.

Gkirtzimanaki P. Aikaterini

Laboratory of Molecular and Cell Biology
Post Graduate Program of 'Molecular Biology and Biomedicine'
University of Crete School of Medicine & IMBB FORTH

Heraklion, 2012

Διδακτορική διατριβή

Μελέτη του ρόλου και της ρύθμισης της Tpl2/ COT (MAP3K8) στην καρκινογένεση του πνεύμονα: ένα πρωτο-ογκογονίδιο με ογκοκατασταλτική δράση.

Γκιρτζιμανάκη Π. Αικατερίνη

Εργαστήριο Μοριακής και Κυτταρικής Βιολογίας
Μεταπτυχιακό Πρόγραμμα Μοριακής Βιολογίας και Βιοϊατρικής
Ιατρική Σχολή Πανεπιστημίου Κρήτης & IMBB ITE

Ηράκλειο, 2012

PhD Thesis

Study of the role and regulation of Tpl2 /COT (MAP3K8) in lung carcinogenesis: a proto-oncogene with a tumor suppressive function.

Supervising Professor: **Eliopoulos Aristides, PhD**

Members of advisory committee:
Eliopoulos A., Associate Professor, Medical School - UoC and IMBB member (Researcher A').
Papadaki E., Full Professor, Medical School - UoC
Mamalaki K., Researcher A', IMBB FORTH

Members of examination committee:
Chalepakis G., Full Professor, Biology Dpt. – UoC
Mavroudis D., Full Professor, Medical School – UoC
Tsatsanis C., Associate Professor, Medical School - UoC
Sourvinos G., Associate Professor, Medical School - UoC

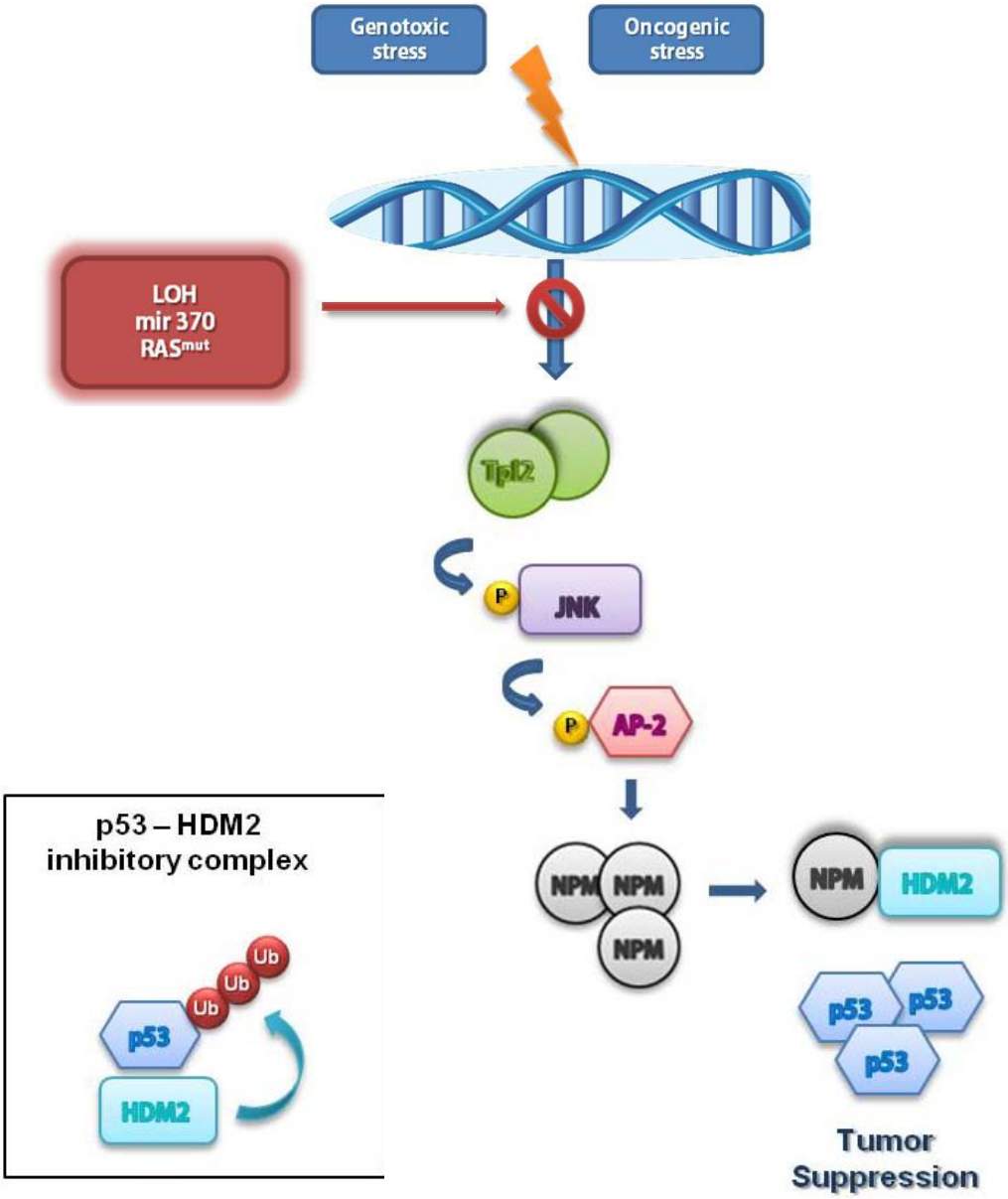
Genotoxic stress
Oncogenic stress
LOH
mir 370
RASmut
Tpl2
P
JNK
P
AP-2
NPM
NPM
NPM
NPM
HDM2
p53
p53
p53
Tumor Suppression
p53 – HDM2 inhibitory complex
Ub
Ub
Ub
p53
HDM2

Dedicated to my family….

Acknowledgments

This dissertation would not have been possible without the guidance and the help of several individuals who contributed in the preparation and completion of this study.
First and foremost, my utmost gratitude to Dr. Eliopoulos Aris, my supervisor, whose guidance and encouragement untill the completion of this research work I will never forget. I am indebted to you for giving me the opportunity to work in your laboratory and have your support. Thank you for the understanding and for the helpful suggestions.
I am also grateful to Dr. Liloglou Triantafyllos whose help was necessary for the successful completion of this project. He offered me the opportunity to expand my knowledge on Genetics and provided me with everything I needed during my visit to Liverpool and the Lung Cancer Institute of UoL.
I would like to express the deepest appreciation to my Advisory Committee members Prof. Papadaki Eleni and Dr. Mamalaki Clio for their expert, sincere and valuable guidance and encouragement extended to me.
I would also like to thank my colleagues Kalliopi, Marina, Sophia, Dimitris, Maria, Aris and Dimitra. They make me realize the value of working together as a team, especially in this working environment, which challenges us every minute. Not to forget my friends Nikoletta, Panos and Michalis for their support and friendship. I have great moments to remember!
A very special thanks to Marianna and Nikos M., as well as Nikos P., Anna and Elena who were always next to me, with their love and support guiding me in all aspects of life and for tolerating me.
I would further like to acknowledge several individuals for their assistance and support throughout my Thesis: Dr. P. Tsichlis, Dr J.K. Field, Dr. Gorgoulis, Dr. J.Penninger, Dr. M.Oren and Dr. A. Malliri as well as the animal facility group members of IMBB.
Financial support to undertake my Ph.D. degree, of which this thesis is an integral part, was provided by the European Commission research program INFLA-CARE and by M.Manassaki's Foundation.
These acknowledgments would not be complete without thanking my family and in particular my parents Paschalis and Maria and my sister Xanthi for their unconditional love and support and for teaching me the most important;to fight for my dreams.

Table of Contents

1.Abstract

Cancer can be perceived as a disease of communication between and within cells. The aberrations are pleiotropic, but mitogen-activated protein kinase (MAPK) pathways feature prominently. Tpl2/COT is a serine-threonine MAPK kinase kinase (MAP3K8) at the crossroad of various signal transduction pathways that control fundamental cellular processes such as growth, proliferation, differentiation, migration and apoptosis. Despite early studies identifying Tpl2 as a proto-oncogene activated by C-terminal truncation in mouse and rat, a detailed evaluation of its expression and function in human malignancy is missing and the physiological role of Tpl2/COT in carcinogenesis remains enigmatic.

One of the three major human tissues where Tpl2 is expressed at highest levels is the lung. Lung cancer is the leading cause of cancer related death worldwide, reflecting the need for a better understanding of the mechanisms that underlie the development of pulmonary carcinomas. The Ph.D. thesis presented here focuses on the characterization of the role and of the mechanisms regulating the expression of Tpl2/COT[1] in lung tumor cells during the onset of lung cancer development and through its progression.

In this regard, we were able to reveal an unprecedented role for Tpl2/COT as suppressor of lung carcinogenesis. This conclusion was based on a number of novel findings obtained through the extensive analysis of human tissue and of *ex vivo* and *in vivo* experimental models. We showed that COT expression is significantly reduced in human lung cancer compared to normal lung tissue providing the first demonstration that COT can be differentially expressed in a human malignancy. Importantly, the downregulation of COT is found to be of clinical relevance as it correlates with a more aggressive tumor phenotype and with poor prognosis in patients with lung cancer.

Our data disclose 3 mechanisms responsible for COT downregulation in primary human lung tumors: (i) allelic imbalance at the COT locus; (ii) global DNA hypomethylation-associated upregulation of miR-370 which targets COT tran-

[1] The term "Tpl2" is used for the mouse gene and protein product whereas the term "COT" refers to the human product.

scripts and (iii) activated Ras signaling affecting both COT transcription and protein stability. The operation of multiple genetic and epigenetic aberrations leading to loss of wild-type COT in primary lung tumors underlines a previously unappreciated broader role for this pathway in lung carcinogenesis. This is corroborated by our experimental data showing that ablation of the Tpl2 gene in mice dramatically accelerates the onset and multiplicity of urethane-induced lung tumorigenesis.

Additionally, we provide mechanistic evidence to suggest that Tpl2/COT antagonizes oncogene-induced cell transformation and survival through a pathway involving the tumor suppressor p53 downstream of JNK. In particular, our studies define Tpl2/COT as a novel physiological antagonist of oncogenic Ras, thus also expanding our understanding of signaling and function of this major human oncogene. An important functional interaction between Tpl2/COT, JNK and p53 which controls apoptosis is revealed, providing a telling example of how tumor cells usurp alternative pathways that lower intrinsic barriers to malignant transformation.

1. Περίληψη

Ο καρκίνος μπορεί να θεωρηθεί ως ασθένεια στην επικοινωνία μεταξύ και στο εσωτερικό των κυττάρων. Οι δυσλειτουργίες που προκύπτουν είναι πλειοτροπικές, αλλά τα μονοπάτια των κινασών που ενεργοποιούνται από μιττογόνα (Mitogen Activated Protein Kinases) φαίνεται να παίζουν εξέχοντα ρόλο στη διαδικασία της καρκινογένεσης. Η Tpl2 είναι μία MAP3 κινάση σερίνης/θρεονίνης στο σταυροδρόμι πολλών και διαφορετικών μονοπατιών σηματοδότησης που ελέγχουν πρωτεύουσας σημασίας κυτταρικές διεργασίες, όπως η κυτταρική αύξηση, πολλαπλασιασμός διαφοροποίηση, μετανάστευση και απόπτωση. Παρά τις αρχικές που οδήγησαν στην ταυτοποίηση της Tpl2 ως πρωτο-ογκογονίδιο που ενεργοποιείται μετά από καρβοξυτελική αποκοπή σε ποντικούς και αρουραίους, μία λεπτομερής εκτίμηση της έκφρασης και της λειτουργίας της Tpl2/COT στην ανθρώπινη κακοήθεια λείπει ακόμη από τη βιβλιογραφεία. Ο φυσιολογικός ρόλος της Tpl2 στην καρκινογένεση παραμένει αινιγματικός.

Ένα από τα 3 κυριότερα όργανα όπου εμφανίζονται από τα υψηλότερα επίπεδα της COT είναι οι πνεύμονες. Ο καρκίνος των πνευμόνων είναι η σημαντικότερη αιτία θανάτου καρκινοπαθών παγκοσμίως, αντανακλώντας την άμεση ανάγκη για καλύτερη κατανόηση των μηχανισμών που διέπουν την ανάπτυξη καρκινωμάτων του αναπνευστικού. Η διδακτορική διατριβή που παρουσιάζεται εδώ εστιάζει στον χαρακτηρισμό του ρόλου και των μηχανισμών που ελέγχουν την έκφραση της Tpl2/COT στα καρκινικά κύτταρα του πνεύμονα, κατά την έναρξη της ανάπτυξης του καρκίνου του πνεύμονα καθώς και κατά τη διάρκεια εξέλιξής του.

Ερευνώντας υπό αυτό το πρίσμα, καταφέραμε να αποκαλύψουμε έναν απροσδόκητο ρόλο για την Tpl2/COT ως καταστολέα της καρκινογένεσης του πνεύμονα . Αυτό το συμπέρασμα βασίστηκε σε έναν αριθμό νέων ευρημάτων στα οποία καταλήξαμε μετά από ενδελεχή ανάλυση ανθρώπινου ιστού και χρήση πειραματόζωων και *ex vivo* μοντέλων. Δείξαμε πως η έκφραση της COT είναι σημαντικά μειωμένη στον καρκίνο του πνεύμονα στον άνθρωπο συγκριτικά με τον φυσιολογικό ιστό, παρέχοντας έτσι την πρώτη απόδειξη πως η COT μπορεί να παρουσιάσει διαφορική έκφραση σε μία ανθρώπινη κακοήθεια. Ανάλογα σημαντικό ήταν

το εύρημα πως η μείωση της COT έχει κλινική προέκταση καθώς συσχετίζεται με πιο επιθετικό φαινότυπο του όγκου και κακή πρόγνωση στους ασθενείς με καρκίνο του πνεύμονα.

Τα δεδομένα μας περικλείουν 3 μηχανισμούς υπεύθυνους για τη μείωση της έκφρασης της COT σε πρωτεύοντες όγκους του πνεύμονα στον άνθρωπο: (i) αλληλική αστάθεια στον γενετικό τόπο της COT (ii) υπερέκφραση του mir370 που στοχεύει τα μετάγραφα της COT μετά από υπομεθυλίωση του γενετικού του τόπου, στα πλαίσια της γενικής υπομεθυλίωσης που συμβαίνει κατά την καρκινογένεση (iii) ενεργοποίηση σηματοδότησης Ras που επηρεάζει και την μεταγραφή και την πρωτεϊνική σταθερότητα της Tpl2/COT.

Η ύπαρξη πολλαπλών γενετικών και επιγενετικών ανωμαλιών που οδηγούν σε απώλεια ή σημαντική μείωση της αγρίου τύπου Tpl2 / COT σε πρωτεύοντες όγκους στον πνεύμονα υπογραμμίζει έναν έως τώρα μη εκτιμημένο, ευρείας σημαντικότητας ρόλο αυτού του μονοπατιού στην καρκινογένεση του πνεύμονα. Αυτό ενισχύεται και επιβεβαιώνεται και από τα πειραματικά μας δεδομένα που δείχνουν πως η έλλειψη του γονιδίου στα πειραματόζωα επιταχύνει δραματικά την έναρξη και την πολλαπλότητα της ογκογένεσης στον πνεύμονα μετά από χορήγηση ουρεθάνης.

Επιπρόσθετα, παρουσιάζουμε μηχανιστικές ενδείξεις που υποδεικνύουν πως η Tpl2/COT ανταγωνίζεται τον επαγόμενο από ογκογονίδια κυτταρικό μετασχηματισμό και επιβίωση, μέσω ενός μονοπατιού που περιλαμβάνει την ογκοκατασταλτική p53 καθοδικά της JNK. Πιο συγκεκριμένα, οι μελέτες ορίζουν την Tpl2/COT ως ένα νέο φυσικό ανταγωνιστή της ογκογόνου Ras, διευρύνοντας ακόμη περισσότερο την κατανόηση της λειτουργίας και της σηματοδότησης ενός τόσο σημαντικού ανθρώπινου ογκογονιδίου. Μία ενδιαφέρουσα λειτουργική αλληλεπίδραση μεταξύ των Tpl2/COT, JNK και p53 που ελέγχει την απόπτωση αποκαλύπτεται, παρέχοντας ταυτόχρονα ένα ενδεικτικό παράδειγμα για το πώς τα καρκινικά κύτταρα εκμεταλλεύονται και καθοδηγούν εναλλακτικά μονοπάτια για να μειώσουν τους έμφυτους φραγμούς στον καρκινικό μετασχηματισμό.

3.Introduction

The origins and general classification of cancer

Lung cancer

- **Classification of lung cancer**
- **Lung cancer treatment**
- **The Ras paradigm**

Cancer Biology

- **The development of a tumor**
- **Genomic Instability**
- **Genome guarding-the p53 case**
- **Epigenetic alterations in cancer**
- **Micro-RNAs and their role in cancer**
- **From genes to pathways**

The MAP Kinase Signal Transduction Pathway

- **MAPKs, the effectors of the pathway**
  - **The ERK family**
  - **The JNK/SAPK family**
  - **The p38 family**
- **MAP3Ks, the first tier in the kinase cascade**

Tpl2/Cot (MAP3K8)

- **History of cloning**
- **Gene and protein product**
- **Activation**
- **Function**
- **Role in cancer**

3.1 The origins and general classification of cancer

The term *carcinos*, the greek word for crayfish, was first introduced by Hippocrates (460 - 370BC) because of "the veins stretched on all sides as the crab has its feet" (1). The latin doctor Celsus (ca. 25BC – 50AD) later translated the greek word “carcinos”, to todays latin word “cancer” (1). Today, the term cancer is commonly used to describe a disease were a group of cells is abnormally proliferating - forming a tumor - and, over time, spread to distant parts of the body and form metastases.

In general, tumors are classified into benign and malignant categories. Benign tumors are separated from surrounding tissue by a basal membrane, can only grow locally restricted and lack the ability to spread into distant parts of the body. Therefore, benign tumors can be retracted by surgery and have a favorable clinical outcome. In stark contrast, due to lack of a basal lamina, malignant tumors grow more aggressively, can spread to distant parts of the body and have a more severe clinical outcome.

Malignant tumors are classified based on the specialized cell type they originate from and the most predominant and clinically most relevant group of malignant tumors are carcinomas. They account for 80% of cancer related deaths in the western world (2) due to the fact that carcinomas can arise from epithelial tissue originating from all three germ layers (ectoderm e.g., lung, mesoderm e.g., ovarian and endoderm e.g., liver).

The remaining cancer related deaths are caused by tumors arising from:

- connective tissues originating from the mesoderm (sarcomas), e.g. osteoblasts;
- blood forming tissues (hematopoietic system), e.g. leukemias and lymphomas; or
- components of the central and peripheral nervous system (neuroectodermal tumors), e.g. gliomas and neuroblastomas.

Taken together, the disease “cancer” means the abnormal proliferation of cells that subsequently form a tumor. Tumors are classified based on the presence of a basal lamina and the organ and tissue where the primary tumor arises from (2).

3.2 Lung cancer

Classification of lung cancer

Lung cancer is a disease of tumor formation in the lung, eventually followed by metastasis into the body. It is the leading cause of cancer-related death worldwide. More people die from lung cancer than from breast, colon and prostate cancer combined (Cancer J. Clin 2011). In Greece, 7000 people die every year from lung cancer. Histologicaly, lung cancer is separated in two major subtypes; non-small cell (NSCLC) and small cell (SCLC) lung cancer. This classification was originally based on the size of cells seen by microscopic examination and mitotic cell division rate.

SCLC typically arises from airway bronchioles and rapidly increases in size due to an average tumor doubling time of 81 days (10, 11). SCLC tumors initially respond dramatically to chemotherapy and radiation treatment but almost all patients suffer from a recurrence; a re-grown tumor being mostly resistant to the initial treatment (11). Five-year overall survival rate for extensive SCLCs is below 5 % .

NSCLC is further divided into several subtypes, depending on the tissue of origin, with adenocarcinomas and squamous-cell carcinomas being the most common subtypes. Adenocarcinomas arise from epithelial cells, forming glandular tissue in the periphery of the alveolar system. They account for approximately 40% (12) of all lung cancer cases, whereas squamous-cell lung carcinomas arise from epithelial cells that form a layer covering the main bronchus. They account for 30 to 35% of all lung cancer cases (12) and are almost invariably associated with smoking (13). Large-cell carcinoma is another histological subtype. In rare cases, these tumors present a neuroendocrine differentiation and are thus called large-cell neuroendocrine lung cancer. Other tumors occurring in the lung include carcinoids, sarcomas and metastases from tumors originating from other sites (e.g., colonic adeno-carcinomas).

Stage I The cancer is located only in the lungs and has not spread to any lymph nodes.

Stage II The cancer is in the lung and nearby lymph nodes.

Stage III Cancer is found in the lung and in the lymph nodes in the middle of the chest, or there is a tumor in the lung plus fluid in the chest cavity. Stage III has two subtypes: If the cancer has spread only to lymph nodes on the same side of the

chest where the cancer started, it is called stage IIIA. If the cancer has spread to the lymph nodes on the opposite side of the chest or caused fluid to form in the chest, it is called stage IIIB.

Stage IV This is the most advanced stage of lung cancer. This is when the cancer has spread to another part of the body, such as the liver or other organs.

Lung cancer treatment

The identification of the exact tumor type from each patient is mandatory to choose the optimal treatment strategy. Patients suffering from a SCLC tumor are initially treated with chemotherapy and radiation of the affected area (12). As mentioned above, these tumors inevitably recur after an initial response and lead to rapid death of the patient. Patients with non-small cell lung tumors (stage I to IIIa) undergo surgery, frequently in combination with chemotherapy (14) leading to a stage dependent median overall survival of up to 80% for stage I and ~23% for stage IIIa patients (Table1). Most patients present with advanced stage lung cancer (IIIb/IV) and cannot undergo complete resection with a curative intention. For these patients palliative chemotherapy is the only therapeutic option and the five-year survival rate is very low (<5%)(12).

Table 1. Survival rate strongly correlates with stage at diagnosis (Schmoll 4th Edition,2005)

Stage	5 year survival rate with treatment	
	SCLC	Non SCLC
Limited disease	10-15%	
Extensive disease	5%	
Stage Ia		75-80%
Stage Ib+IIa		55-60%
Stage IIb		35-45%
Stage IIIa		~25%
Stage IIIb		5%
Stage IV		<1%

The Ras paradigm

Lung cancer is a heterogeneous disease both at clinical and molecular level, posing conceptual and practical bottlenecks in defining key pathways affecting its initiation and progression. Molecules with central role in lung carcinogenesis are likely to be targeted by multiple deregulated pathways and may have prognostic, predictive and/or therapeutic value. Recent advances in the understanding of the molecular biology of lung adenocarcinomas have led to the identification of genomic alterations with therapeutic implications. A representative example of such an alteration, especially significant in lung cancer, implicates the gene K-ras (21). Activating mutations of the Ras gene are found in one-quarter to one-half of human lung adenocarcinomas. Ras is a membrane-associated GTPase signaling protein that regulates proliferation, differentiation, and cell survival (22). Missense mutations at codons 12, 13, and 61 result in decreased GTPase activity, which leads to constitutive signaling (Figure I1).

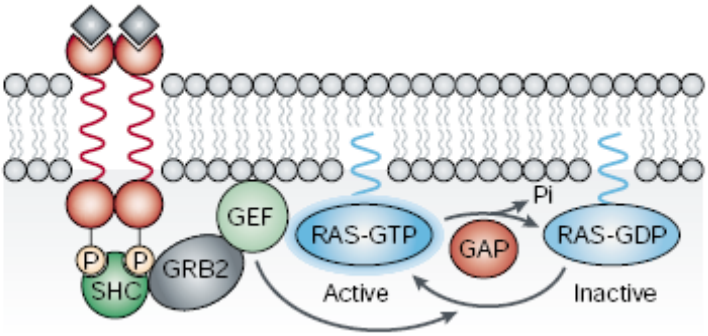

Figure I1: Signaling upstream of RAS. The activation state of RAS is controlled by the cycle of hydrolysis of bound GTP, which is catalyzed by GTPase activating proteins (GAPs), and the replacement of bound GDP with fresh GTP, which is catalyzed by guanine nucleotide exchange factors (GEFs). The best-studied activation mechanism involves the assembly of complexes of activated, autophosphorylated growth-factor receptor tyrosine kinases with the GEF Sos through the adaptor protein Grb2, and possibly Shc, resulting in the recruitment of Sos to the plasma membrane, where Ras is located. Several other GEFs exist that have distinct regulatory mechanisms. In addition, a wide range of GAPs have now been identified for Ras, some of which are also subject to regulation. Ras is also activated through GEFs in response to activation of a wide range of G-protein-coupled receptors.

In tumors harboring Ras mutations, the activated Ras protein contributes significantly to several aspects of the malignant phenotype, including the deregulation of tumor-cell growth, programmed cell death and invasiveness, and the ability to induce new blood-vessel formation (23). Kinase inhibitors that block either Raf or mitogen-activated protein (MAP) kinase kinase MEK in the Raf/MAP kinase pathway downstream of Ras have been developed and show promise in early clinical trials. However, their potential might be even greater, as many tumors that lack Ras mutations have found other ways to activate the same pathways. Furthermore, clinical responses to single-agent targeted anticancer therapeutics are almost invariably followed by relapse due to de novo or acquired drug resistance (23, 24, 25, 26). Identification of resistance mechanisms in a manner that elucidates alternative 'druggable' targets may inform effective long-term treatment strategies for lung cancer.

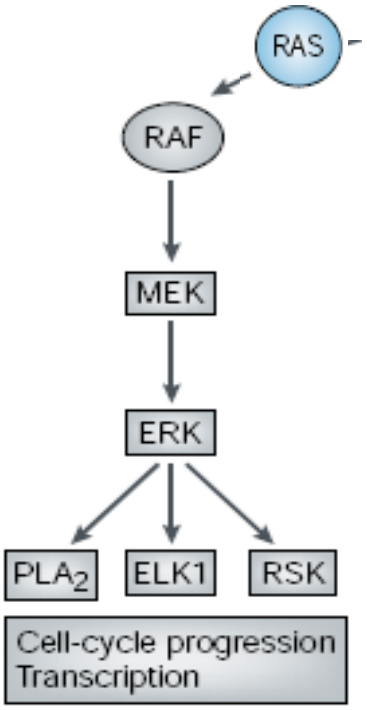

Figure I2: Signaling downstream of Ras. Once in its active, GTP-bound state, Ras will interact with several families of effector proteins, resulting in stimulation of their catalytic activity. Raf protein kinases initiate the mitogen-activated protein (MAP) kinase cascade, which leads to Erk activation. This kinase has numerous substrates both in the cytoplasm and in the nucleus, including Ets family transcription factors such as Elk1 which forms part of the serum response factor that regulates the expression of Fos; in addition, Erk phosphorylates c-Jun. This leads to activation of the AP1 transcription factor, which is made up of Fos–Jun heterodimers. As a result of stimulating these transcriptional regulators, key cell-cycle regulatory proteins, such as D-type cyclins, are expressed, which enables the cell to progress through the G1 phase of the cell cycle. So, Ras activation can promote cell-cycle progression, at least in conjunction with other signals.

3.3 Cancer Biology

The development of a tumor

From a cell-biology point of view, the process of tumor development must include several key steps in order to facilitate the malignant phenotype. A commonly accepted idea for a “skill set”- of distinctive and complementary capabilities that enable tumor growth and metastatic dissemination- that a tumor cell has to acquire, was proposed by Douglas Hanahan and Bob Weinberg in the year 2000 and updated in 2011, namely sustaining proliferative signaling, evading growth suppressors, resisting cell death, enabling replicative immortality, inducing angiogenesis and activating invasion and metastasis.

These six hallmarks of cancer are defined as acquired functional capabilities that allow cancer cells to survive, proliferate, and disseminate; these functions are acquired in different tumor types via distinct mechanisms and at various times during the course of multistep tumorigenesis. Their acquisition is made possible by two enabling characteristics. Most prominent is the development of genomic instability in cancer cells, which generates random mutations including chromosomal rearrangements; among these are the rare genetic changes that can orchestrate hallmark capabilities. A second enabling characteristic involves the inflammatory state of premalignant and frankly malignant lesions that is driven by cells of the immune system, some of which serve to promote tumor progression through various means.

Genomic Instability

During cellular transformation, the genome is affected by a multitude of alterations ultimately leading to a fully transformed malignant tumor. Genomic alterations accumulate over the years and may also get accelerated by external mutagenic agents (e.g., tobacco smoke (3,4)). Genetic instability refers to a set of events capable of causing unscheduled alterations, either of a temporary or permanent nature, within the genome. This term encompasses diverse genetic changes, which can be classified in a variety of ways. For simplicity I will categorize them into two major groups, instability occurring at the chromosomal level and at the nucleotide level.

Instability at the nucleotide level occurs due to faulty DNA repair pathways such as base excision repair and nucleotide excision repair and includes instability of microsatellite repeat sequences (MSI) caused by defects in the mismatch repair pathway.

The second form or chromosomal instability (CIN), defines the existence of accelerated rate of chromosomal alterations, which result in gains or losses of whole chromosomes as well as inversions, deletions, duplications and translocations of large chromosomal segments. Aneuploidy, which refers to an abnormal karyotype is a hallmark of many cancer cells and is thought to develop as a result of CIN. The observation that cancer cells harbour an abnormal number of chromosomes was made almost a century ago (Boveri, 1914; von Hansemann, 1890) and since then we have come a long way in understanding the causes behind this type of instability. To date several pathways and processes have been implicated in CIN including :

a) pathways involved in telomere and centromere stability,

b) cell cycle checkpoint pathways and kinases,

c) pathways regulating diverse proteins via post-translational modifications,

d) sister chromatid cohesion and chromosome segregation, and

e) centrosome duplication.

When certain combinations of genomic alterations accumulate in the same cell, transformation takes place and tumorigenic cell behavior occurs (2). Certain mutant genotypes confer selective advantage on subclones of cells, enabling their outgrowth and eventual dominance in a local tissue environment. Accordingly, multistep tumor

progression can be portrayed as a succession of clonal expansions, each of which is triggered by the chance acquisition of an enabling mutant genotype. The extraordinary ability of genome maintenance systems to detect and resolve defects in the DNA ensures that rates of spontaneous mutation are usually very low during each cell generation. In the course of acquiring the roster of mutant genes needed to orchestrate tumorigenesis, cancer cells often increase the rates of mutation (28,29). This mutability is achieved through increased sensitivity to mutagenic agents, through a breakdown in one or several components of the genomic maintenance machinery, or both. In addition, the accumulation of mutations can be accelerated by compromising the surveillance systems that normally monitor genomic integrity and force genetically damaged cells into either senescence or apoptosis (30, 31, 32). The role of the p53 protein is central here, leading to its being called the ‘‘guardian of the genome’’ (33).

Genome guarding-the p53 case

The process of tumorigenesis not only involves mutations that activate oncogenes; it also requires several mutations that disrupt the activities of proteins that function to suppress tumorigenesis (34). Among these is the paradigm tumor-suppressor protein p53, maybe the more frequently mutated gene in human cancers. The p53 complex is a key regulator of stress response in cells. It acts as a critical monitor preventing survival of cells with irreparable genetic damage. Under normal conditions, p53 is locked in an inactive state in the cytoplasm, tightly controlled by its negative regulator Hdm2 and its levels are allowed to rise only during severe cellular stress. Stabilization and activation of p53 translates into a cellular alert signal that can either assist in recovery from the damage or provoke cell death by apoptosis. Loss of p53 results in tolerance to aberrant cell signaling and DNA damage thereby fostering tumor development.

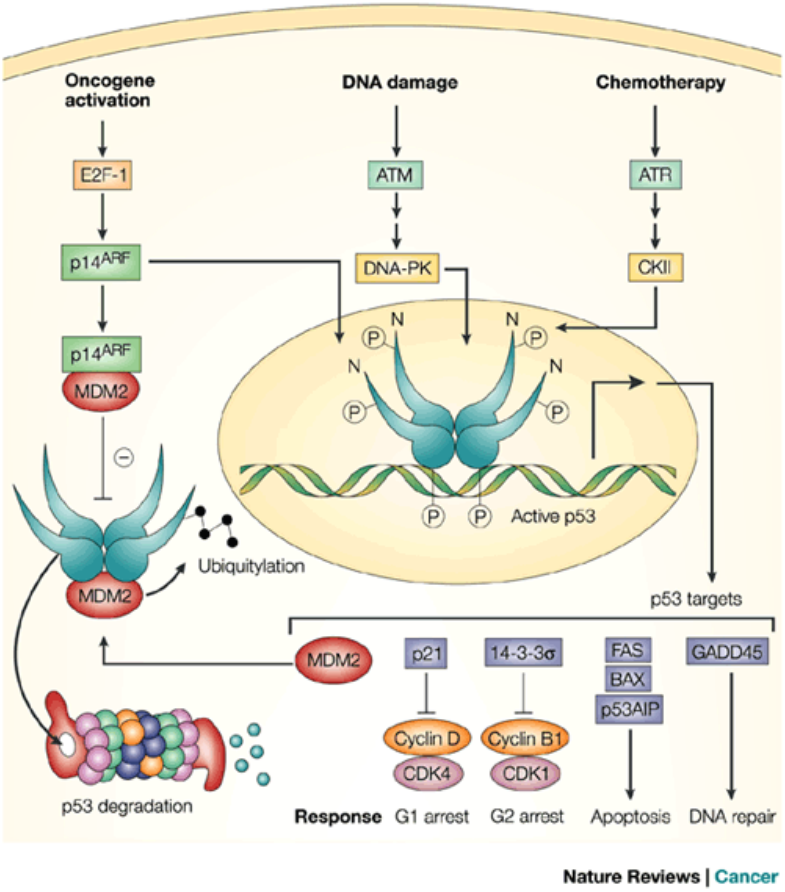

Figure I3: A negative regulatory feedback loop controls cellular levels of p53. In normal cells, p53-dependent transcription of MDM2 (HDM2) promotes p53 degradation. Cellular stress, such as oncogene activation, induces p14ARF, which sequesters MDM2. In addition, DNA damage and chemotherapeutic agents activate protein kinases, such as ATM and ATR, which, through DNA-dependent protein kinase (DNA-PK) and casein kinase II (CKII), respectively, phosphorylate the amino terminus of p53 to prevent MDM2 binding, and the carboxyl terminus of p53 to increase sequence-specific DNA binding. These events increase p53 levels and activate the transcription of p53 target genes. p21 and 14-3-3 promote growth arrest at the G1 and G2 DNA-damage checkpoints by inhibiting cyclin-dependent protein kinase (CDK) activity; FAS, BAX and p53AIP promote apoptosis if repair is not possible; and GADD45 promotes DNA repair.

Epigenetic alterations in cancer

Some mitotically and meiotically heritable phenotypes of clonal expansions leading to tumor development may well be triggered by non-mutational changes, affecting the regulation of gene expression and not the primary DNA sequence itself (35, 36, 37). Epigenetic alterations may involve covalent modifications of amino acid residues in the histones around which the DNA is wrapped, and changes in the methylation status of cytosine bases (C) in the context of CpG dinucleotides within the DNA itself.

In humans, DNA methylation is typically found as a covalent modification at the fifth carbon position of cytosine residues within CpG dinucleotides (38, 39, 40, 41, 42) What is interesting is the existence of CpG-rich regions—"CpG islands"—that are associated with the 5′-end regulatory regions of almost all housekeeping genes as well as with half of tissue-specific genes. When these promoter CpG islands are methylated, the associated genes tend to be transcriptionally inactive. Faithful propagation of the methylation state of a CpG dinucleotide occurs directly after DNA replication by an enzymatic methyl transfer reaction at cytosine residues in the unmethylated nascent DNA strand across from methylated CpG dinucleotides. This activity, which uses hemi-methylated CpG dinucleotides as a substrate, is referred to as maintenance methylation activity. Loss of methylation can occur by the failure of maintenance methylation, but acquisition of DNA methylation at a previously nonmethylated CpG cannot be accomplished by maintenance methylation activity. This requires a methylation activity that can recognize unmethylated CpG dinucleotides and is referred to as *de novo* methylation activity. Aberrant DNA methylation patterns have been associated with a large number of human malignancies and found in two distinct forms: hypermethylation and hypomethylation compared to normal tissue. Hypermethylation typically occurs at CpG islands in the promoter region and is associated with gene inactivation. Global hypomethylation has also been implicated in the development and progression of cancer through different mechanisms mainly leading to silencing abolishment in previously eterochromatinic genetic loci.

The other critical epigenetic marks are chemical modifications of the N-terminal tails of histone proteins. Histones, once considered mere DNA-packaging proteins, regu-

late the underlying DNA sequences through complex post-translational modifications such as lysine acetylation, arginine and lysine methylation, or serine phosphorylation. It has been proposed that distinct combinations of modifications presented on histone tails form a “histone code” that regulates gene activity.

Micro-RNAs and their role in cancer

MicroRNAs (miRNAs) are small, often phylogenetically conserved, non–protein-coding RNAs that mediate posttranscriptional gene repression by inhibiting protein translation or by destabilizing target transcripts. miRNAs recognize target sites, most commonly found in the 3′-untranslated regions (UTRs) of cognate mRNAs, through imperfect base-pairing, with 1 or more mismatches in sequence complementarity. miRNAs are believed to fine-regulate a diverse array of biological processes, and a convergence of genetic, biochemical, and structural studies has led to rapid growth in understanding of their synthesis and molecular mechanisms (150). miRNAs are initially expressed as part of one arm of an imperfect ∼80-nt RNA hairpin that, in turn, forms part of a longer transcript termed a primary miRNA (pri-miRNA) (151). The first step in miRNA biogenesis is the excision of the upper part of this RNA hairpin by the nuclear RNase III enzyme Drosha to produce an ∼65-nt intermediate, termed a pre-miRNA (152, 153). Pre-miRNAs, which form short RNA hairpins bearing a 2-nt 3overhang, are then bound by the nuclear export factor Exportin 5, which transports them to the cytoplasm (154, 155, 156). Here, a second RNase III enzyme termed Dicer removes the terminal loop of the pre-miRNA to generate an ∼20-bp RNA duplex with 2-nt 3′ overhangs (151, 157, 158). The mature miRNA, which forms one strand of this duplex, is then incorporated into a large protein complex, termed the RNA induced silencing complex (RISC), where it functions to guide RISC to complementary mRNA targets (159, 160, 161). Through the seed region (nt 2 to 8), the miR can then bind to the 3’UTR of target mRNA sequences, preventing protein translation, leading to mRNA degradation. More recently, miRs have also been described to target 5’UTR, and even coding regions of transcripts (59) (Figure I4).

The current miRDatabase (http://www.mirbase.org) has catalogued more than 1,300 human sequences. Given their ability to target mRNA with imperfect complementari-

ty, and predicted to regulate the expression of approximately one-third of all human transcripts (60), miRs are considered to be among the largest class of gene regulators (61, 62). Multiple mechanisms can mediate miR dysregulations in human cancers, including chromosomal gains or losses (63), mutations of miR located loci (64), or epigenetic aberrations (64). Any misstep in miR biogenesis (Figure I4) can also affect miR expression (65, 66), exemplified by the down-regulation of Drosha and Dicer being associated with worse survival in ovarian, lung, and breast cancers (67). MiRs can be either over- or under-expressed, functioning as tumor suppressors or oncogenes, depending on their downstream target genes (68).

More recently, the role of mRNA or miRs as cancer biomarkers have also been investigated and developed. The prototype mRNA signature is Oncotype DX, the 21-gene set utilized to predict recurrence risks for patients with breast cancer (69). MiR expression profilings could distinguish different cancer types (68), classify sub-types of prostate or breast cancers (70), identify the tissue origin of tumors (71), and facilitate the diagnosis of colon (72), or lung cancers (73). MiRs can also predict outcome, such as let-7a (73) and miR-155 (74) for lung cancer, and select patients for targeted therapy (for example, breast cancer (75)). Finally, predictive miR signatures have been reported for several malignancies, such as lung (76-79), hepatocellular (80), esophageal (81), gastric (82), prostate (83) cervical (84) and colon cancers (85).

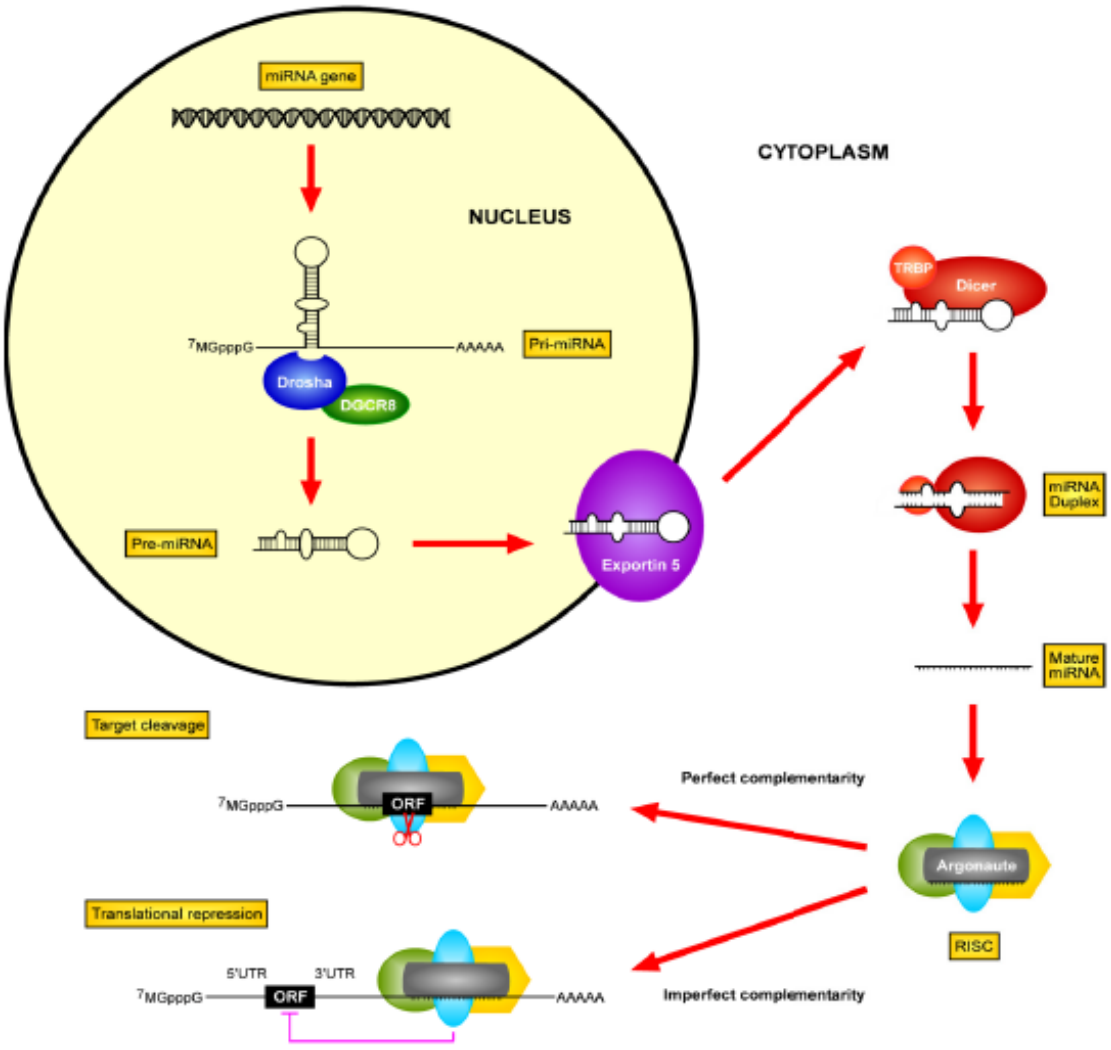
miRNA gene
NUCLEUS
CYTOPLASM
7MGpppG
AAAAA
Pri-miRNA
Drosha
DGCR8
Pre-miRNA
Exportin 5
TRBP
Dicer
miRNA Duplex
Mature miRNA
Target cleavage
ORF
Perfect complementarity
Argonaute
RISC
Translational repression
5'UTR
3'UTR
Imperfect complementarity

Figure I4: Micro-RNA biogenesis. MiR's are synthesized initially as large RNA precursors (pri-miRs), processed in the nucleus by RNAse III Drosha, and DGCR8 into approximately 70 nt pre-miR, which are transported to the cytoplasm by exportin-5, with subsequent cleavage by another RNAse III enzyme Dicer, with its co-factor TRBP, releasing the approximately 22-nt mature dsmiR. MiR's can negatively regulate their targets in one of two major ways, depending on the degree of complementarity to its target. First, and probably most commonly, one strand of this duplex is incorporated into the RNA-induced silencing complex (RISC), then binds with imperfect complementarity to the 3'-UTR (untranslated region) of mRNA targets, preventing protein translation. Alternatively, miRs can bind with perfect complementarity to the ORF (open reading frame) of target mRNA's with subsequent degradation. Recent evidence also indicates miRs can also bind to either promoters, or coding regions of mRNAs as additional mechanisms of regulation.

From genes to pathways

Since cancer is a disease of the genome, the translational interpretation of the alterations in genomic constitution which leads to a transformed cell physiology is absolutely significant in order to develop new treatment strategies for cancer patients. Advances in high-throughput sequencing technologies enabled a comprehensive view on the genomic changes in cancer. The sheer amount of genomic alterations observed in tumor cells is staggering (*5*-*7*) with more than 150 subtle genomic changes observed in one single tumor (*5*). Thus, it is tempting to conclude that every tumor is absolutely unique on its own, suggesting that no effective therapeutic strategy could be developed against molecularly defined classes of tumors. However, a careful analysis of functional cell signaling pathways affected by the multitude of cancer genome alterations has revealed that ultimately, all of these alterations affected only a limited repertoire of pathways that are required for transformation according to the Hanahan and Weinberg dogma (9,10). Therefore, in addition to a genetic “driver”-oriented view of cancer genomics (wherein single alterations functionally support the acquisition of more than one of the Hanahan and Weinberg criteria), these observations support a pathway-oriented view, which takes into account multiple genetic possibilities for the activation of each required pathway.

3.4 The MAP Kinase Signal Transduction Pathway

The MAP (Mitogen Activated Protein) Kinase signal transduction pathways are complex multiprotein pathways that are necessary to interpret signals received at the cell surface and initiate appropriate cellular responses. The name mitogen-activated protein kinase was assigned to these enzymes to acknowledge the fact that they had first been detected as mitogen-stimulated tyrosine phosphoproteins in the early 1980s, during an intense search for tyrosine kinase substrates (43). MAP kinase pathways are three-tiered signaling cascades with protein activation events occurring through phosphorylation of serines, threonines, and tyrosines. The basic structure of this pathway is conserved among eukaryotes from yeast to humans and involves the downstream activation of the MAP kinase kinase kinase (MAP3K) serine/threonine kinases, to the downstream MAP kinase kinase (MAP2K) dual specificity tyrosine and threonine kinases, to a MAP Kinase (MAPK). The MAPK translocates from the cytoplasm into the nucleus to elicit further molecular activities including phosphorylation of nuclear proteins and regulation of transcription factors (44, 45, 46). Activation of the limited number of MAPKs is controlled by the MAP3Ks which provide the stimulus and cell context specificity of signaling responses. The MAP3Ks tend to be the most diverse and contain regulatory domains not found in MAP2Ks. The domains are necessary for cooperation with a variety of upstream inputs, scaffolding proteins, and anchoring proteins that determine the proper association and activation of the downstream MAP2Ks (44). On the other hand MAP2Ks tend to be highly specific in phosphorylation of MAPKs - each MAP2K phosphorylates only one or a few of the MAP kinases- but there is limited understanding of how these proteins integrate the activation signals for their downstream phosphorylation events (45). It is known that the different MAP2Ks recognize specific Thr-X-Tyr activation motifs on their downstream substrates based on the tertiary structure. Phosphorylation at these specific motifs is necessary to activate and regulate the downstream MAPK protein (46). The MAPKs are the final kinase in the three-tiered pathway, but are not the final phosphorylation event to occur. Activation of the MAPKs through phosphorylation of the Thr-X-Tyr motif induces nuclear translocation and phosphory-

lation of different MAPK substrates including transcription factors, protein kinases, phospholipases, and cytoskeletal associated proteins (46).

There are several characteristics of MAP kinases that result from their activation by kinase cascades. Important among these is that the intermediates provide distinct mechanisms for detecting inputs from other signaling pathways to enhance or suppress the signal to the MAP kinase (48, 49, 50). Another is signal amplification. Amplification can occur if each successive protein in the cascade is more abundant than its regulator. This may be true at one or both steps within MAP kinase modules. Another feature of MAP kinase cascades derives in part from the dual phosphorylation of the MAPK by the MAP2K. In the case of ERK1/2, the kinases are phosphorylated on tyrosine before threonine is phosphorylated both in vitro and in cells (51, 52). The result of this nonprocessive phosphorylation is the establishment of a threshold (53, 54). The tyrosine-phosphorylated proteins are not active but must accumulate before phosphorylation of threonine. Once this accumulation threshold has been reached, the kinases are rapidly converted to the active state, as threonine is phosphorylated. It may be generally true that the MAP2K-MAPK step exists to enhance the cooperativity of activation of the MAPK and to allow modulation by other signaling events, in addition to or rather than amplifying the MAP2K signal.

A specific MAP3K enzyme may regulate either a single or multiple MAP2Ks depending upon the enzymatic specificity of the MAP3K, the cellular and subcellular distribution of the signaling components, the formation of protein complexes, and the activating stimuli. Consequently, significant differences in both the magnitude and kinetics of MAPK activation may occur in response to a given agent under different circumstances. Many kinases acting at the MAP3K level have been identified, adding to the complexity of unraveling signaling mechanisms. There is no apparent similarity among these proteins outside of their kinase catalytic domains. The relative contribution of each MAP3K to the activation of individual MAPK, with the possible exception of Raf in the ERK1/2 module, is unclear.

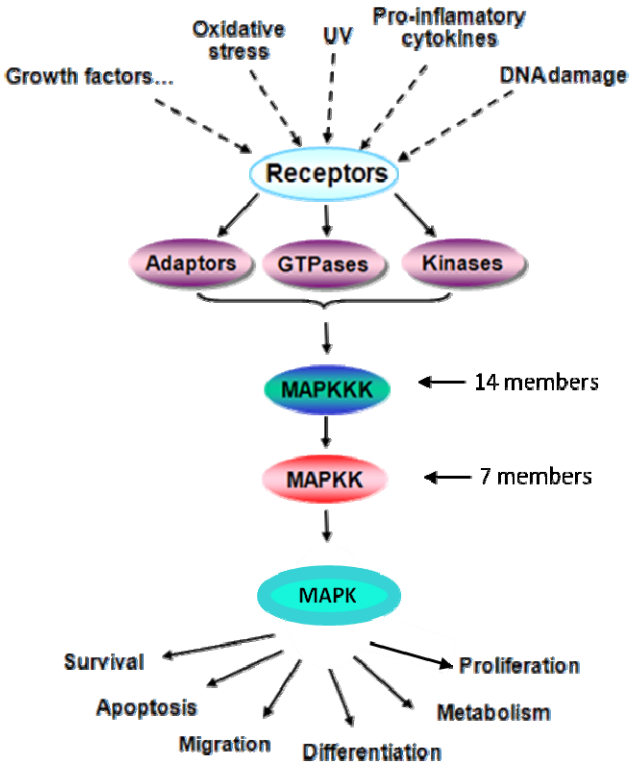

MAPKs, the effectors of the pathway

The ERK family

To date three distinct families of MAPKs have been characterized in mammals; extracellular signal-regulated kinases (ERK 1/2, 3/4, 5, 7/8), Jun N-terminal kinases (JNK 1/2/3) and the p38 isoforms (a/b/g(ERK6)/d) (55, 56, 57, 58).

The ERK pathway is the best studied of the mammalian MAPK pathways with the ERK1 and ERK2 members being the most popular of the family (for the purposes of this dissertation I will focus on ERK1 and 2 for simplicity). ERK1 and ERK2 are proteins of 43 and 41 kDa that are nearly 85% identical overall, with much greater identity in the core regions involved in binding substrates (86, 87). Both are ubiquitously expressed, although their relative abundance in tissues is variable. They are stimulated to some extent by a vast number of ligands and cellular perturbations, with some cell type specificity (88). In fibroblasts (the cell type in which the generalizations about their behavior and functions have been developed) they are activated by serum (mitogens), growth factors, cytokines, certain stresses, ligands for G protein-coupled receptors (GPCRs), and transforming agents, to name a few. In the ERK MAPK module, ERK1 and ERK2 are activated by a pair of closely related MEKs, MEK1 and MEK2 (89 –95). Both of these MEKs have been shown to fully activate ERK1/2 in

vitro (96,97). Active ERKs phosphorylate numerous cytoplasmic and nuclear targets, including kinases, phosphatases, transcription factors and cytoskeletal proteins (162). ERK signaling can, depending on the particular cell type, regulate processes such diverse as proliferation, differentiation, survival, migration, angiogenesis and chromatin remodelling (162, 163).

The JNK/SAPK family

The JNK family of MAP kinases (alternatively called stress-activated protein kinases, SAPKs) are predominantly activated by cytokines, UV radiation, growth factor deprivation, DNA-damaging agents, certain G-protein coupled receptors and serum (164). The family is encoded by three genes: Jnk1, Jnk2 and Jnk3. Jnk1 and 2 are ubiquitously expressed, whereas Jnk3 expression is restricted to the brain, heart and testis. Alternative splicing of these genes creates a total of 10 JNK isoforms. JNK activation requires dual phosphorylation on tyrosine and threonine residues at a distinctive TPY motif, a reaction is catalyzed by MEK4 and MEK7. Two MEK family members, MKK4 (SEK1, MEK4, JNKK1, SKK1) and MKK7 (MEK7, JNKK2, SKK4), have been implicated in JNK/SAPK pathways. In vitro MKK4 preferentially phosphorylates the tyrosine residue in the TPY activation loop motif of JNK/SAPKs, and MKK7 preferentially phosphorylates the threonine residue. Based on these specificity differences, it has been suggested that these kinases cooperate to activate JNK/SAPKs, perhaps allowing for signal integration (98, 99). JNKs translocate/ relocate from the cytoplasm to the nucleus following activation. A major substrate for JNK is the transcription factor c-Jun, which when phosphorylated at serines 63 and 73, results in the enhancement of AP-1 transcriptional activity (165). The localization of active JNK is not restricted to the nucleus but relatively little is known about the nature of cytoplasmic JNK substrates. In response to stresses such as UVB radiation, oxidative stress and DNA-damage, JNK binds to and phosphorylates p53 (166). Depending on the site phosphorylated, this can result in an increase in p53 transcriptional activity and p53 stabilization (167-170). JNK has also been reported to regulate p53 stability in the absence of stress by an HDM2-dependent mechanism (171).

The p38 family

The four vertebrate isoforms of p38, a, b and g (ERK6) and d are characterized by the presence of the conserved Thr-Gly-Tyr (TGY) phosphorylation motif in their activation loop (172). This motif is phosphorylated by MEK3 and MEK6 which themselves are induced by physical and chemical stresses, such as oxidative stress, hypoxia, X-ray and UV irradiation and cytokines. In some instances p38 can also be activated by MEK4, a kinase that is better known as an activator of JNK. Once active, p38 proteins can translocate from the cytosol to the nucleus where they phosphorylate serine/threonine residues of their many substrates. In addition to its role in stress responses, the p38 pathway also plays a role in the regulation of apoptosis, cell cycle progression, growth and differentiation. This is due, in part, to the ability of a broad range of extracellular stimuli such growth factors and hormones that activate this pathway. p38 is required for expression of TNFa and interleukin-1 during inflammatory responses and most stimuli that activate p38 also induce expression of the p38 protein (173). Characterization of the function of p38 has been facilitated by the anti inflammatory drug SB203580, an inhibitor of p38 (174).

MAP3Ks, the first tier in the kinase cascade

A specific MAP3K enzyme may regulate either a single or multiple MAP2Ks depending upon the enzymatic specificity of the MAP3K, the cellular and subcellular distribution of the signaling components, the formation of protein complexes, and the activating stimuli. Consequently, significant differences in both the magnitude and kinetics of MAP kinase activation may occur in response to a given agent under different circumstances. Many kinases acting at the MAP3K level have been identified, adding to the complexity of unraveling signaling mechanisms. There is no apparent similarity among these proteins outside of their kinase catalytic domains. The relative contribution of each MAP3K to the activation of individual MAP kinases, with the possible exception of Raf in the ERK1/2 module, is unclear.

Aside from Raf isoforms, the first of these to be isolated was the 195-kDa protein MEKK1. It is one of a family of molecules most closely related to the yeast kinase Ste11p, all of which contain C-terminal kinase domains and N-terminal regions of

variable length (100). In their catalytic domains, MEKK2 and MEKK3, each approximately 70 kDa, and MEKK4, about 150 kDa, are nearly 50% identical to MEKK1 (101-104). The other enzymes with MAP3K activity mentioned next are less similar with identities to MEKK1 generally in the 30–40% range. The following MAP3K level kinases activate JNK/SAPKs when overexpressed or by *in vitro* reconstitution with MAP2Ks: MEKKs 1–4 (101-104), MAP three kinase(MTK1) (101, 103-106), Tpl-2/Cot (111), dual leucine zipper kinase (DLK) (107), mixed lineage kinase MLK2/MST (107), MLK3/PTK-1/SPRK (108, 109), transforming growth factor-b (TGFb)-activated kinase (TAK1) (109), apoptosis signal-regulating kinases (ASK1)/MAPKKK5 (112, 113) and ASK2/MAPKKK6 (114), and thousand and one amino acid kinases 1,2 (TAOs1, 2) (115, 116). Of these, MEKKs (1–3) and Tpl-2 can also activate the ERK1/2 pathway (111); MEKK3 and Tpl-2 also activate the ERK5 pathway (117, 118); and TAK1, ASK1, TAOs1/2, and MTK1 also activate the p38 pathway (113, 115, 116).

MAPK pathways in cancer

Abnormalities in MAPK signaling impinge on most, if not all the processes previously mentioned as “hallmarks” of cancer and play a critical role in the development and progression of cancer. The ERK pathway is deregulated in approximately, one-third of all human cancers. Historically, ERK signaling was synonymous with cell proliferation but it is now clear that deregulation of this pathway is linked to many other aspects of the tumor phenotype. Most cancer-associated lesions that lead to constitutive activation of ERK signaling occur at early steps of the cascade, namely, overexpression of receptor tyrosine kinases, activating mutations in receptor tyrosine kinases, sustained autocrine or paracrine production of activating ligands, Ras mutations and B-Raf mutations . However, there is also amplification or deregulation of its nuclear transcription factor targets, most notably myc and AP-1. In addition, cancer cells may switch the repertoire of extracellular matrix receptors they express to one that favours the transmission of pro-growth signals. Such growth promoting integrins can activate ERK signaling (175). Thus, the fact that deregulation of this pathway in cancer occurs at several levels underlines its importance.

As mentioned before, cancer cells are exposed to various stress conditions including hypoxia, detachment from substrate, inflammation and metabolic stress arising from dysregulation of energy production. Added to this are genotoxic and pharmacological stress during chemotherapy or radiotherapy. Thus, an important part for stress-activated kinases (JNK and p38 pathway) in cancer has also emerged, mainly in modulatory roles that impinge on DNA damage response, apoptosis and inflammation. Generally, their effect is anti-proliferative and proapoptotic, but dependent on the cellular context they also may contribute to tumorigenesis.

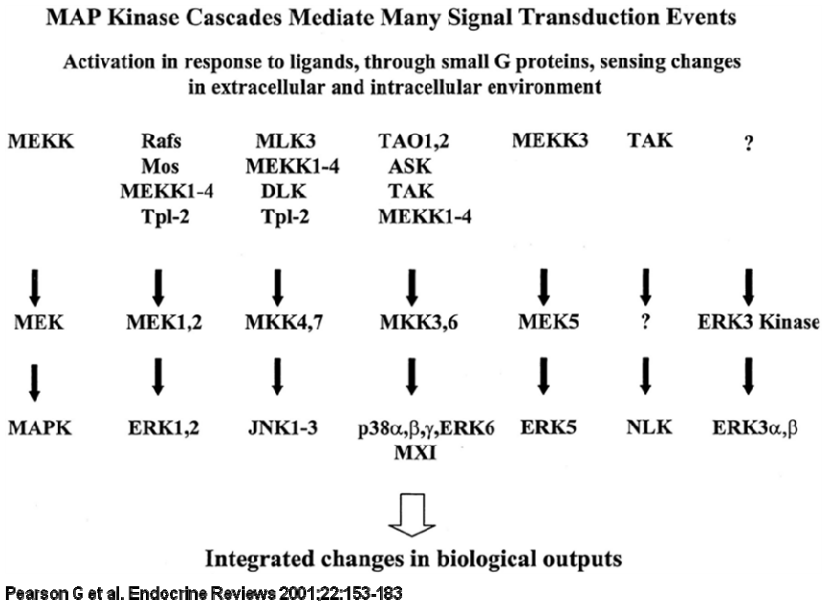

Pearson G et al. Endocrine Reviews 2001:22:153-183

3.5 Tpl2 / Cot

History of cloning

Tpl2 (tumor progression locus 2) also known as COT (cancer Osaka thyroid) and MAP3K8 is a Ser/Thr MAP3K, independently discovered in three different laboratories in the early 1990s. Initially, Miyoshi et al. (15) identified Cot as an oncogene, using DNA isolated from a human thyroid carcinoma cell line, to transform the SHOK hamster embryonic cell line in vitro. The rat homolog of human Cot, called Tpl2, was subsequently identified as a target for provirus integration in Moloney murine leukemia virus (MoMuLV)-induced T-cell lymphomas and demonstrated to transform NIH 3T3 fibroblasts *in vitro* (16). More recently, MoMuLV insertion into the murine Tpl2 locus was also found in two genome-wide screens for oncogenes using genetically sensitized mouse strains (17, 18). It has also been reported that the murine Tpl2 locus is a site of Mouse Mammary Tumor Virus (MMTV) proviral integration associated with the induction of mammary carcinomas in mice (19). Proviral activation of Tpl2 oncogenicity consistently results in production of Tpl2 proteins truncated at the C terminus compared to the wild-type protein (generically termed TPL-2ΔC here), suggesting important roles of the C terminus in regulation of TPL-2 oncogenic activity. Consistent with this hypothesis, generation of transgenic mice expressing rat TPL-2 or TPL-2ΔC in their T cells has revealed that C-terminal deletion is essential for TPL-2 to induce the formation of T cell lymphoblastic lymphomas (20). As the overexpression of wild-type TPL2 did not exert similar oncogenic effects in vivo, it was proposed that TPL2 is a proto-oncogene activated by C-terminal truncation (20)

Gene and protein product

The Tpl2 gene localizes to human chromosome 10p11.2 and has highly conserved homologues in the rat and mouse genome. Human MAP3K8 is composed of 9 exons, the second of which is alternatively spliced (Sanchez-Gongora et al., 2000). Exon 3 contains the two alternative translation initiation sites resulting in two protein isoforms, full-length M1-Tpl2 (p58) and M30-Tpl2 (p52). M30- Tpl2 is translated from the same mRNA transcript as M1-Tpl2 by alternative translational initiation at methionine 30 (Figure C M30, black arrowhead). Both M1-and M30- Tpl2 proteins are predominantly localized in the cytoplasm. Of the two TPL2 isoforms, p58 TPL2 is believed to be the catalytic subunit responsible for transducing ERK activation signals, whereas the p52 isoform plays a role in stabilizing p58 in the NF-κB1/ABIN2/TPL2 complex (119).

The Tpl2 kinase domain (KD) is located in the centre of the protein, flanked by N-terminal and C-terminal regions with largely unknown functions. C-terminal truncation, however, results in a protein (Tpl2ΔC) with increased kinase-specific activity, suggesting that this region may inhibit Tpl2 kinase activity (20). Furthermore, a proposed degron sequence [435-457, shaded box] is located within the C terminus and confers destabilizing properties to full-length Tpl2 (120). Consequently, Tpl2ΔC has increased protein stability and is expressed at higher levels. The positions of oncogenic truncations in Tpl2 identified in MoMuLV- and MMTV-induced murine tumors [424], human Tpl2 (COT) in transformed SHOK cells [397] and in a human lung adenocarcinoma [421] are indicated by red arrowheads. Several phosphorylation sites in Tpl2 have been identified by mass spectrometry (121). Two of these sites, T290 and S400, are known to regulate Tpl2 MEK kinase activity *in vivo*. T290 phosphorylation may also regulate Tpl2 release from its binding partner p105 (see Figure 4). The physiological significance of the sites shown in italics is not yet known.

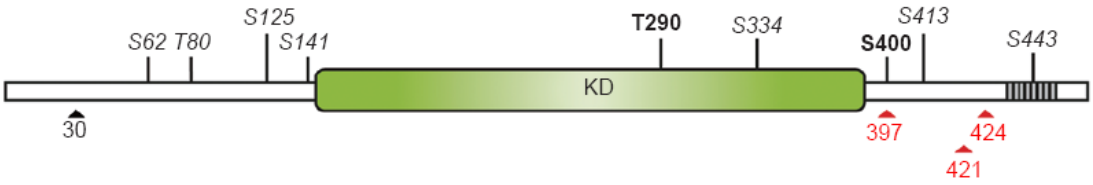

In unstimulated cells, TPL-2 is stoichiometrically complexed with the C-terminal half of NF-κB inhibitory protein NF-κB1 p105, which blocks TPL-2 access to its substrate MEK, and the ubiquitin-binding protein ABIN-2 (A20-binding inhibitor of NF-κB 2), both of which are required to maintain TPL-2 protein stability. Following agonist stimulation, the IKK complex phosphorylates p105, triggering its K48-linked ubiquitination and degradation by the proteasome. This releases TPL-2 from p105-mediated inhibition, facilitating activation of MEK, in addition to modulating NF-κB activation by liberating associated Rel subunits for translocation into the nucleus. However, TPL-2 is only associated with a small fraction of total cellular p105. It therefore remains possible that TPL-2 regulates the proteolysis of this pool of p105, which is likely to contribute to only a fraction of total NF-κB activity.

In unstimulated cells, all detectable TPL-2 is complexed with NF-κB1 p105 and ABIN-2. The TPL-2 kinase domain (KD) directly interacts with the death domain (DD) of p105. This regulates TPL-2 MEK kinase activity by blocking access of the substrate to the active site. The TPL-2 C terminus [398-467] interacts with a region [497-539] of p105 within the “processing inhibitory domain” [PID; 474-544] (122), which also mediates p105 dimerization (123). These two distinct interactions contribute to a very strong association between TPL-2 and p105, and dissociation of recombinant TPL-2/p105 complex produced in insect cells requires high concentrations of urea (8 M) (124). The importance of TPL-2 regulation by p105 is highlighted by the dysregulated TPL-2 MEK kinase activity and tumorigenic potential of C-terminal truncated TPL-2, which lacks one of the binding sites for p105 (see text for details). The same region of TPL-2 that mediates binding to the PID of p105 is also the principal interaction site with ABIN-2. The binding site on ABIN-2 [194-250] contains ABIN-homology domain (AHD) 4 [203-220], which is also present in ABIN-1 and ABIN-3 (125). ABIN-2 interaction is critical to maintain TPL-2 protein stability, and steady-state levels of TPL-2 are dramatically reduced in cells deficient in ABIN-2.

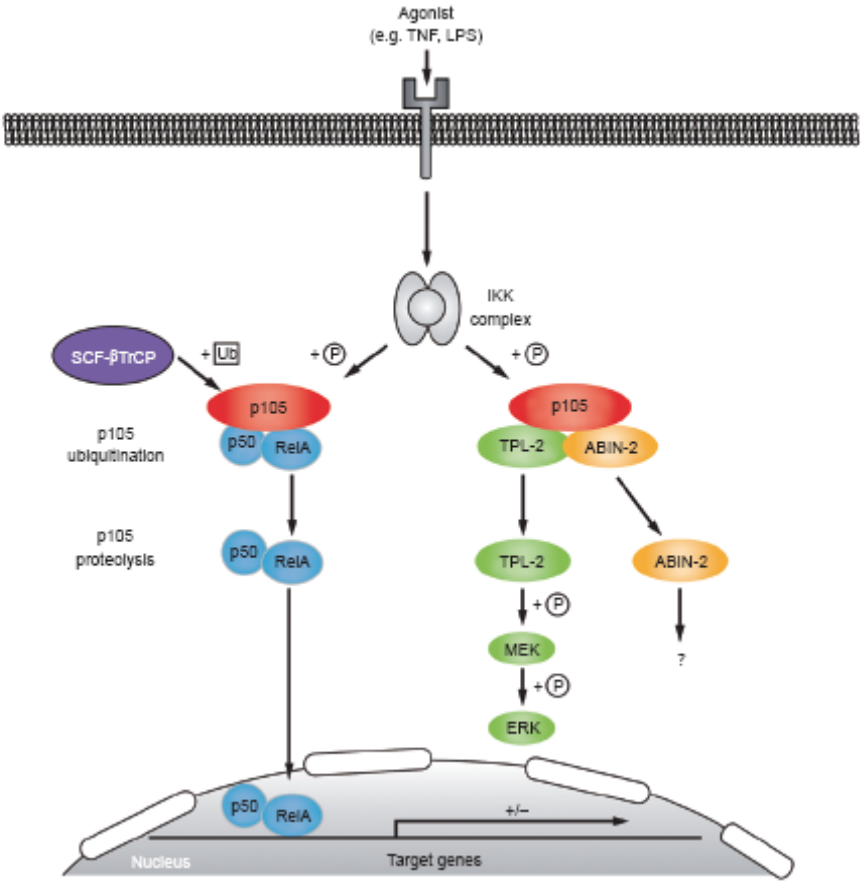

Figure I4: Tpl2 is confined to a cytoplasmic complex with the NF-κB1 precursor protein p105, and the ubiquitin-binding protein ABIN-2. Cellular stimulation with various agonists, such as TLR ligands, IL-1β, TNF and CD40L, induces the formation of receptor proximal complexes that trigger activation of the MAP3 kinase TAK1 [101]. Activation loop phosphorylation of IKK2 by TAK1, in turn, activates IKK2 to phosphorylate the target residues S927 and S932 in p105, creating a binding site for the SCFβTrCP ubiquitin E3 ligase complex. K48-linked ubiquitination of p105 by SCFβTrCP triggers its complete degradation by the 26S proteasome. After liberation from p105, Tpl2 directly phosphorylates MEK and thereby activates downstream ERK MAP kinase signaling. Activation of Tpl2 MEK kinase activity additionally requires trans-/autophosphorylation of S400 by an unknown kinase and autophosphorylation at T290 in the Tpl2 activation loop. Proteasomal degradation of p105 also releases ABIN-2 from association with p105 and Tpl2. The function and downstream targets of ABIN-2 are not known

Activation

Similar to other MAP3 kinases (130), TPL-2 signaling function is regulated by phosphorylation. Activation of TPL-2 requires autophosphorylation of T290 in the activation loop of its kinase domain (131), which may also regulate the association of TPL-2 with p105 (119). The phosphorylation event at Thr290 is induced preferentially to the catalytic isoform p58 and is required for its release from p105 NF-κB1 (126). The released subunit is active towards its physiological substrate MEK1 but unstable and is rapidly targeted for proteasome-mediated degradation, thus restricting prolonged activation of ERK signaling (126, 127).TPL-2 must also be phosphorylated on S400 in its C-terminal tail to activate MEK following LPS stimulation of macrophages (126). Different experimental systems have suggested that S400 is either autophosphosphorylated by TPL-2 (IL-1β-stimulated IL-1R-293T cells) or transphosphorylated by an unknown kinase (LPS-stimulated RAW264.7 macrophages) (126, 128) . The way by which Ser400 phosphorylation contributes to kinase activation is still unclear. As this residue is within the C-terminus of TPL2, its phosphorylation is proposed to act as an essential control step for kinase activation, by inducing a conformational change which releases the inhibitory intermolecular interaction between the C-terminal tail and the kinase domain of TPL2 (129).

An important aspect of TPL2 activation is its interplay with upstream components of NF-κB signaling, such as the IκB kinase β (IKKβ, also known as IKK2). Studies in IKKβ-null fibroblasts have demonstrated that IKK activity is required for the activation of the TPL2-ERK axis. This has been attributed to the phosphorylation of p105 by IKKβ, an event which is essential for the signal-induced liberation of p58 from the p105 complex (123) (Figure 1). In addition, the signal-induced phosphorylation of the TPL2 catalytic subunit at Thr290, which largely contributes to dissociation of TPL2 from p105 NF-κB1, has been shown to depend on IKKβ activity (129). However, despite its essential role, IKKβ activation is not sufficient to induce TPL2 activity.

Function

While the potential of truncated Tpl2 to behave as a transforming oncoprotein kinase was clear, the physiological function of wild-type Tpl2 was initially less evident.

Early northern blot analyses of rat tissues demonstrated that Tpl2 mRNA is expressed at highest levels in the spleen, thymus and lungs, with low levels in the brain, testis and liver (16, 132). In the mid 1990s, DNA sequence homology comparisons revealed that Tpl2 kinase domain is related to the MAP3 kinases STE11 and MEK kinase (111, 133), suggesting that Tpl2 might regulate MAP kinase signaling pathways.

Consistent with this hypothesis, Tpl2 overexpression in COS-7 and 3T3 cells activates ERK, JNK, p38γ and ERK5 MAP kinases (111, 118, 133). Immunoprecipitated Tpl2 phosphorylates MEK-1, MKK-4 (also known as SEK-1), MEK-5 and MKK-6, suggesting that it functions directly as a MAP3 kinase (111, 118). This was subsequently confirmed using recombinant Tpl2 purified from lysates of baculovirus-infected insect cells and recombinant MEK protein as a substrate (124). Overexpression of Tpl2 also activates NFAT (nuclear factor of activated T cells) in Jurkat T cells and induces IL-2 (interleukin-2) production (134). In addition, overexpression experiments in COS-7 cells demonstrate that Tpl2, may regulate NF-κB activation by inducing p105 proteolysis, releasing associated Rel subunits for translocation into the nucleus (135).

Overexpression of kinases can result in artifactual phosphorylation of cellular proteins, and it remained unclear for several years whether Tpl2 really regulated the activation of so many downstream signaling pathways under physiological conditions. This was clarified through the generation of a Tpl2−/− mouse strain by the Tsichlis laboratory. Tpl2−/− mice display no overt phenotype, are of normal size and weight and have a normal lifespan under pathogen-free conditions (136). The development of immune cells (T cells, B cells, dendritic cells (DC), natural killer cells and macrophages) occurs normally.

Analysis of Tpl2−/− macrophages revealed an essential function for TPL-2 in LPS activation of MEK-1/2 and ERK-1/2, but not of p38, JNK or NF-κB. Furthermore, LPS stimulation activates the MEK kinase activity of TPL-2 (127, 138). TPL-2 is also required for TLR2, TLR9 and TNF induced activation of ERK in macrophages (139-141) and CD40 induced activation of ERK in B cells (139). In other cell types, the function of TPL-2 may not be restricted to the regulation of the ERK MAP kinase pathway. Consistent with this idea, TPL-2 is required for optimal activation of ERK and JNK in

embryonic fibroblasts after TNF or IL- 1β stimulation, and for maximal p38 activation in LPS and CpG-stimulated DC (137, 140).

Tpl2−/− mice were found to produce very low levels of TNF after intraperitoneal LPS injection and to be resistant to septic shock induced by LPS and d-galactosamine (136). TPL-2 is also required for optimal TNF production by LPS stimulated macrophages, the major cellular source of TNF during inflammatory responses, while LPS-induced TNF production by DC is partially dependent on TPL-2 (136, 141). However, TPL-2 is not universally involved in induction of TNF in macrophages, since curdlan stimulation of dectin-1, which activates ERK via Raf, induces TNF independently of TPL-2 expression (141, 142). The requirement for TPL-2 in TNF-induced innate immune responses is, therefore, both cell- and stimulus specific.

Together, analyses of primary cells from Tpl2−/− mice indicate that the major physiological function of TPL-2 is to regulate ERK MAP kinase activation in immune responses following stimulation of receptors of the TLR and TNF-R families. However, TPL-2 may also regulate the activation of other MAP kinases and NF-κB in a cell type- and stimulus-specific fashion.

Role in cancer

Despite early studies identifying COT as a proto-oncogene activated by C-terminal truncation in mouse and rat, mutations in Tpl2 are rarely observed in humans (143, 144) and the physiological role of TPL2 in carcinogenesis remains enigmatic. Whilst elevated levels of TPL2 have been reported in human gastric/colon adenocarcinomas (145)], large granular T cell neoplasias (146), breast cancer (135, 147) and Epstein-Barr virus (EBV)-related nasopharyngeal carcinoma and Hodgkin's disease , a detailed evaluation of Tpl2 expression and function in human malignancy and normal tissue is still missing. Although multiple studies have demonstrated that Tpl2 can function as an oncogene in some situations, recent studies implicate Tpl2 in tumor suppressive activity. For example, Tpl2−/− mice bred onto an MHC Class I-restricted T-cell antigen receptor (TCR) transgenic background develop T-cell lymphomas due to hyperresponsiveness of CD8+ T cells following TCR stimulation (22). A genome-wide RNA interference (RNAi) screen showed that COT is required for TRAIL-induced

apoptosis in human breast cancer cells (176). Therefore, COT may impact on oncogenic events including the cellular response to therapy in a tissue type and stimulus-dependent manner.

5. Objectives

The present study sought to delineate the role of Tpl2/COT in carcinogenesis. More specifically, the objectives of the study were :

1. **To dissect the contribution of Tpl2/COT in the initiation and during different stages of the progression of lung carcinogenesis in human.**

2. **To investigate how ablation of Tpl2 shapes the disease after chemical induction of lung carcinogenesis *in vivo*.**

3. **To decipher the molecular mechanism(s) involved in the development of the epithelial response to carcinogenesis in the absence of Tpl2.**

Results obtained from these objectives, indicated that Tpl2 /COT is preferentially downregulated in epithelial cells of the lung during the human disease and its ablation accelerates carcinogenesis. Tpl2/ COT may act as a tumor suppressor, participating in both initiation and progression of tumor development. Therefore a new series of questions were raised:

1. **Which is the physiological role of COT in human lung cancer? Is it of clinical importance?**

2. **How is Tpl2/COT regulated in epithelial cells *in vivo?* Which are the statistically significant mechanisms really affecting its *in vivo* levels?**

3. **Since industry has already invested in systemic Tpl2 inhibition as a drug target wouldn't it be wiser to elucidate its physiological role in epithelial homeostasis at fist?**

6. Materials & Methods

Mouse maintenance, carcinogenesis protocol and histological analyses

Single-cell suspension preparation from lungs, lymph nodes and spleen and Flow Cytometry

Mouse lung lysis for Western Blotting

Human tissue

DNA and RNA isolation and cDNA synthesis

Quantitative PCR expression assays

DNA Methylation Analysis

Allelic Imbalance (AI) analysis

Mutational analysis of human K-ras

Statistical Analyses

Cell culture, transfections and RNA interference.

Immunoblotting

Reporter Assay

Quantitative measurement of apoptosis

Soft agar assay

Light microscopy

Immunohistochemical detection of Tpl2

Mouse maintenance, carcinogenesis protocol and histological analyses

Tpl2+/+ and Tpl2-/- mice (C57/BL6 background, obtained by the SPF facility of IMBB-FORTH) (Dumitru et al., 2000) were housed in plastic cages containing hardwood bedding and dust covers in a HEPA-filtered, environmentally controlled room (24^{o}C, 12-h/12-hrs light/dark cycle), and were given Rodent Lab Chow and water *ad libitum*. For the induction of lung tumors, a chemical carcinogenesis protocol based on urethane (ethyl-carbamate) was applied, as previously described for C57/BL6 mice (Miller et al., 2003). 7-week-old mice were injected intra-peritoneally with 1 mg/g freshly prepared sterile urethane (Sigma-Aldrich) in 0.9% NaCl once weekly, for a total of 10 doses and tumor multiplicities were examined at several time points after the last injection. Lungs were dissected out and incubated in 10% buffered formalin overnight at 4°C followed by PBS wash (6h at room temperature). Fixed tissues were then dehydrated through a graded ethanol series (30% (6h), 50% (6h), 70% (6h), 80% (6h), 90% (6h) and 100%(6h) RT). Tissues were cleared with chloroform (12h) at room temperature and then embedded in melted paraffin wax at 56-58°C for 12-24 hrs, with 3 changes of wax. Sections cut into 4 μm size were prepared and placed on glass slides, stained with hematoxylin and eosin, and reviewed in a blinded fashion and in consensus in case of discrepancy more than 10%. The same procedure was followed for lung inflammation grade evaluation, under the guidance of expert pathologist Gorgoulis V. The histopathological classification of the pulmonary lesions was performed in accordance with the recommendations of the mouse models of human cancers consortium, NIH/NCI, 2004 (Nikitin et al., 2004). To estimate the growth rate of tumors, the percentage of tumor cells expressing the proliferation marker Ki67 was measured. A proliferation index was calculated for each tumor lesion by counting the total number of tumor cell nuclear profiles and the number of Ki67-positive nuclear profiles in randomly selected fields. The same procedure was followed for lung inflammation grade evaluation. Animal experiments were approved by the local ethical committee of the University of Crete Medical School, Greece, licence number 1406/14-03-2006.

Single-cell suspension preparation from lungs, lymph nodes and spleen and Flow Cytometry

Lungs, draining lymph nodes and spleens were removed from euthanized mice animals at several time points following urethane administration, washed with HBSS, and mashed into single-cell suspensions using 7μm cell strainers. Erythrocytes were lysed and cells were isolated by centrifugation. Cells were then washed twice with PBS/5% FCS and stained with fluorescently labeled antibodies for 20 min at 4 ^{0}C in PBS/5% FCS against CD3 (145-2C11), NK1.1 (PK136), CD4 (GK1.5), CD8α (53-6.7), CD69 (H1.2F3), F4/80 (BM8), CD11c (N418), Gr1 (RB6-8C5) and CD11b (M1/70). Antobodies were purchased from eBioscience, UK.

Mouse lung lysis for immunoblotting

Lysates from tumor and normal areas of mouse lung tissue were obtained according to the protocol proposed at "Current Protocols in Protein Science", Ch. 4.2.10. Briefly, normal tissue and lung tumors from each mouse were dissected, tumors were pooled together (tumors from different mice were not mixed; each pool corresponds to one animal) and all samples were weighed and chopped into small pieces. Samples were homogenized in modified RIPA buffer (50 mM Tris-HCl, pH 7.4, 1% Triton X-100, 0.2% sodium deoxycholate, 0.2% sodium dodecylsulfate (SDS), 1 mM sodium ethylenediaminetetraacetate, 1 mM phenylmethylsulfonyl flouride, 5 μg/ml of aprotinin, 5 μg/ml of leupeptin). Tissue and cell debris was removed by centrifugation. Protein concentration was determined with Bio-Rad protein assay. The lysate was boiled for 5 min in 1 x SDS sample buffer (50 mM Tris-HCl pH 6.8, 12.5% glycerol, 1% SDS, 0.01% bromophenol blue) containing 5% b-mercaptoethanol. Lysates from mouse lungs expressing K-RASG12D (Schramek et al., 2011) were kindly provided by Josef Penninger, Austrian Academy of Sciences, Austria.

Human tissue

Frozen tissue from 124 NSCLCs (46 adenocarcinomas and 78 squamous cell carcinomas), as well as 100 adjacent normal lung tissues were obtained from Liverpool Heart and Chest Hospital (Liverpool, UK). In 100 of the NSCLCs, matched normal tis-

sue was available. 82 patients were males and forty two were females. Specimens comprised the following pathological stages (pT): 8 T1, 103 T2, 9 T3 and 2 T4. Ethical approval has been obtained from Liverpool Ethics Committee for this study and informed consent was obtained from each individual.

DNA and RNA isolation and cDNA synthesis

DNA and total RNA extraction from tissues were performed using the DNeasy and miRNeasy kits (Qiagen, UK) respectively following the manufacturer's protocol. 20-40 µm frozen sections from each patient sample were utilised. The first and last sections underwent pathological review to ensure ≥80% tumor cell content. 500 ng total RNA was reverse transcribed in a 20 µl reaction using the Quantitect kit (Qiagen, UK) and following the supplier's protocol.

Quantitative PCR expression assays

A TaqMan™ gene expression assay for COT (MAP3K8; ID Hs00178297_m1, FAM labeled) as well as β-actin (ACTB; 4326315E) as endogenous control (VIC-labeled) were purchased from Applied Biosystems, Warrington, UK . Assays were performed in 20 µl, containing 10 µl Taqman expression master mix (Applied Biosystems), 1µl of the target primer/probe mix, 1 µl endogenous control and 2 µl of cDNA following the universal conditions (2 min at 50^{o}C, 95^{o}C for 10 min, 50 cycles of 94^{o}C for 30 sec, 60^{o}C for 45 sec) on an Applied Biosystems 7500 FAST real-time PCR instrument. For micro RNA analysis, the hsa-miR-370 (assay ID 2275) and RNU48 (assay ID 1006) were used as target and endogenous control respectively, following the manufacturer's protocol. Briefly 10 ng total RNA were used in each reverse transcription reaction followed by PCR amplification with the corresponding primer/probe mix on an Applied Biosystems 7500 FAST real-time PCR instrument. For micro RNA analysis, the hsa-miR-370 (assay ID 2275) and RNU48 (assay ID 1006) were used as target and endogenous control respectively, following the manufacturer's protocol. Briefly 10 ng total RNA was used in each reverse transcription reaction followed by PCR amplification with the corresponding primer/probe mix on a 7500FAST instrument. All assays were run in triplicate and the mean value was used for the analysis. mRNA and

miRNA levels were expressed as relative quantification (RQ) values which were calculated as: RQ=2(-ΔΔCt), where the expression of IMR-90 human lung fibroblasts was used as a calibrator in each run.

DNA Methylation Analysis

Pyrosequencing® assays were developed using the Pyromark Assay Design 2.0 software (Qiagen) in order to measure the DNA methylation levels of MAP3K8 promoter and miR-370 region. One assay (TPLmeth1) covered the transcription start site (TSS) and proximal promoter (CpGs at positions -42, -40, -37, -16, -4, 1 and 5 relative to TSS). The second assay (TPLmeth2) covered CpGs within the 5'UTR (positions 27, 30, 38, 53, 55, 68 and 70 relative to TSS). The miR-370 methylation assay covered CpGs at positions -9, -18, -42, -48, -60 and -80 relative to the TSS of the pre-miRNA sequence. The primer sequences used are the following:

TPLmeth1-Fb 5' biotin-GAGGTTTTGGGTTATTAGGTT

TPLmeth1-R 5' CCCTCATTTACCCTCTAAAC

TPLmeth1-S 5' CCTCATTTACCCTCTA

TPLmeth2-Fb 5' biotin-GTTTAGAGGGTAAATGAGGG

TPLmeth2-R 5' ATTACAAAATAAACCAAAACCC

TPLmeth2-S 5' TTACAAAATAAACCAAAAC

mir370meth-F: 5' GGGTTATTTGAGGGATGG 3'

mir370meth-Rb: 5' biotin-AACCTAACTTCTCTATCTTATACCC 3'

mir370meth-S: 5' TTATTTGAGGGATGGG

Oligonucleotides were supplied by Eurofins MWG Operon (Germany). 1 μg of genomic DNA was treated with sodium bisulphite (EZ DNA methylation Kit™, ZymoResearch) following the manufacturer's protocol. PCR amplifications were performed in a final volume of 25 μl using Qiagen HotStarTaq Master Mix, 150 nM biotinylated primer, 300 nM non-biotinylated primer and approximately 60 ng of bisulphite treated genomic DNA. The thermal profile was: 95^{o}C for 5 min followed by 40 cycles consisted of 14 94^{o}C for 30 sec, 52^{o}C for 30 sec, and 72^{o}C for 30 sec. For Pyrosequencing analysis, the PyroMark Gold Q96 SQA Reagents and the PyroMark Q96 ID instrument (Qiagen) were used following the suppliers protocol. The methyl-

ation index (MtI) for each promoter was calculated as the mean value of mC/(mC+C) for all examined CpGs in the target sequence(Daskalos et al., 2011).

Allelic Imbalance (AI) analysis

Four microsatellite repeats (designated MS1-4) were identified in the vicinity of the COT (MAP3K8) gene. As shown in Supplementary Figure 4, MS1 (CA)n repeat lies 18.8 kb upstream the gene's TSS, MS2 (GA)n repeat is located in the proximal promoter, MS3 (TTA)n repeat is found in intron 4 while MS 4 (GT)n repeat is located 40.3 Kb downstream the TSS. Primers flanking the repeat regions were designed. The forward primers were labeled with FAM (MS1, MS3) and HEX (MS2, MS4) dyes. The primer sequences were:

MS1-F: CATTGTATGTAACATATATGAAGA

MS1-R: GCATCATAGTAGACCCTGT

MS2-F: GAATCTGGGTTGTGCCTG

MS2-R: CTAGGAGCCATGTAAGGTCG

MS3-F: GGCAGAAACTGGGAAGGAGG

MS3-R: ACCCCGACACTGCACTCC

MS4-F: AATTAGTCAAGGAAATAACTGG

MS4-R: GCTTTCTTTATTGTGAGAGACT

The thermal profile was: 95^{o}C for 5 min followed by 25 cycles consisted of 94^{o}C for 30 sec, 52^{o}C for 30 sec, and 72^{o}C for 30 sec. A final 20 min extension step at 72^{o}C was introduced to enhance non-template A addition and reduce split peaks. 2 μl of the PCR reactions were mixed with 10 μl formamide, denatured at 95^{o}C for 2 min, chilled on ice and analysed on a 3130 capillary sequencer (Applied Biosystems). Genemapper software was used to analyse the signal and quantify allelic peak areas. Allelic imbalance was scored if the allelic ratio tumor/normal was outside the region 0.75-1.25 (Liloglou et al., 2001).

Mutational analysis of human K-ras

K-ras mutational analysis for the hot-spot codons 12 and 13 was carried out by PCR and direct sequencing. The primer sequences were:

Krasc12-FOR GCCTGCTGAAAATGACTGA

Krasc12-REV TATCAAAGAATGGTCCTGCAC

Krasc12-SEQ TTCGTCCACAAAATGATTCTG

50 ng of genomic DNA was amplified in a 25 ml reaction containing 12.5 ml and 10 pmoles of each primer. PCR products were cleaned by a standard spin column method (EZ kit, NBS Biologicals, UK) and sequencing was performed using the Big Dye v3.1 chemistry and a 3130 genetic analyser (Applied Biosystems, UK). Mutations were determined by comparing each tumor to the K-ras codon 12/13 wild-type sequence (GGTGGC)

Statistical Analyses

The 1-sample Smirnov-Kolmogorov test was used to assess normal distribution in continuous variables (e.g. expression and methylation levels). In the absence of normal distribution non-parametric tests were used. The Mann-Whitney (independent) and Wilcoxon's ranking (paired comparisons) tests were employed to determine significant differences in expression and methylation levels among groups. Pearson's chi square test was performed to assess differences in categorical data groups, while Spearman's correlation assessed the relationship between continuous variables. Survival analysis was undertaken by constructing Kaplan Meier curves and utilizing log-rank test.

Cell culture, transfections and RNA interference

Lung cancer cell lines were purchased from ATCC, USA, and cultured according to the provider's instructions. Whilst A549 cells carry mutated K-ras alleles, they do not display dependency ("addiction") on the endogenous K-ras oncogene in as much as their proliferation, survival, ERK phosphorylation or PI3 kinase activation status remain unaffected upon RAS knock-down, presumably because of low K-ras oncogene copy number (Singh et al., 2009). Liposome-mediated transfections were performed using Lipofectamine (Invitrogen) in Optimem media (Invitrogen) according to the instructions of the manufacturer. RASG12V-expression vectors were a kind gift of Dr A. Malliri, Paterson Institute for Cancer Research, Manchester, UK. TPL2 expression

vectors have been previously described (Eliopoulos et al., 2002; Tsatsanis et al., 2008). For the delivery of siRNAs and miR370, $5x10^4$ A549, A549/H-rasG12V clone 2 or H1299 cells were plated into each well of a 24-well plate (Costar) and 2 rounds of transfection with siRNA duplexes were performed as previously described (Knox et al., 2011) using the siIMPORTER transfection reagent according to the instructions of the manufacturer (Upstate Biotechnology). The COT siRNA (Cat. No AM16708) and miR-370 (Cat. No hsa-miR-370) were purchased from Ambion (Applied Biosystems). The control siRNA duplex comprised the sequence CGUACGCGGAAUACUUCGAUU and the corresponding antisense strand. The p53 shRNA vector was kindly provided by Reuven Agami (The Netherlands Cancer Institute, Netherlands). Cells transfected with siRNAs targeting Cot or the unrelated luciferase (Luc) gene were then exposed (in the case of the indicated experiments where cells underwent genotoxic stress) to 25μM cis-platin for various time-intervals. Chemical kinase inhibitors (zVAD-fmk, JNK SP600125, MEK PD98059, Tpl2 #616373) were purchased from Calbiochem and dissolved in dimethyl sulfoxide prior to use.

Immunoblotting

Specific antibodies against COT/Tpl2, pERK, β-ACTIN, NFKB1, P53, JNK, pJNK, NPM, BAX, were used at dilutions of 1:500–1:1000. Phospho-specific antibodies were diluted in 5% bovine serum albumin in Tris-buffered saline-0.1% (vol/vol) Tween 20 (TBS-T); all other antibodies were diluted in 5% milk in TBS-T. The MAP3K8 (Tpl2 M20) antibody was purchased from Santa-Cruz Biotechnology Inc., the IκBα L35A5 mAb from Cell Signaling Technology, phospho-specific ERK antibody (M8159) was from Sigma and the β-ACTIN clone C4 antibody from Millipore. The NF-κB1 antibody (clone E381) was purchased from Novus Biologicals. The anti-p53 mAb 1801 was a kind gift from Moshe Oren (Weizmann Institute, Israel). The anti-rabbit IgG-horseradish peroxidase (HRP) and anti-mouse IgG-HRP were obtained from Sigma-Aldrich. Immunoblotting was performed as previously described (Eliopoulos et al., 2003). 15 to 40 μg of whole cell lysates were separated by sodium dodecyl sulfate (SDS)-polyacrylamide gel electrophoresis, transferred onto polyvinylidene difluoride membrane (0.45 μM; Millipore), and blocked for 45 min at room temperature with

5% nonfat milk dissolved in TBS-T. Following three washes with TBS-T, membranes were incubated overnight at 4°C with primary antibody and 1 h at room temperature with the appropriate secondary antibody and then subjected to enhanced chemiluminescence analysis using an ECL kit (Amersham).

Reporter Assay

Tpl2 promoter cloning:

A sequence of 865bp (mentioned as -900) containing 2 κB elements of the Tpl2 promoter, was PCR amplified from genomic DNA isolated from EJ cells (primer sequences are shown in Table 2).

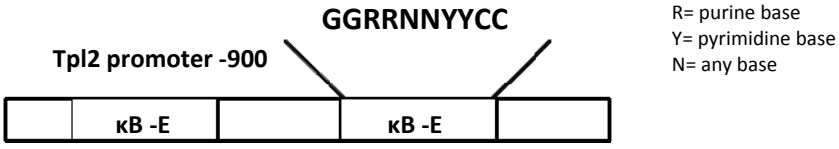

The products, carrying a different R.E. binding sequence on each of the 5' and 3' ends, were initially cloned into the pCR2.1 plasmid (TOPO TA cloning kit, Invitrogen). After the correct sequence was confirmed by sequencing, the inserts were digested and ligated between the KpnI/BglII sites of the pGL3-Basic vector (Promega), upstream the luciferase gene.

Table 2

Tpl2-Luc R	5' GGA AGA TCT GGG ACT AGG GAG GAG CAG AG 3' (BglII site)	Product size
Tpl2-Luc F	5'CGG GGT ACC GGT TCC TAG TGG GTG CTT GA 3' (KpnI site)	~900bp

Quantitative measurement of apoptosis

Quantitative determination of apoptosis in A549 and A549/H-rasG12V clone 2 cells was performed 24 hours post-transfection with Myc epitope-tagged (MT) COT in the presence or absence of shRNA targeting p53 and of the pan-caspase inhibitor zVAD-fmk (15uM). Mean values (± sd) from 3 independent experiments were calculated. For the assessment of apoptosis, we took into consideration the guidelines for the

use and interpretation of assays for monitoring cell death (Galluzzi et al., 2009a) and performed multiple, methodologically unrelated assays to quantify dead cells.

Annexin V staining

Cells were lightly trypsinized and incubated with Annexin V-FITC (BD) and propidium iodide for 15 min before assessment of fluorescence intensity on a flow cytometer (BD FACSCalibur).

Soft agar assay

60mm tissue culture dishes were layered with 3ml 0.7% (w/v) SeaPlaque Low Melting Point Agarose (FMC Bioproducts, Maine, USA) dissolved in serum-containing medium. A549 or H1299 cells were then mixed with 1.6 ml of 0.35% (w/v) warm agar (42^{o}C) in serum-containing medium and plated on the solidified agarose layer. Fresh agar was added weekly and cellular foci were enumerated on day 17.

Light microscopy

Morphological changes related to apoptosis were observed using an inverted microscope (DMIRE2; Leica) equipped with a digital camera (DFC300 FX; Leica). Camera image acquisition was controlled by IM50 software (Leica), and single images were exported as TIFF files. Individual frames were prepared for presentation using Photoshop (Adobe). Cells were seeded into 4-well, chambered coverglass units with coverslip-quality glass bottoms (Laboratory-Tek; Thermo Fischer Scientific) and, after treatment, were examined with a 63× dry objective lens.

Immunohistochemical detection of Tpl2

Paraffin embedded tissue sections 3 μm thick were deparaffinized and subjected to low-temperature antigen retrieval, in 1 mM EDTA (pH 8.0), with 0.1% Tween 20, on a hot plate stirrer at 65°C for 16 min. Following antigen retrieval, sections were washed in Tris-buffered saline (TBS; pH 7.6), and primary antibody to Tpl-2 (M20; Santa Cruz Biotechnology) was applied at a dilution of 1/100 for 1 h at room temperature (RT). Slides were washed in TBS (pH 7.6) containing 0.001% Tween 20. For the immunodetection, UltraVision LP Detection System: HRP Polymer Quanto (Thermo

Scientific, Cheshire, UK) was utilized, with Diaminobenzidine (DAB) as chromogen. Sections were then washed in tap water, counterstained in Harris hematoxylin (BIOSTAIN, Manchester, UK), dehydrated, cleared, and mounted. Negative controls consisted of consecutive lung tissue sections in which non-immune serum was substituted for primary antibody. Lung macrophages served as internal positive controls. An external positive control was always used in each run. For slide reading a Nikon Eclipse E400 optical microscope with plan lenses was used. Digital photographs were taken by the Nikon Digital Sight DS-5M camera.

7.Results

Tpl2 downregulation/ ablation promotes lung carcinogenesis in an inflammation-independent way

Tpl2 levels are reduced in human lung tumors and associate with poor patient survival.

Figure R1: Inspection of transcriptome profiles registered in the Oncomine database indicates that expression of Tpl2 mRNA is approximately 4 times lower in human lung tumors compared to the normal bronchial epithelium.

Figure R2: Tpl2 levels are reduced in human lung tumors and associate with poor patient survival.

Tpl2 deficiency enhances susceptibility to experimental lung carcinogenesis.

Figure R3: Tpl2 suppresses lung cancer growth *in vivo*.

Table R1: Summary of histopathology data of Tpl2+/+ and Tpl2-/- mouse lung sections isolated at 4 and 6 months post-treatment with the chemical carcinogen urethane.

Figure R4: Tpl2 ablation promotes both tumor initiation and progression *in vivo.*

Figure R5: Tpl2 reduction directly favors cancer cell survival and prliferation.

The increased susceptibility of Tpl2 -/- mice in chemically induced lung carcinogenesis is inflammation independent.

Figure R6: Analysis of lymphoid cell populations in the spleens of Tpl2+/+ and Tpl2 -/- mice exposed to urethane.

Genetic and epigenetically-controlled mechanisms account for TPL2 down-regulation in human lung cancer

52% of the human lung cancer speciments inspected harbored LOH in *tpl2* locus.

Figure R7: Data mining of the genome-wide SNP analysis database indicates LOH in the Tpl2 locus in human lung cancer lines

Figure R8: Correlation between Tpl2 mRNA and protein levels in hu man lung tumor cell lines.

Figure R9: Allelic imbalance partly accounts for the down-regulation of TPL2 in hu-man lung cancer.

Figure R10: The Tpl2 promoter is not differentially methylated in hu man lung cancer vs normal lung tissue.

DNA hypomethylation-associated upregulation of miR-370 is in part respons-ible for Tpl2 downregulation

Table R2: sequence of microRNA-370

Figure R11: An epigenetic mechanism of Tpl2 expression regulation involving miR370.

Oncogenic Ras mediates down-regulation of TPL2.

Figure R12: Down-regulation of TPL2 levels by activated Ras associates with cell sur-vival and oncogenic transformation.

Down-regulation of TPL2 levels by activated RAS associates with cell survival and oncogenic transformation.

Figure R13: TPL2 antagonizes oncogenic Ras in transformed cells by modulating apoptosis induction in a p53-dependent manner.

Functional role of Tpl2 in lung cancer

TPL2 regulates p53 via a JNK-NPM signaling pathway.

Model R1: Tpl2 → JNK → NPM → p53 proposed pathway

Figure R14: Tpl2 leads to JNK activation, which is necessary and suffi cient for NPM transactivation and thus p53 stability.

Model R3: oncogenic / genotoxic stress → LOH, mir370, Ras^{mut} → Tpl2 regvgvbt43tgr3r duction →inhibition of JNK activation → inhibi tion of NPM transactivation → inhibition of p53 stabilisation → halt ed tumor suppression.

Tpl2 downregulation/ ablation promotes lung carcinogenesis in an inflammation-independent way

TPL2 levels are reduced in human lung tumors and associate with poor patient survival.

Our mining of transcriptome profiles (Beer et al., 2002) registered in the Oncomine database (www.oncomine.org) indicated that TPL2/MAP3K8 expression is reduced in lung tumors compared to normal bronchial epithelium (Figure R1). To validate this finding, we determined TPL2 mRNA levels by qPCR in 100 human lung carcinomas and paired adjacent normal tissue. The results (Fig. R2A) demonstrated a significant downregulation of TPL2 in the malignant tissue. Lower expression of TPL2 was confirmed in protein lysates from representative primary lung tumor biopsies compared to normal tissue (Fig. 1B). Investigating the clinical relevance of TPL2 mRNA expression in human lung carcinomas, we found no association with histology, TNM or differentiation status, age, gender and smoking history. Interestingly, however, low TPL2 expression correlated with reduced patient survival (Log rank test; p=0.009) (Fig. 1C). In line with this prediction was the inverse correlation between TPL2 mRNA levels and Ki67 proliferation index (Fig. 1D), indicating that reduced levels of TPL2 are associated with a more aggressive tumor phenotype. To exclude the possibility that this reduction associates with the presence of normal cells in the tumor stroma and confirm that it reflects changes in the malignant cells, we analyzed TPL2 by immunohistochemistry in 20 representative NSCLC specimens containing tumor and non-tumoral tissue. In non-tumoral bronchial epithelium TPL2 displayed a strong, homogeneous, cytoplasmic granular staining with a prominent apical orientation. In contrast, TPL2 expression in malignant cells was significantly reduced in a heterogeneous manner (Fig. 1E). Of note, tumor cells in one NSCLC case were found negative for TPL2 expression.

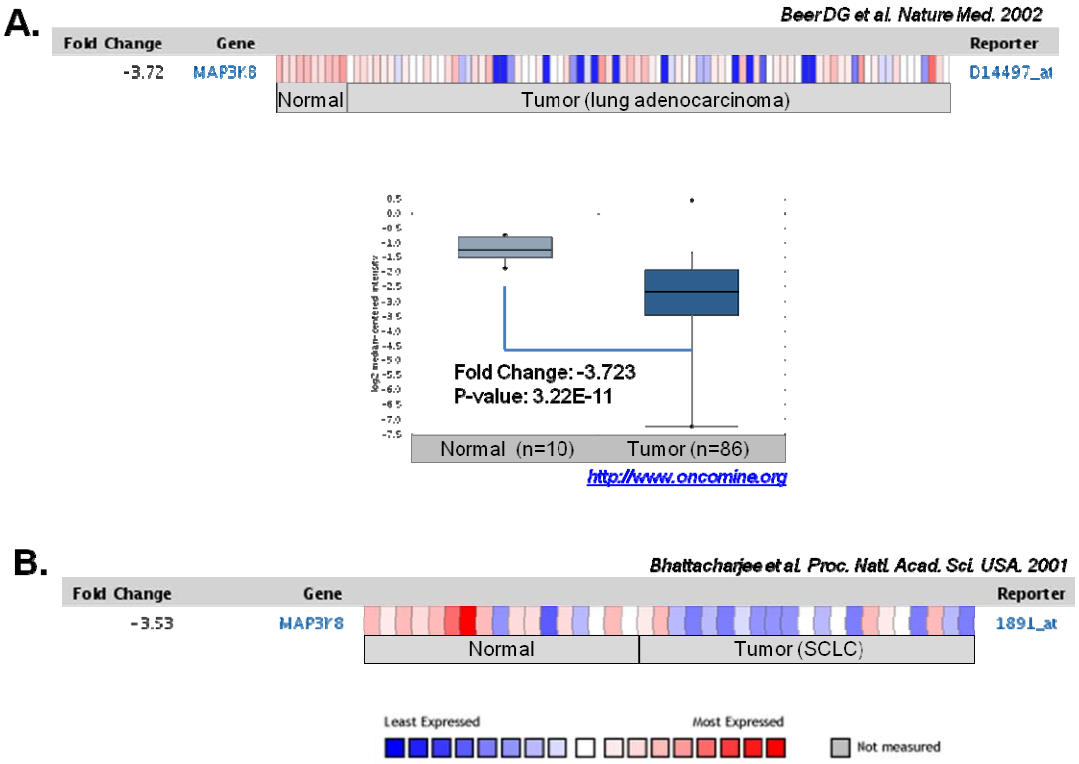

Figure R1: Inspection of transcriptome profiles registered in the Oncomine database indicates that expression of Tpl2 mRNA is approximately 4 times lower in human lung tumors compared to the normal bronchial epithelium. The Tpl2 profile in (A) has been retrieved from *Beer et al.* and in (B) from Bhattacharjee *et al.* . The log2 median-centered intensity of the tumor versus normal lung Tpl2 expression in the study by Beer *et al*. is also shown in (A).

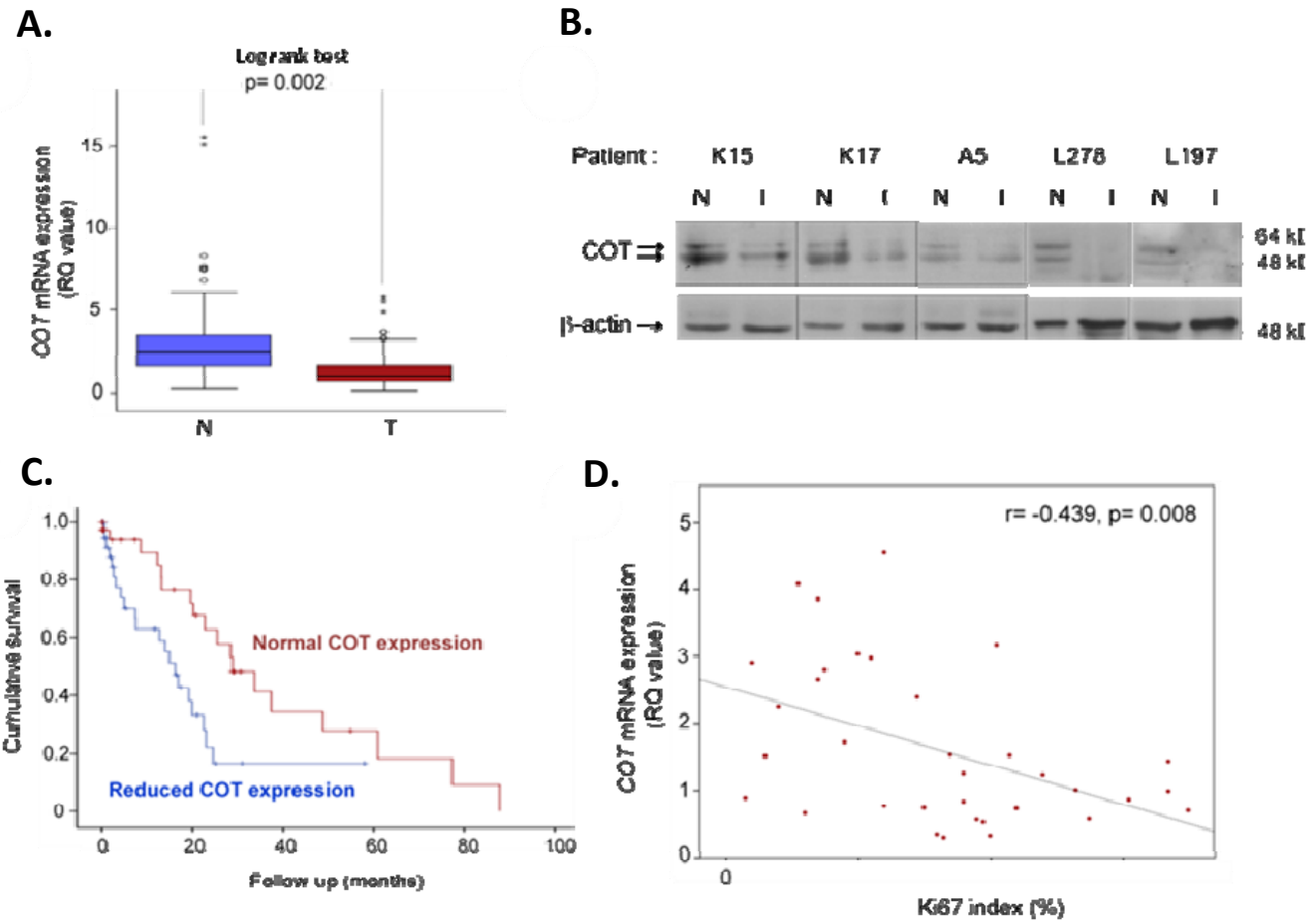
A.
Log rank test
p= 0.002
COT mRNA expression (RQ value)
15
10
5
0
N
T
B.
Patient :
K15
K17
A5
L278
L197
N
T
COT
β-actin
64 kD
48 kD
48 kD
C.
Cumulative survival
1.0
0.8
0.6
0.4
0.2
0
Normal COT expression
Reduced COT expression
0
20
40
60
80
100
Follow up (months)
D.
r= -0.439, p= 0.008
COT mRNA expression (RQ value)
5
4
3
2
1
0
0
Ki67 index (%)
E.
200uM
200uM

Figure R2: Tpl2 levels are reduced in human lung tumors and associate with poor patient survival. (A) Comparison of COT mRNA expression in the 100 available pairs of NSCLCs (37 adenocarcinomas and 63 squamous cell carcinomas) and adjacent normal lung tissues by qPCR. Results were normalized to the housekeeping β-actin gene and are expressed as relative quantification (RQ) values utilizing the IMR-90 human fibroblast cell line as calibrator. The reduction of COT mRNA levels in tumor (T) versus normal (N) tissue is profound (p value obtained from Wilcoxon's test). Stars and circles in the box plot indicate outliers. (B) COT protein levels are reduced in primary lung tumor samples compared to adjacent normal tissue. COT is expressed as 2 isoforms, noted with arrows, generated by the utilization of alternative translation start sites at methionine 1 and methionine 30. (C) Kaplan-Meier survival plot showing the cumulative survival of lung cancer patients who displayed more than 2-fold reduction in COT mRNA levels in their tumors compared to normal tissue and of patients with < 2-fold reduction in expression levels. Patients with low COT expression have median survival of 16.2 months (95% CI 11.8-20.6) compared to those with < 2-fold reduction who have median survival of 28.8 months (95% CI 18.4-39.2) (p= 0.009; Log rank test).(D) Inverse correlation between COT mRNA levels and Ki67 expression in cancer subset of NSCLC samples within this study (n= 35) for which Ki67 data were available (r coefficient and p values obtained from Spearman's correlation). (E) Representative immunohistochemical analysis showing a marked down-regulation of TPL2 expression in malignant cells (arrowheads) compared to normal epithelium (arrows) (400X final magnification, objective lense 40X/0.65). Bars correspond to 200μm.

TPL2 deficiency enhances susceptibility to experimental lung carcinogenesis.

On the basis of the aforementioned findings we experimentally evaluated the functional significance of TPL2 down-regulation in lung carcinogenesis. We thus examined the relative susceptibility of *tpl2*$^{-/-}$ *versus* *tpl2*$^{+/+}$ mice to develop lung tumors when exposed to urethane, a chemical carcinogen which induces lung tumors in mice that have similar molecular and histological features to human lung adenocarcinoma (Malkinson, 1992; To et al., 2008; Zhang et al., 2001). Interestingly, at 4 months post-treatment all *tpl2*$^{-/-}$ mice were found to already harbor multiple lung adenomas whereas only hyperplasia, without atypia, had developed in wild-type animals (Fig. R3A and R3B and Table R1). Ki67 staining was increased in hyperplastic lesions from *tpl2*$^{-/-}$ compared to *tpl2*$^{+/+}$ mice (Fig. R4A and R4B). At six months after urethane administration, lungs from *tpl2*$^{-/-}$ animals contained significantly higher numbers of adenocarcinomas compared to *tpl2*$^{+/+}$ mice. The tumors developed in *tpl2*$^{-/-}$ mice showed loss of normal alveolar architecture, increased nuclear/cytoplasmic ratio, cytologic atypia and invasion into adjacent bronchioles. Urethane-exposed *tpl2*$^{+/-}$ mice were also found to possess higher number of lung adenocarcinomas compared to wild-type animals. At 12 months, the effect of Tpl2 deficiency was macroscopically evident by the dramatic difference in the size of lung tumors developed in these animals (Fig. R4C), indicating that Tpl2 ablation not only influences the carcinogenic process at an early stage but also exerts positive effects during tumor growth. In agreement with the latter observation, urethane-induced mouse lung tumors express lower levels of Tpl2 than normal lung tissue (Fig. R5A) and the knock-down of TPL2 in A549 and H1299 human lung carcinoma cells increased their anchorage-independent growth *in vitro* (Fig. R5C).

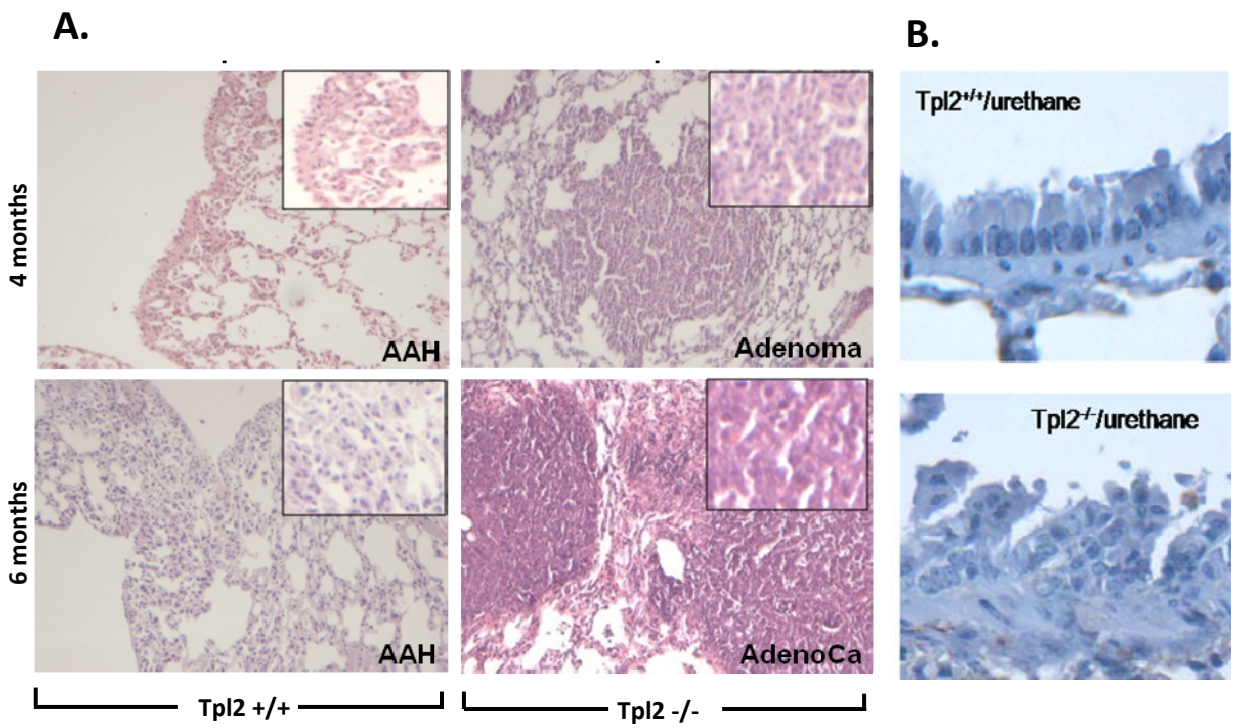

Number and histopathology of lesions per slide (n=5 animals per group)						
4 months	$Tpl2^{+/+}$	1 AAH	3 AAH	2 AAH	2 AAH	2 AAH
	$Tpl2^{-/-}$	6 Adenomas + Multiple foci of AAH	4 Adenomas + Multiple foci of AAH	2 Adenomas + Multiple foci of AAH	2 Adenomas + Multiple foci of AAH	6 Adenomas + Multiple foci of AAH
6 months	$Tpl2^{+/+}$	2 Adenomas + Multiple foci of AAH	Multiple foci of AAH	Multiple foci of AAH	1 AdenoCa + Multiple foci of AAH	1 AdenoCa – Multiple foci of AAH
	$Tpl2^{-/-}$	6 AdenoCa	5 AdenoCa	4 AdenoCa	> 10 AdenoCa	> 10 AdenoCa

Figure R3: Tpl2 suppresses lung cancer growth *in vivo*. (A) Hematoxylin and eosin staining of lung tissue isolated from $Tpl2^{+/+}$ and $Tpl2^{-/-}$ mice at 4 and 6 months post-treatment with the chemical carcinogen urethane. *AAH*: atypical adenomatous hyperplasia ; *AdenoCa*: adenocarcinoma. (B) The basal membrane and the alveolar architecture are significantly disrupted in $Tpl2^{-/-}$ mice sacrificed in less than 4 months post treatment, while wild type animals remain unaffected.

Table R1: Summary of histopathology data of $Tpl2^{+/+}$ and $Tpl2^{-/-}$ mouse lung sections isolated at 4 and 6 months post-treatment with the chemical carcinogen urethane. A total of 3 independent experiments using 15 $TPL2^{+/+}$ and 18 $TPL2^{-/-}$ mice have been performed with similar results.

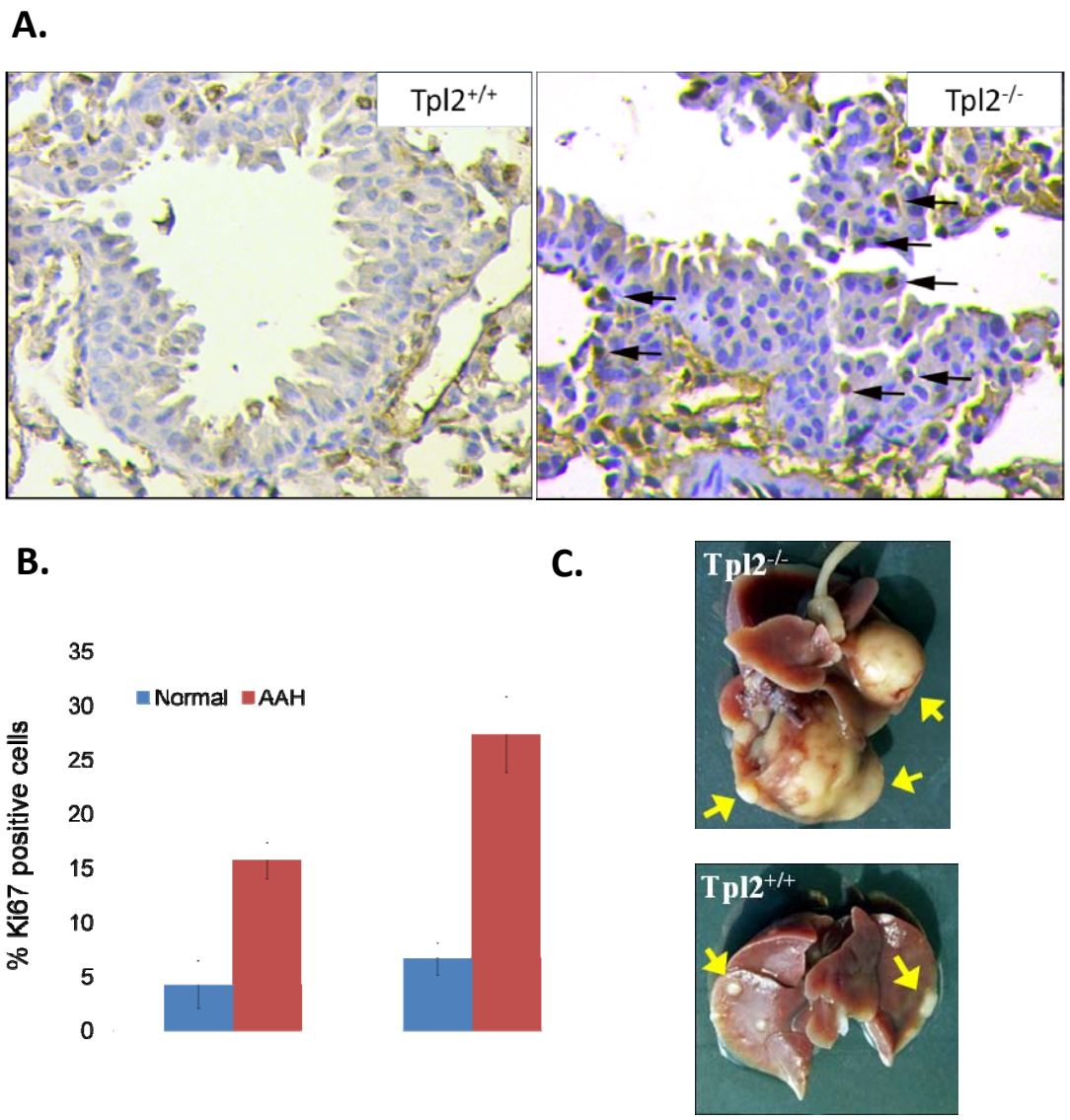

Figure R4: Tpl2 ablation promotes both tumor initiation and progression *in vivo*. (A) Representative immunohistochemical analysis of Ki67 status in hyperplastic lung tissue from urethane-treated $Tpl2^{+/+}$ and $Tpl2^{-/-}$ mice. The arrows show Ki67-positive cells. (B) Collective data of Ki67 staining in normal and AAH from urethane-treated $Tpl2^{+/}$+ and $Tpl2^{-/-}$ mice (n=4) Ki67 proliferation index is increased in hyperplastic $Tpl2^{-/-}$ compared to $Tpl2^{+/+}$ lung lesions. (C) Lungs of TPL2+/+ and TPL2-/- mice at 12 months post-treatment with the chemical carcinogen urethane. Representative tumors are shown by arrow.

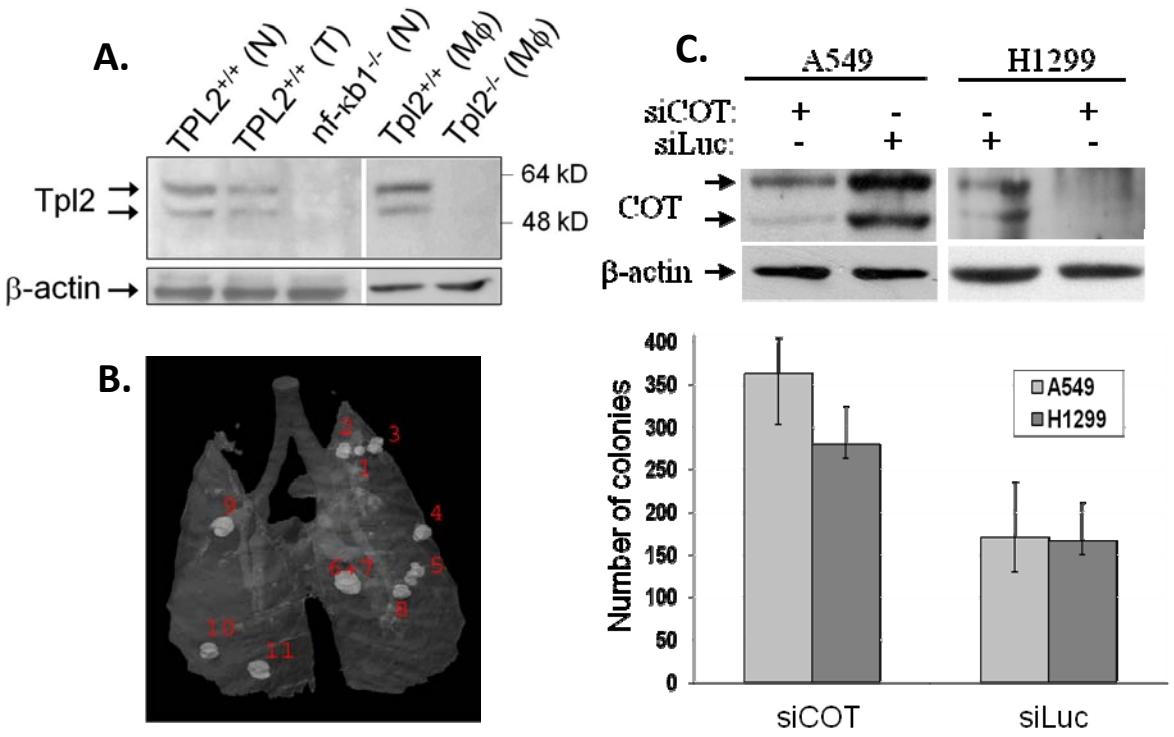

Figure R5: Tpl2 reduction directly favors cancer cell survival and proliferation. (A) Lung tumors dissected and pooled together (a.k.a. areas 1-11 as depicted in (B)) from wild type mice exposed to urethane display reduced Tpl2 levels compared to normal lung tissue. Lysates of tumor vs normal lung tissue from each mouse were analysed individually (C) Tpl2 knock-down enhances anchorage-independent growth in lung cancer cell lines, as determined by colony formation assays in soft agar. The number of colonies formed per 30000 plated cells was measured and presented in histogram form as the mean ±s.d. of three independent experiments.

The increased susceptibility of Tpl2 $^{-/-}$ mice in chemically induced lung carcinogenesis is inflammation independent

It has recently been reported that TPL2 ablation enhances inflammation induced by the Apc ^{min} mutation resulting in dramatic increase in polyposis (Serebrennikova et al., 2012). Theoretically, an exaggerated inflammatory response caused by urethane administration in TPL2$^{-/-}$ mice could be responsible for their increased susceptibility to lung tumorigenesis. We thus analyzed immune cell content in lungs, draining lymph nodes and spleens from TPL2$^{-/-}$ and TPL2$^{+/+}$ mice at 2 and 10 weeks following urethane treatment, that is during the early stages of adenoma development. Histological assessment of H&E-stained lung tissue sections did not reveal differences in immune cell load between mouse strains before or after urethane administration (data not shown). Flow cytometric analysis of CD3+, CD4+ and CD8+ T cells, macrophages and natural killer cells (NK) in the lungs and the draining lymph nodes and of CD3+, CD4+, CD8+, macrophages, NK, Gr1+/CD11b+ myeloid-derived suppressor cells (MDSCs), and natural killer T (NKT) cells in the spleens of Tpl2-/- and Tpl2+/+ mice exposed to urethane also did not reveal differences between strains (Fig. R6). Finally, quantification of soluble mediators of inflammation, such as TNF, IL-10 and IL-6 in blood serum by ELISA did not reveal any changes above background level in either TPL2$^{-/-}$ or TPL2$^{+/+}$ mice (data not shown). Collectively, these data do not indicate an association between TPL2 status and systemic or local inflammation at early stages of urethane-induced lung carcinogenesis.

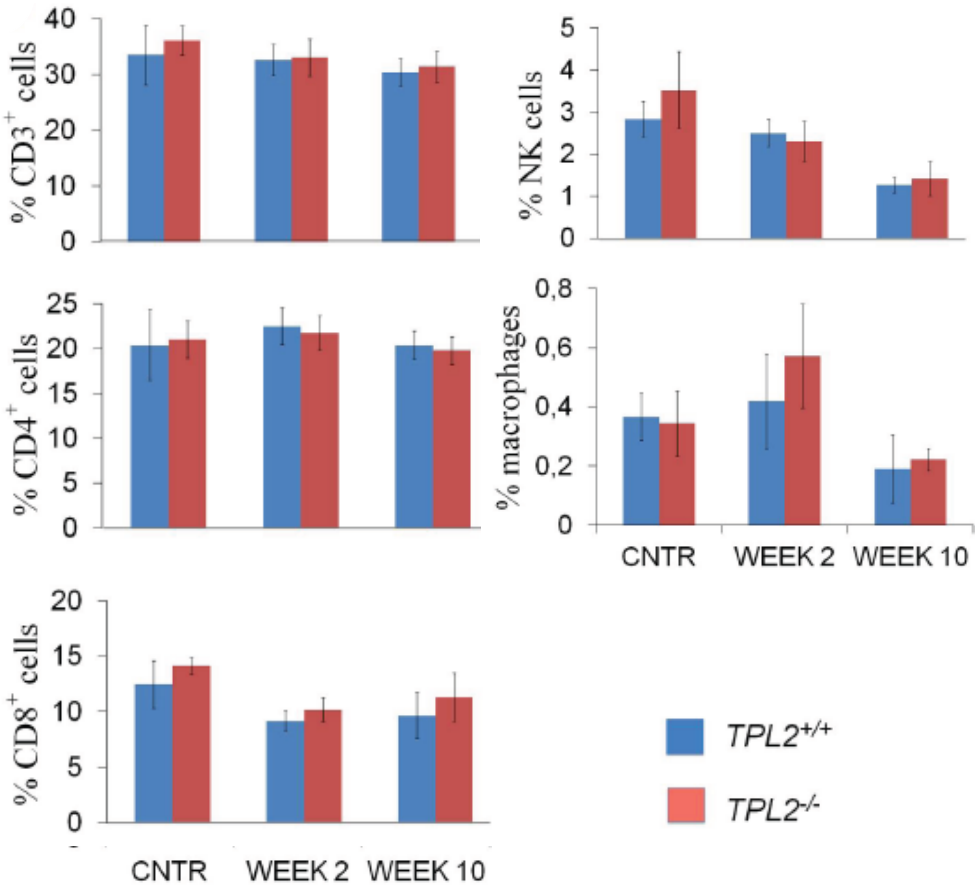

Figure R6: Representative results after analysis of lymphoid cell populations in the spleens of Tpl2+/+ and Tpl2 -/- mice exposed to urethane. No statistically significant difference between the two strains was revealed.

Genetic and epigenetically-controlled mechanisms account for TPL2 down-regulation in human lung cancer.

52% of the human lung cancer speciments inspected harbored LOH in *tpl2* locus

The aforementioned observations suggest that TPL2 may physiologically function as a suppressor of lung carcinogenesis and warranted further investigations into the molecular mechanisms that account for the reduced TPL2 expression in human lung cancer. Our inspection of the genome-wide loss of heterozygosity (LOH) and DNA copy number database of tumor cell lines available at the Wellcome Trust Sanger Institute Cancer Genome Project web site http://www.sanger.ac.uk/ genetics/CGP) indicated allelic imbalance at the MAP3K8 locus (chr 10p11.23) in a number of human lung cancer cell lines (Fig. R7) which correlated with reduced TPL2 expression (Fig. R8). We thus employed fluorescent microsatellite analysis at four positions on the TPL2 gene (two internal and two flanking; Fig. R9A), to assess loss of heterozygosity (LOH) in the available set of human primary lung tumors. Allelic imbalance at the TPL2 locus was observed in a significant 52% of primary lung tumors (Fig. R9B). Cases with LOH displayed lower TPL2 mRNA levels although at borderline significance (Mann-Whitney test p=0.051; Fig. R9C), indicating contribution of additional mechanisms affecting TPL2 expression in lung cancer.

We thus surmised that TPL2 could be subject to epigenetic silencing, as observed in certain tumor suppressor genes. The presence of a putative CpG island located at positions -973 to +981 relative to the TPL2 transcription start site (Fig. R9A), indicated by *in silico* analysis (http://cpgislands.usc.edu/) was in line with this notion. However, the results of Pyrosequencing methylation analysis (PMA) demonstrated absence of TPL2 promoter methylation in either normal or malignant tissue (Fig. R10).

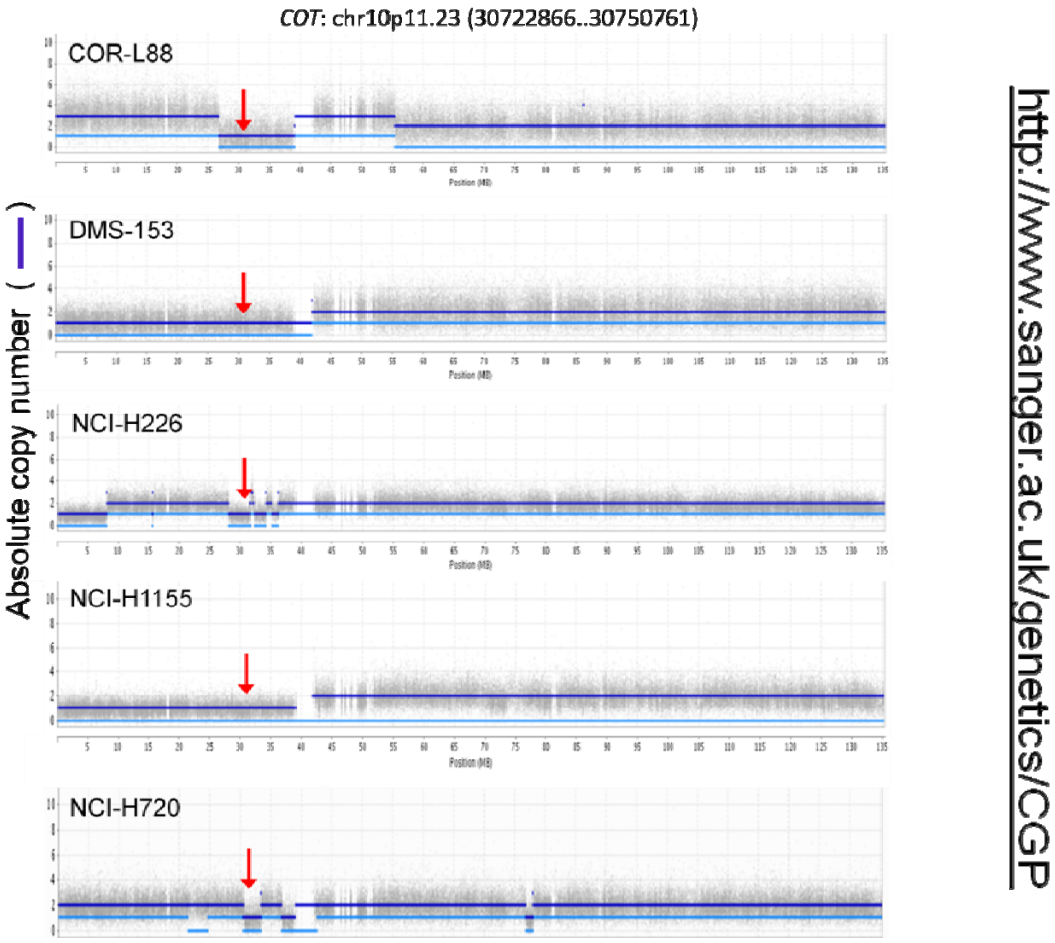

Figure R7: Data mining of the genome-wide SNP analysis database indicates LOH in the Tpl2 locus in human lung cancer lines. Red arrows correspond to the area of the genome where the *tpl2* locus is mapped. Absolute copy number < 2 means loss of the allele mapped in the specific locus of the genome.

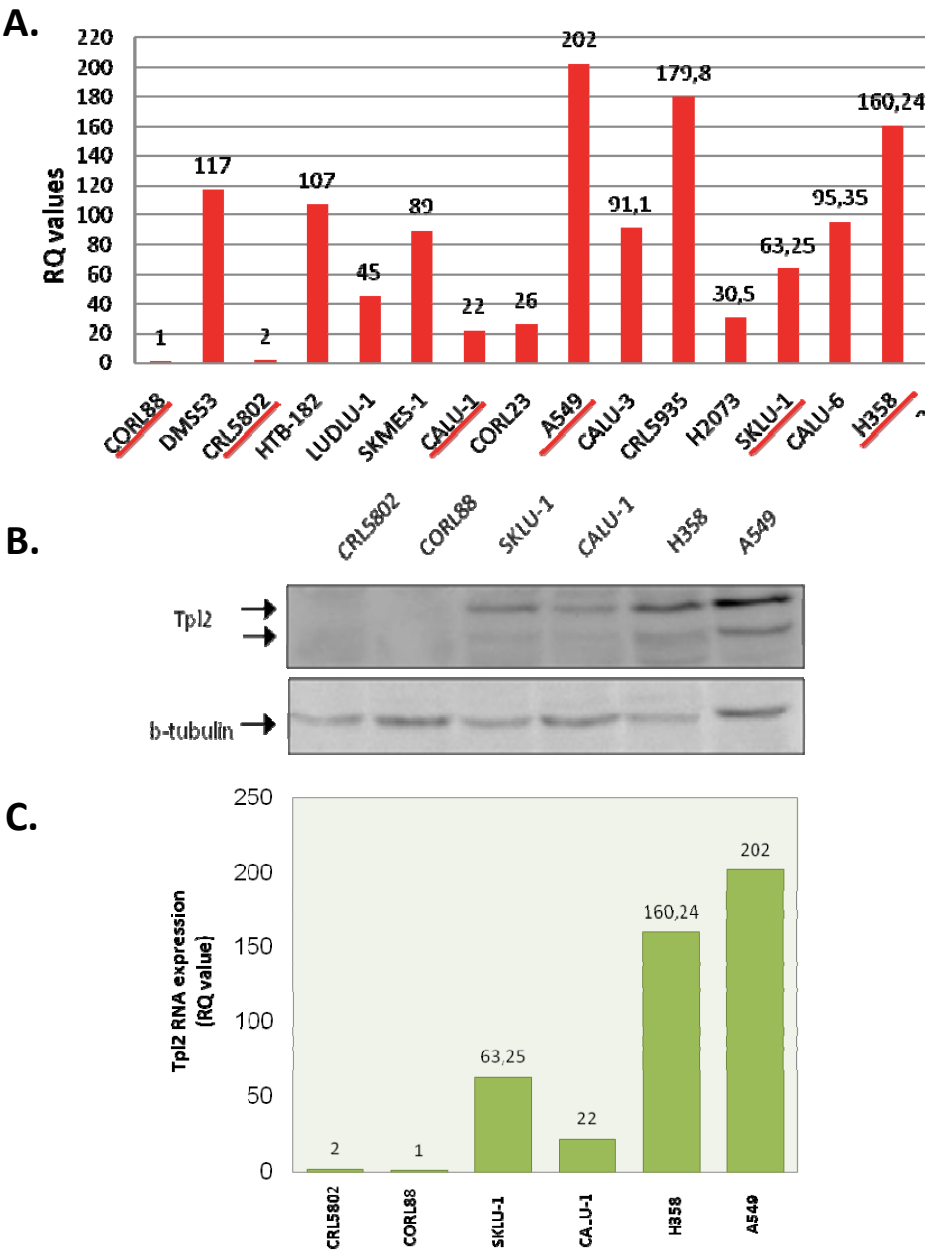

Figure R8: Correlation between Tpl2 mRNA and protein levels in human lung tumor cell lines. (A) mRNA from human lung cancer cell lines available in our lab was subjected to Real Time PCR and representative lines with low, median and high expression of Tpl2 were chosen to be further analysed. (B) CRL5802, CORL88, CALU-1, SKLU-1, H358 and A549 cells were then subjected to immunoblotting using anti- Tpl2 or anti-β-tubulin antibodies. (C) RNA from the same cultures was subjected to Real Time PCR to confirm that protein levels correlate directly with the transcriptional changes of tpl2 expression levels.

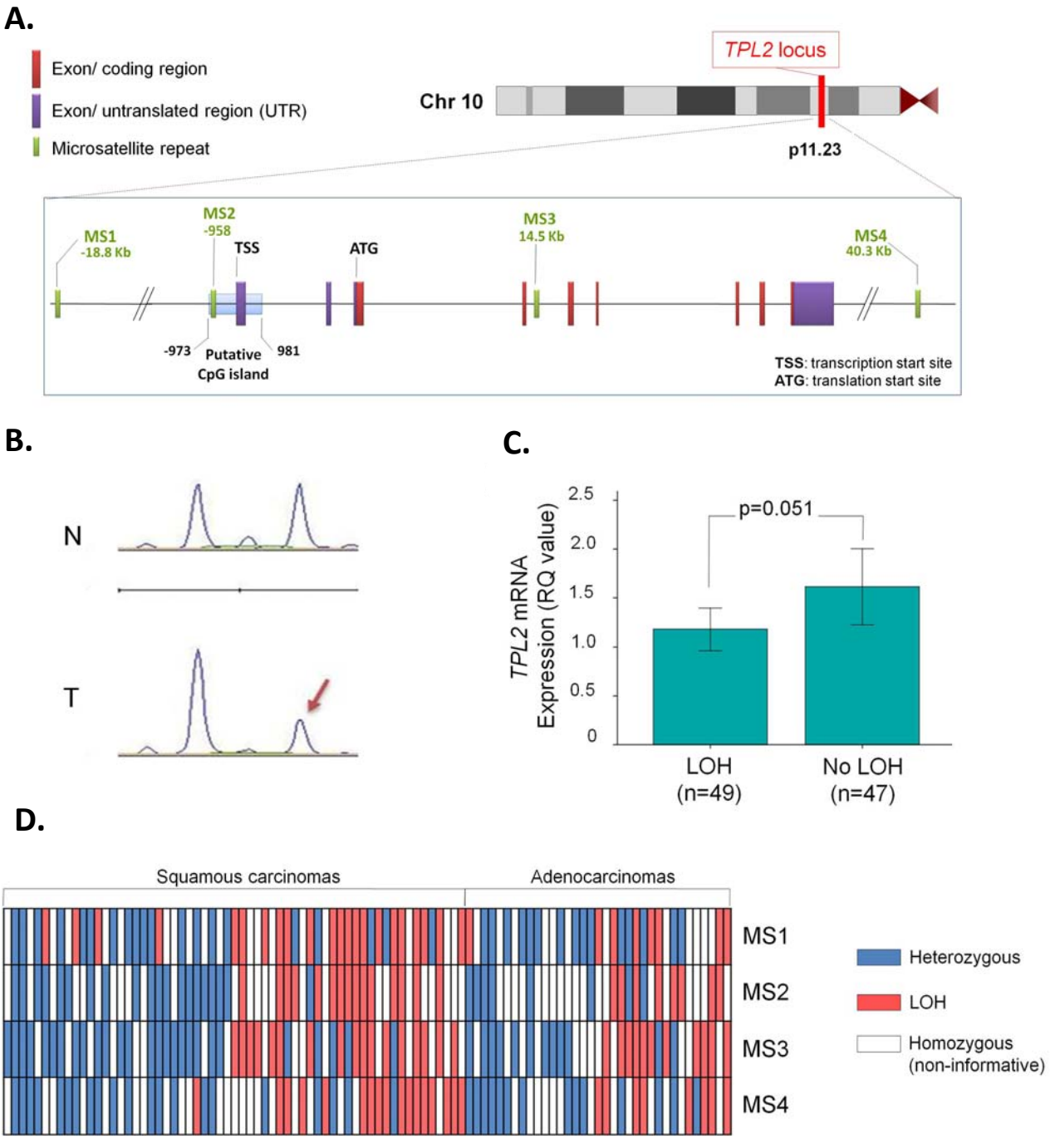
A.
Exon/ coding region
Exon/ untranslated region (UTR)
Microsatellite repeat
TPL2 locus
Chr 10
p11.23
MS1
-18.8 Kb
MS2
-958
TSS
ATG
MS3
14.5 Kb
MS4
40.3 Kb
-973
Putative
CpG island
981
TSS: transcription start site
ATG: translation start site
B.
N
T
C.
TPL2 mRNA
Expression (RQ value)
2.5
2.0
1.5
1.0
0.5
0
p=0.051
LOH
(n=49)
No LOH
(n=47)
D.
Squamous carcinomas
Adenocarcinomas
MS1
MS2
MS3
MS4
Heterozygous
LOH
Homozygous
(non-informative)

Figure R9: Allelic imbalance partly accounts for the down-regulation of TPL2 in human lung cancer. (A) Schematic representation of the *tpl2* locus on human chromosome 10 and relative positions of microsatellite repeats MS1, MS2, MS3 and MS4, used as markers for detection of LOH. Numbering refers to the transcription start site, TSS. The position of a putative CpG island in the TPL2 promoter is also indicated. (B) Example of allelic imbalance / loss of heterozygocity (LOH) in the tpl2 locus in a pair of normal and tumor sample from a lung cancer patient. Electropherogram traces for the normal (N) and tumor (T) genotypes are shown, with the two peaks representing the two alleles. An allelic ratio cut-off level of 0.75 (25% reduction of one allele intensity) was used to score LOH (Liloglou et al., 2001). (C) Expression of Tpl2 RNA, measured by Real Time PCR, in relation to allelic imbalance (LOH) in the *tpl2* locus. (D) Collective data of allelic imbalance analysis of the Tpl2 locus in 96 pairs of NSCLC and normal adjacent tissue using the 4 microsatellite markers shown in (A). Red boxes represent LOH, blue boxes show retention of heterozygosity and white boxes represent homozygous (non-informative) loci.

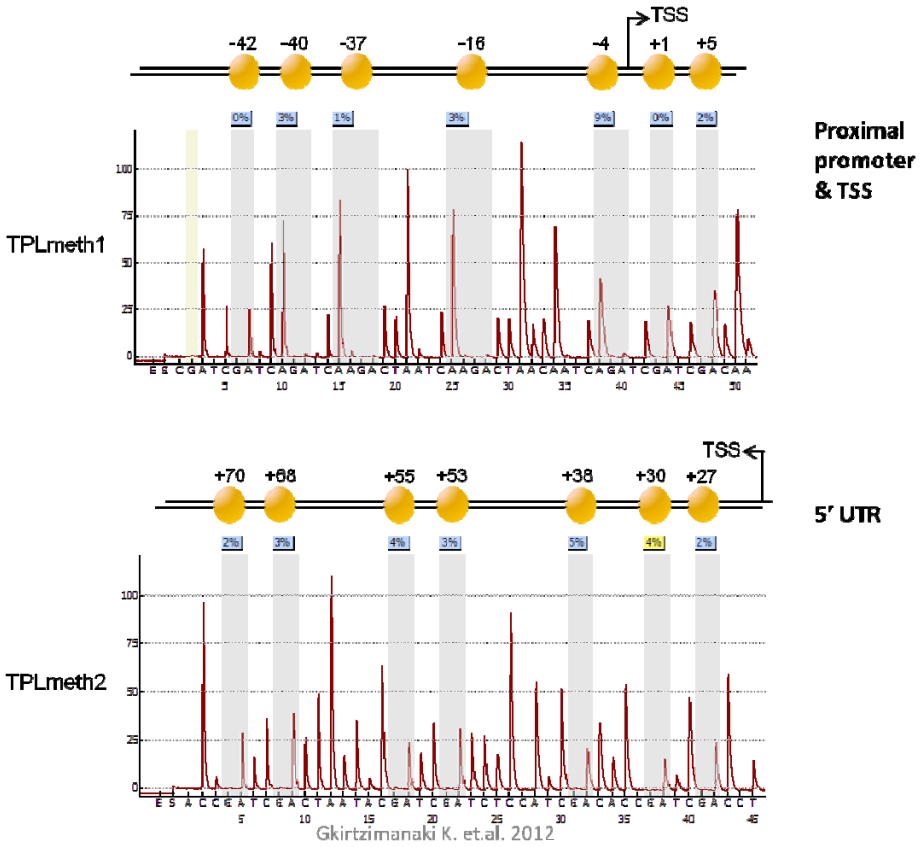

Figure R10: The Tpl2 promoter is not differentially methylated in human lung cancer vs normal lung tissue. Representative pyrograms from Pyrosequencing-Methylation Analysis of the Tpl2 promoter in a human lung tumor sample. One assay (Tplmeth1) covered the transcription start site (TSS) and proximal promoter (CpGs at positions -42, -40, -37, -16, -4, 1 and 5 relative to TSS) as schematically represented by the orange circles in the upper panel. The second assay (Tplmeth2) covered CpGs within the 5'UTR (positions 27, 30, 38, 53, 55, 68 and 70 relative to TSS). The letters below each graph represent the dispensation order (E, enzyme mix; S, substrate; A, G, C, T, nucleotides). Grey lanes indicate the CpG sites that were analyzed and the y-axis depicts the light levels produced following the incorporation of each nucleotide.

DNA hypomethylation-associated upregulation of miR-370 is in part responsible for Tpl2 downregulation

Recent work has indicated that miR-370 (Table R2) negatively regulates the expression of TPL2 in malignant cholangiocytes (Meng et al., 2008). In agreement with this report, we have found that transfection of miR-370 in A549 lung cancer cells results in a time-dependent reduction in TPL2 protein levels (Fig. R11A). To determine if this pathway could operate in human lung cancer, we evaluated miR-370 expression by Real Time PCR in the lung cancer set under evaluation. This analysis demonstrated that miR-370 levels are elevated in the malignant *versus* normal tissue (Wilcoxon's test p=0.001) (Fig. R11B). As miR-370 is embedded in a CpG island and is subject to epigenetic control (Meng et al., 2008), we evaluated by PMA the methylation status of this region (Fig. R11C). The results showed a statistically significant reduction of miR-370 methylation levels in the tumor tissue ($p<0.001$; Wilcoxon's test; Fig. R11D). Moreover, this reduction closely correlated with the methylation status of the retrotransposable LINE-1 element (Chalitchagorn et al., 2004; Daskalos et al., 2009) suggesting that miR-370 hypomethylation in NSCLC is most likely the result of global genome hypomethylation (Spearman's $r=0.621$, $p<10^{-6}$; Fig. R11E).

A.

```
      agaa        ca gu   u    u   a ag
agacag    gccaggu  c  cuc gcag uac c  c
||||||    |||||||  |  ||| |||| ||| |  u
ucuguc    uggucca  g  ggg cguc gug g  c
      ----        ag ug   u    c   a ca
```

B.

48 - gccugcuggggguggaaccuggu – 69

Table R2: hsa-microRNA 370. (A) Stem loop sequence of pre-mir370. Pink coloured bases correspond to the mature sequence. (B) mature mir370 sequence

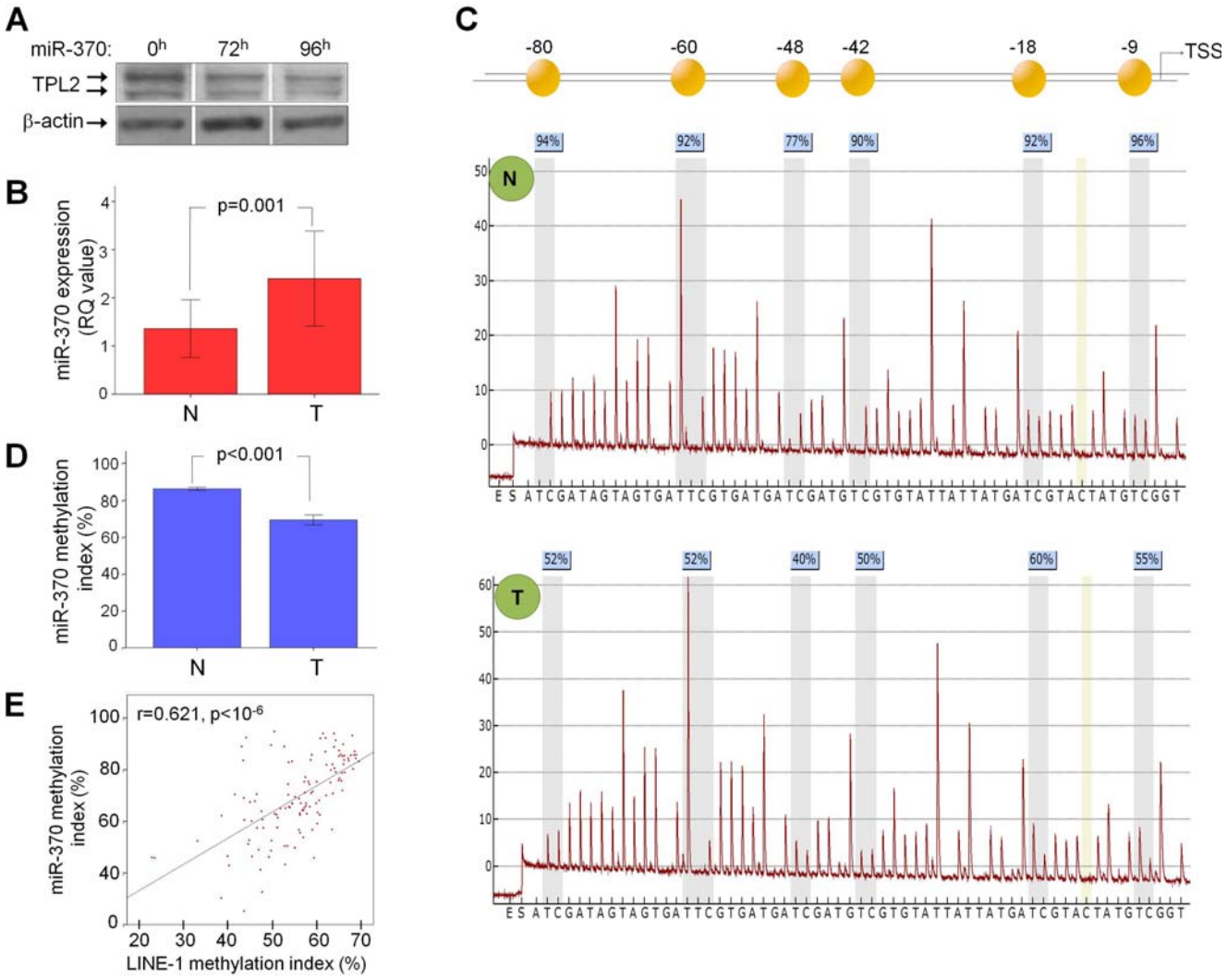
A
miR-370:
0h
72h
96h
TPL2
β-actin
B
miR-370 expression (RQ value)
p=0.001
N
T
C
-80
-60
-48
-42
-18
-9
TSS
94%
92%
77%
90%
92%
96%
N
E S A T C G A T A G T A G T G A T T C G T G A T G A T C G A T G T C G T G T A T T A T T A T G A T C G T A C T A T G T C G G T
52%
52%
40%
50%
60%
55%
T
E S A T C G A T A G T A G T G A T T C G T G A T G A T C G A T G T C G T G T A T T A T T A T G A T C G T A C T A T G T C G G T
D
miR-370 methylation index (%)
p<0.001
N
T
E
miR-370 methylation index (%)
r=0.621, p<10-6
LINE-1 methylation index (%)

Figure R11: An epigenetic mechanism of Tpl2 expression regulation involving miR370. (A) Tpl2 protein levels are reduced in A549 lung cancer cells transfected with miR-370 for different time points. Results are representative of 3 independent experiments. (B) Expression of miR-370 (RQ value) was measured in 96 carcinoma specimens and paired normal lung tissue by Real Time PCR, demonstrating significantly higher miR-370 levels in the tumor tissues (Wilcoxon's test, p=0.001). (C) Representative pyrograms from Pyrosequencing-Methylation Analysis of the miR-370 locus in a lung tumor (T) and corresponding normal (N) adjacent tissue. Grey areas indicate the CpG sites that were analyzed at positions -9, -18, -42, -48, -60 and -80 relative to the transcription start site (TSS) of the pre-miRNA sequence, which are schematically represented by orange circles in the upper panel. The letters below each graph represent the dispensation order (E, enzyme mix; S,substrate; A, G, C, T, nucleotides). The y-axis depicts the light levels produced following the incorporation of each nucleotide. Percentages indicate the extent of bisulfate conversion of C to T; unmethylated C should be fully converted to T. (D) The miR-370 locus is significantly (Wilcoxon's test, $p<0.001$) hypomethylated in lung tumors (T) compared to normal lung epithelium (N). The methylation index of the miR-370 locus was calculated from Pyrosequencing-Methylation Analysis of 96 carcinoma specimens and paired normal lung tissue and is depicted in histogram form as methylation index. (E) Correlation between the methylation indexes of miR-370 and LINE-1. Methylation of miR-370 correlates with LINE-1 element methylation index suggesting that miR370 hypomethylation in NSCLC is a result of global genome hypomethylation (r coefficient and p value obtained from Spearman's correlation).

Oncogenic Ras mediates down-regulation of TPL2

Activating mutations in ras genes have been recorded in 25-40% of lung tumors. A recent study has shown that oncogenic RAS stimulates a TBK1-dependent signaling pathway *in vitro* which leads to reduction in p105 NF-κB1 protein levels (Barbie et al., 2009). NFκB1 physically interacts with and regulates the stability of TPL2 as highlighted by the fact that TPL2 is absent in macrophages (Beinke et al., 2003; Waterfield et al., 2003) and lung tissue (Fig. S1) from NFKB1-/- mice. We therefore reasoned that by modulating NF-κB1 levels, activated RAS may impact on TPL2 expression. We have explored this association in A549 and H1299 human lung carcinoma cells stably transfected with HA-tagged H-RASG12V expression vector or infected with K-RASG12V-expressing retrovirus, respectively. Interestingly, we found that the expression of either form of oncogenic RAS mediates dramatic down-regulation of TPL2 concomitant to reduction in NF-κB1 expression (Fig. 5A & 5B). The lower protein levels of TPL2 in A549/H-RASG12V clones associated with impaired ERK phosphorylation in response to TNF (Fig. 5C), a hallmark of TPL2 signaling defect in macrophages (Eliopoulos et al., 2003). The functional link between reduced TPL2 expression and defective ERK activation was confirmed in parental A549 cells transfected with TPL2 siRNA. As shown in Figure 5D, the RNAi-mediated knock-down of TPL2 impaired TNF induced ERK phosphorylation. Stable expression of mutated RAS also diminished TPL2 mRNA levels (Fig. 5E), suggesting that oncogenic RAS signaling may affect TPL2 gene transcription in addition to protein stability. In line with this observation, stable or transient expression of oncogenic forms of K-RAS or H-RAS in transformed (Fig. 5F) and non-transformed (Fig. 5G) cells suppressed TPL2 promoter activity. We furthermore observed reduced levels of TPL2 (Fig. 5H) in lysates from mouse lungs expressing K-RASG12D (Schramek et al., 2011) suggesting that oncogenic RAS may also down-regulate TPL2 expression *in vivo*.

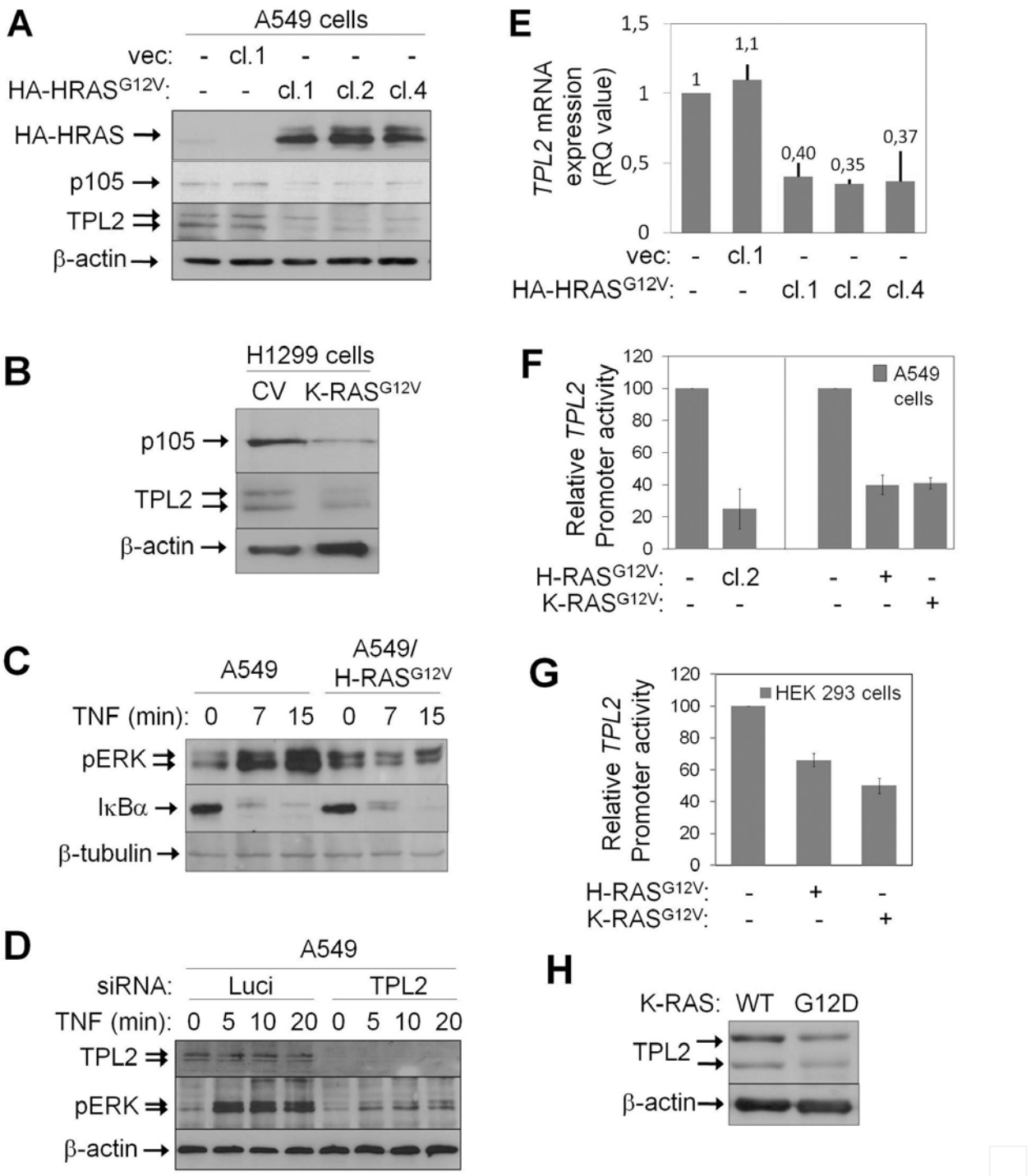
A
A549 cells
vec: - cl.1 - - -
HA-HRAS^{G12V}: - - cl.1 cl.2 cl.4
HA-HRAS
p105
TPL2
β-actin
B
H1299 cells
CV K-RAS^{G12V}
p105
TPL2
β-actin
C
A549
A549/ H-RAS^{G12V}
TNF (min): 0 7 15 0 7 15
pERK
IκBα
β-tubulin
D
A549
siRNA: Luci TPL2
TNF (min): 0 5 10 20 0 5 10 20
TPL2
pERK
β-actin
E
TPL2 mRNA expression (RQ value)
1,5
1
0,5
0
1
1,1
0,40
0,35
0,37
vec: - cl.1 - - -
HA-HRAS^{G12V}: - - cl.1 cl.2 cl.4
F
Relative TPL2 Promoter activity
120
100
80
60
40
20
0
A549 cells
H-RAS^{G12V}: - cl.2 - + -
K-RAS^{G12V}: - - - - +
G
Relative TPL2 Promoter activity
120
100
80
60
40
20
0
HEK 293 cells
H-RAS^{G12V}: - + -
K-RAS^{G12V}: - - +
H
K-RAS: WT G12D
TPL2
β-actin

Figure R12: Down-regulation of TPL2 levels by activated Ras associates with cell survival and oncogenic transformation. (A) Stable transfection of oncogenic ras leads to down-regulation of p105 NF-κB1 and TPL2 expression. Lysates from parental (lane 1), control vector (vec)-transfected (lane 2) or three HAtagged H-RASG12V – transfected A549 clones (lanes 3-5) were immunoblotted with antibodies against HA, NF-κB1, TPL2 or β-actin, as indicated. (B) Expression of K-RASG12V in retrovirus-transduced H1299 lung cancer cells results in reduced p105 NF-κB1 and TPL2 levels. CV; control virus. (C) Defective TNF-induced ERK activation in lung cancer cells expressing oncogenic ras. A549/H-RASG12V cells were stimulated with 25ng/ml TNF and lysates were analyzed for IκBα degradation, a hallmark of canonical NF-κB signaling, ERK phosphorylation (pERK) and β-tubulin expression by immunoblot. Results are representative of 3 independent assays. (D) The knock-down of TPL2 in A549 cells results in defects in TNF-induced ERK response cells were transfected with siRNA targeting Tpl2 or control siRNA and then stimulated with TNF as described in (C). Results are representative of at least 3 independent experiments. (E) TPL2 mRNA expression, easured by qPCR, is reduced in the H-RASG12V – expressing A549 clones described in (A). (F) Stable expression of H-RASG12V (clone 2) or transient transfection of H-ASG12Vor K-RASG12Vin A549 tumor cells results in suppression of tpl2 promoter activity measured by luciferase reporter assays. (G) Transient expression of H-RASG12V or K-RASG12V in non-tumorigenic 293 cells results in suppression of TPL2 promoter activity. HEK 293 cells were co-transfected with 50ng of a reporter construct containing the Luciferase gene under the control of the TPL2promoter, a Renilla reporter to control for transfection efficiency and 30ng of ras vectors as indicated. The mean relative luciferase values (ratio of Luciferase to Renilla activities ± SD) from 4 independent experiments ware determined and expressed relative to control vector which was given the arbitrary value of 100. (H) TPL2 levels are reduced in lysates from mouse lungs expressing K-RASG12D.

Down-regulation of TPL2 levels by activated RAS associates with cell survival and oncogenic transformation.

To assess the biological significance of the impact of oncogenic RAS on TPL2 levels, we transiently introduced a TPL2-expressing vector in A549/HRas G12V cell clones which display strong suppression of endogenous TPL2 (Fig. 5A), and observed decreased cell proliferation (not shown) and elevated levels of apoptosis (Fig. 6A). TPL2-mediated cytotoxicity required caspase activation as it was abolished by treatment with the pan-caspase inhibitor zVAD-fmk. Moreover, the pro-apoptotic effect of TPL2 on RASG12V – transfected cells correlated with increased p53 accumulation (Fig. 6B) which was alleviated by the RNAi-mediated knock-down of p53 (Fig. 6A). These data suggest that TPL2 antagonizes oncogenic RAS in transformed cells at least partly by modulating p53 activity and apoptosis induction. We next investigated whether TPL2 also counteracts the oncogenic effects of K-RASG12V in non transformed cells. Immortalized 208F fibroblasts were transfected with K-RASG12V in the presence or absence of a TPL2 expression vector and cell transformation was quantified by anchorage-independent growth in soft agar. As shown in Figure 6C, expression of TPL2 reduced the number of foci formed by activated K-RAS by 60% whereas a kinase-inactive TPL2 mutant had no effect. To determine if the observed novel link between TPL2 and p53 applies to genotoxic insults in addition to oncogenic stress, A549 cells were transfected with siRNA targeting TPL2 and then exposed to the DNA damaging agent cis-platin. The knock-down of TPL2 was found to significantly attenuate p53 accumulation and to increase the survival of drug-treated cells (Fig. 6D & 6E). Moreover, the expression of two known p53 regulated genes, cdkn1a encoding p21 and bax, was attenuated in lungs from TPL2-/- mice exposed to urethane suggesting that TPL2 may also influence the p53 pathway *in vivo* (Fig. 6F). Next we examined the mechanism by which TPL2 impacts on p53 levels.

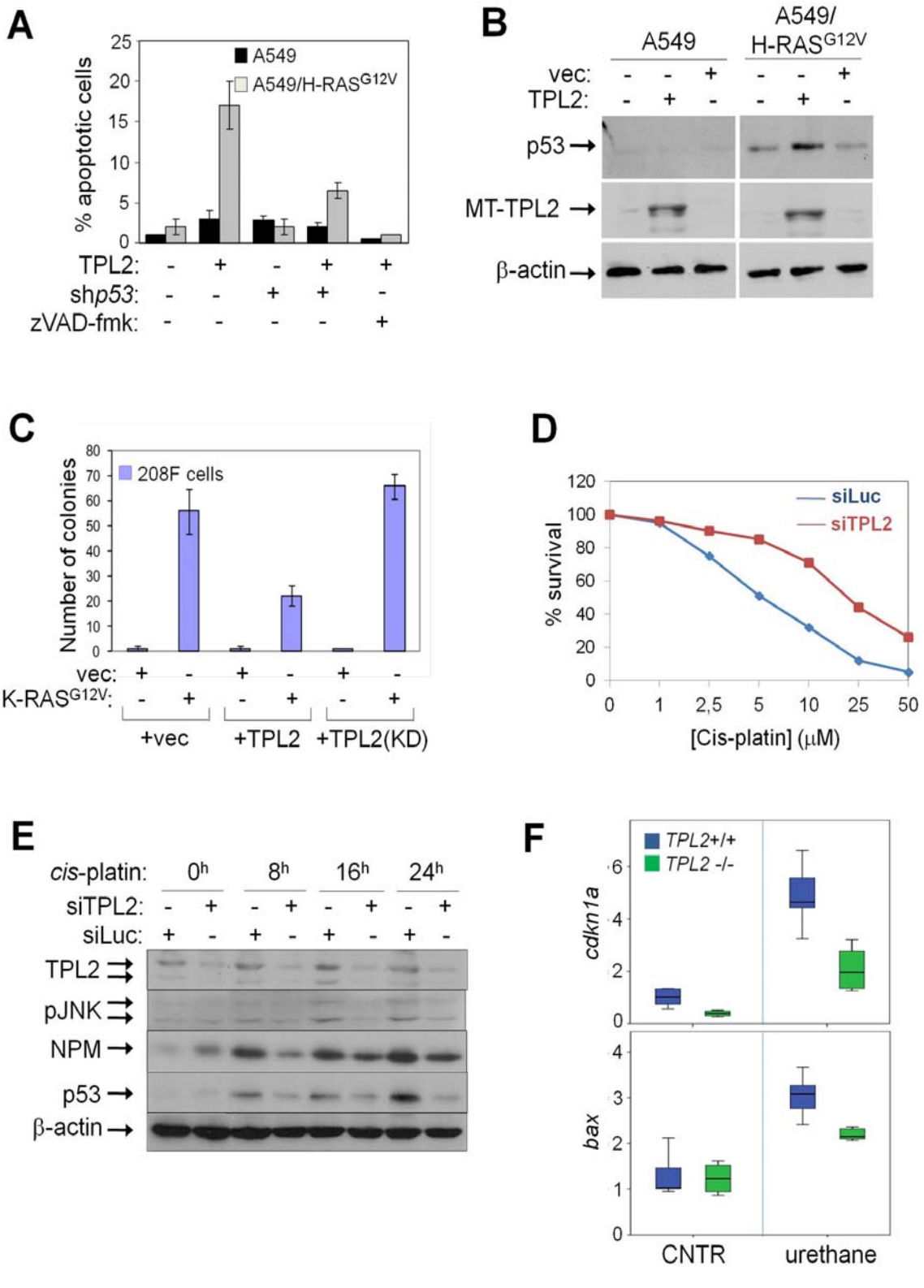
A
% apoptotic cells
A549
A549/H-RASG12V
TPL2:
shp53:
zVAD-fmk:
B
A549
A549/ H-RASG12V
vec:
TPL2:
p53
MT-TPL2
β-actin
C
Number of colonies
208F cells
vec:
K-RASG12V:
+vec
+TPL2
+TPL2(KD)
D
% survival
siLuc
siTPL2
[Cis-platin] (μM)
E
cis-platin:
0h
8h
16h
24h
siTPL2:
siLuc:
TPL2
pJNK
NPM
p53
β-actin
F
TPL2+/+
TPL2 -/-
cdkn1a
bax
CNTR
urethane

Figure R13: TPL2 antagonizes oncogenic Ras in transformed cells by modulating apoptosis induction in a p53-dependent manner. (A) Quantitative determination of apoptosis in A549 and A549/H-RASG12V clone 2 cells was performed 24 hours post-transfection with Myc epitope-tagged (MT) TPL2 in the presence or absence of shRNA targeting p53. The TPL2-mediated A549/H-rasG12V cell death was abolished by the pan-caspase inhibitor zVAD-fmk (15µM). Mean values (± sd) from 3 independent experiments are shown. (B) TPL2 expression results in increased accumulation of p53 in A549/H-RASG12V cells. A549 and A549/H-RASG12V clone 2 cells were transfected with MT-TPL2 or control vector (vec) and analyzed for the expression of TPL2, p53 and β-actin, as indicated. Similar results were obtained with A549/H-RASG12V clone 3 cells (data not shown). (C) TPL2 suppresses oncogenic RAS-mediated transformation. Immortalized 208F fibroblasts were transfected with K-rasG12V in the presence or absence of TPL2 or a kinase-inactive TPL2 mutant (KD), plated in soft agar and the number of foci formed 2 weeks later was measured and presented in a histogram form. Data are the mean ± s.d. of three independent experiments. (D) Knock-down of TPL2 in A549 cells confers resistance to cis-platin induced cytotoxicity. Cells were transfected with TPL2 or luciferase siRNA and then treated with 25µM cis-platin for 48 hours. Cell survival was determined by using the MT conversion assay. Data shown are the average of triplicates from a representative experiment. Three additional experiments were performed with similar results. (E) Knock-down of TPL2 reduces the NPM and p53 induction and the extent of JNK phosphorylation in cis-platin treated A549 cells. Cells were transfected with siRNAs targeting TPL2 or the unrelated luciferase (Luc) gene and then exposed to 25µM cis-platin for various timeintervals. Lysates were analyzed by immunoblot as indicated. Results are representative of at least 4 independent experiments. (F) TPL2 impacts on p53 in vivo. To quantitatively assess p53 activation in vivo, RNA was isolated from TPL2+/+ and TPL2-/- mouse lungs at 2 weeks following urethane treatment and used to determine the levels of two established p53-regulated genes, cdkn1a encoding p21 and bax by qPCR. The y-axis represents the RQ values determined as described in Figure 1A.

Functional role of Tpl2 in lung cancer

TPL2 regulates p53 via a JNK-NPM signaling pathway.

Nucleophosmin (NPM/B23) is a DNA damage-response gene (Grisendi et al., 2006; Wu and Yung, 2002) which negatively regulates the interaction of p53 with HDM2 and thus controls p53 stability (Colombo et al., 2002; Kurki et al., 2004). After confirming these findings, we found that the knock-down of NPM in A549 cells reduces p53 accumulation following cisplatin treatment. Our *in silico* analysis of the NPM promoter (Chan et al., 1997) indicated the presence of multiple binding sites of cJun/AP1, a transcription factor that is activated by the JNK signaling pathway. As TPL2 directly phosphorylates MKK4/7, the JNK kinases (Das et al., 2005; Salmeron et al., 1996), we surmised that TPL2 may influence the p53 response through JNK-mediated NPM transactivation. Indeed, TPL2 knock-down attenuated both JNK phosphorylation and NPM upregulation in cisplatin-treated cells (Fig. R13E). Conversely, the overexpression of TPL2 in A549/H-RASG12V clones stimulated JNK phosphorylation and led to increased NPM levels concomitant to p53 stabilization (Fig. R14A). To provide further support for the association between JNK signaling and NPM transactivation, A549 cells were exposed to the JNK inhibitor SP600125 (Bennett et al., 2001) prior to cisplatin treatment. As shown in Figures R14B and C, inhibition of JNK activity diminished the effect of cisplatin on NPM protein and mRNA expression levels. Collectively, these observations identify TPL2 as a novel physiological regulator of p53 that operates through a JNK-NPM signaling pathway (Model R1).

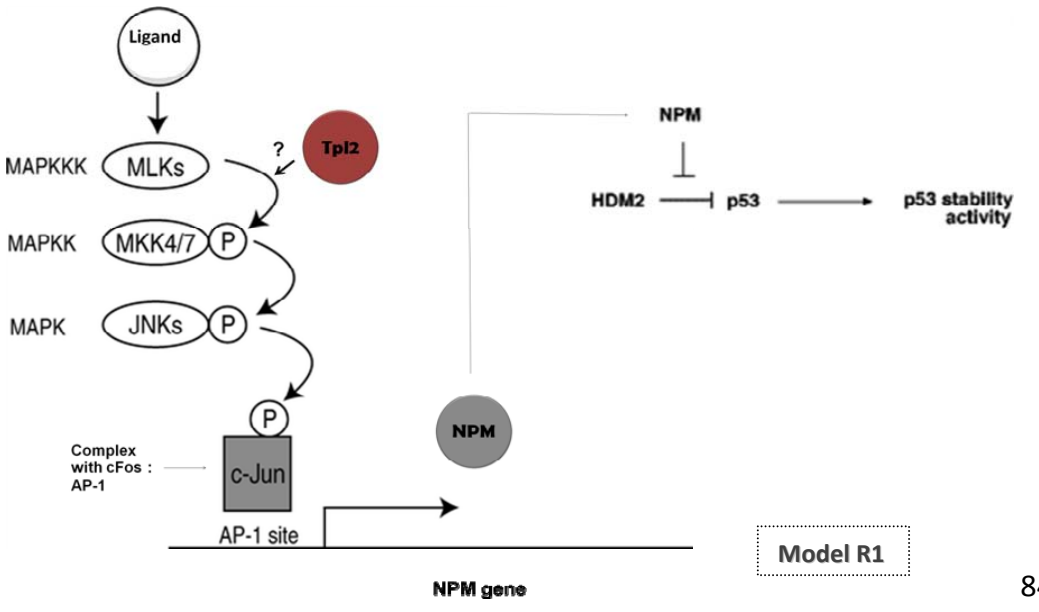

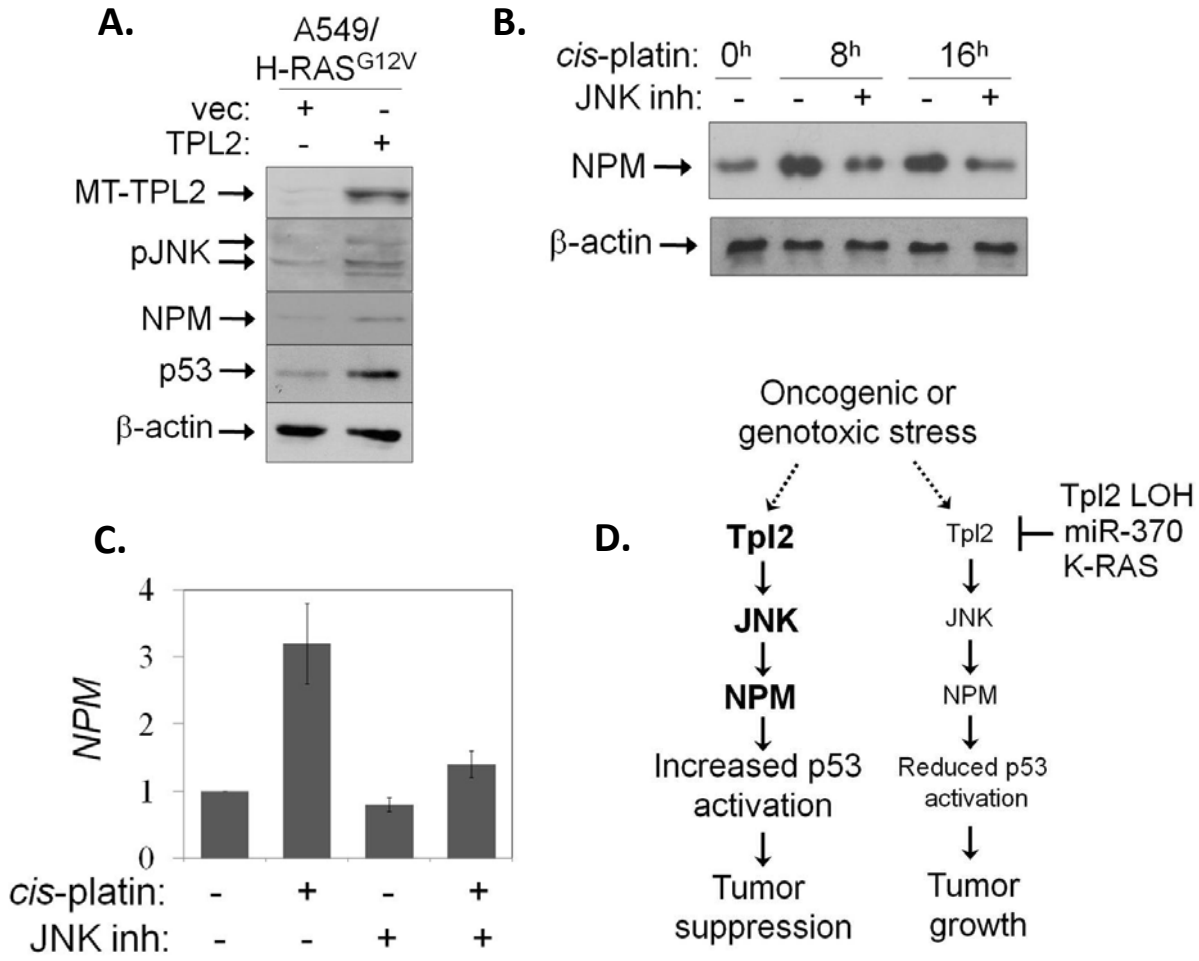
A.
A549/
H-RAS^{G12V}
vec: + -
TPL2: - +
MT-TPL2
pJNK
NPM
p53
β-actin
B.
cis-platin: 0h 8h 16h
JNK inh: - - + - +
NPM
β-actin
C.
NPM
4
3
2
1
0
cis-platin: - + - +
JNK inh: - - + +
D.
Oncogenic or
genotoxic stress
Tpl2
JNK
NPM
Increased p53
activation
Tumor
suppression
Tpl2
JNK
NPM
Reduced p53
activation
Tumor
growth
Tpl2 LOH
miR-370
K-RAS

Figure R14: Tpl2 leads to JNK activation, which is necessary and sufficient for NPM transactivation and thus p53 stability. (A) TPL2 expression results in increased accumulation of p53 and NPM and elevated phosphorylation of JNK in A549/H-RASG12V cells. A549/H-RASG12V clone 2 cells transfected with MT-TPL2 or control vector (vec), were analyzed for the expression of TPL2, NPM, p53, phosphorylated JNK and β-actin, as indicated. (B) Treatment of A549 cells with the JNK inhibitor (inh) SP600125 reduces the cis-patin induced NPM upregulation. Immunoblot results are representative of 3 independent experiments. Treatment with the MEK inhibitor PD98059 had no effect on NPM levels (not shown). (C) SP600125 (20μM) inhibits the cis-patin induced upregulation of NPM mRNA, measured by qPCR. (D) (Model R2) On the basis of the data presented in this PhD thesis, we propose that TPL2 suppresses lung carcinogenesis by mediating JNK-dependent NPM upregulation and p53 accumulation in response to DNA damage induced by genotoxic agents or oncogenic stress. The downregulation of TPL2 as a result of genetic or epigenetic aberrations (LOH, overexpression of miR-370 or oncogenic Ras signaling) diminishes JNK and p53 responses leading to reduced cell death and accelerated cell transformation.

8.Discussion

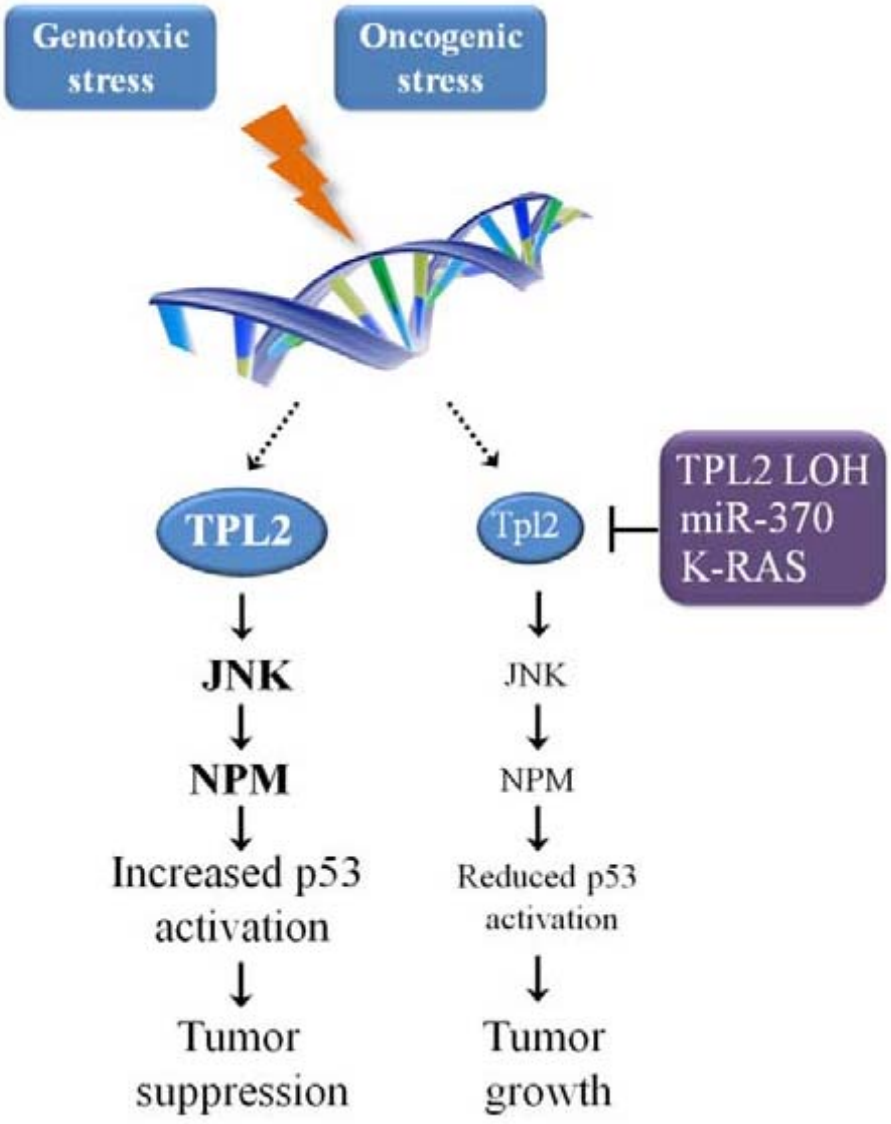

Data presented in this study delineate a novel function for TPL2 in lung cancer. Based on the analysis of primary human lung tissue and established cell lines, we propose that the operation of multiple genetic (LOH, ras mutations) and epigenetic (miR-370 hypomethylation) aberrations leading to loss of TPL2 in lung cancer is not coincidental and points to a previously unappreciated significant role for the TPL2 pathway in this type of malignancy. This is corroborated by the poor prognosis of lung cancer patients carrying reduced TPL2 tumor levels and the reverse association of TPL2 expression with Ki67 index. Further evidence is provided by the demonstration that TPL2-deficient mice display increased susceptibility to chemically-induced lung carcinogenesis during both the initiation and progression of the disease. This finding, coupled with the recently published work showing that TPL2 ablation enhances the oncogenic potential of the Apc^{min} mutation in the gut (Serebrennikova et al., 2012), indicates that TPL2 may have a broader role as negative regulator of carcinogenesis. However, whereas the enhancement of polyposis in $Apc^{min/+/}$ $TPL2^{-/-}$ mice was found to be partially (but not exclusively) hematopoietic cell-driven, the *in vitro* and *in vivo* data shown in this thesis suggest that TPL2 also confers significant effects on epithelial cells in response to genotoxic and oncogenic insults. In agreement with these observations, urethane is known to metabolize to mutagenic mediators in Clara and type II alveolar epithelial cells, the progenitors of lung adenomas (Meuwissen and Berns, 2005; Tuveson and Jacks, 1999), and the accelerated early lesions observed in $TPL2^{-/-}$ mice occur in the absence of heightened systemic or local inflammatory response compared to wild-type animals.

Human lung cancer is characterized by extensive alterations of microRNA expression and allelic imbalance which may influence cancer-related genes and thus impact on patient survival (Herbst et al., 2008; Yanaihara et al., 2006). Known targets of loss of heterozygocity (LOH) in lung cancer include tumor suppressor genes such as RASSF1A, p16 and p53 (reviewed in Herbst et al., 2008). Our data demonstrate for the first time that the TPL2 gene locus is subject to LOH in a human malignancy resulting in reduced TPL2 expression (Fig. 3). LOH and diminished TPL2 levels were also noted in established lung cancer cell lines such as COR-L88, NCI-H226 and NCI-H720 (our unpublished observations).

The molecular mechanisms accounting for the altered expression of microRNAs in lung cancer are unclear (Herbst et al., 2008; Yanaihara et al., 2006). Our finding that miR-370 is upregulated in primary lung tumors and is closely associated with reduced TPL2 levels (Fig. 4) expands our appreciation of the *in vivo* effects of microRNAs on gene expression. Moreover, our data reveal a novel mechanism of *in vivo* regulation of microRNA expression influenced by global DNA hypomethylation.

Aberrant methylation of CpG dinucleotides is a commonly observed epigenetic modification in human malignancies and includes both global genomic hypomethylation and hypermethylation of gene promoter regions. The latter is often associated with transcriptional silencing of tumor suppressors, such as p16, FHIT, APC and DAPK in lung cancer (Herbst et al., 2008). Despite the presence of a rich CpG island in the TPL2 promoter, we found no evidence of it being differentially methylated in tumor versus normal lung tissue. However, we propose that TPL2 gene expression may indirectly be affected by global genomic DNA hypomethylation through the epigenetic regulation of miR-370. Indeed, a close association between miR-370 and LINE-1 methylation indexes was noted in primary human lung tumors (Fig. 4E). Hypomethylation of LINE-1 serves as a surrogate marker of global methylation status (Chalitchagorn et al., 2004), correlates with genomic instability (Daskalos et al., 2009) and has been identified as independent marker of poor prognosis in early stage NSCLC (Saito et al., 2010). It is thus tempting to speculate that the down-regulation of TPL2 associated with miR-370 hypomethylation may impact on the early stages of the disease in humans, similar to the effects of TPL2 ablation on urethane-induced lung cancer initiation in the mouse.

Clinical studies have shown that 25-40% of human NSCLC carry activating mutations in K-ras (Slebos et al., 1990) and infrequently H-ras (Sugio et al., 1992) genes which represent an early event in lung carcinogenesis and mark poor prognosis. Experimental evidence supporting the role of this gene in lung cancer comes from transgenic mice expressing mutated K-ras in which atypical adenomatous hyperplasia and adenocarcinoma develop (Meuwissen and Berns, 2005; Tuveson and Jacks, 1999). K-ras is also mutated in a proportion of urethane-induced lung tumors (Massey et al.,

1995). In these models, oncogenic RAS promotes carcinogenesis through a signaling pathway which critically depends on c-RAF (Blasco et al., 2011) and NF-κB (Meylan et al., 2009; Stathopoulos et al., 2007) and is inhibited by wild-type RAS (Zhang et al., 2001). *In vitro* analyses based on RNAi screens also point to NF-κB and the atypical IκB kinase family member TBK1 as positive regulators of survival and tumorigenicity of human lung cancer cells bearing mutated K-ras (Barbie et al., 2009). Data presented in this thesis show that elevated levels of oncogenic RAS mediate the downregulation of TPL2 *in vitro* (Fig. 5A & 5B) and *in vivo* (Fig. 5H) and that co-expression of these genes is incompatible for optimal tumor cell survival and malignant transformation *in vitro* (Fig.6A & 6C). These findings thus identify TPL2 as a novel physiological antagonist of activated RAS in both transformed and non-transformed cells and provide a mechanistic explanation for the down-regulation of TPL2 expression by oncogenic RAS (Fig. 7). Which is the molecular pathway that modulates the antagonistic relationship between RAS and TPL2?

Our results suggest that in response to oncogenic stress or genotoxic agents, TPL2 participates in JNK-dependent up-regulation of NPM, thereby influencing p53 stabilization (Fig. 7). P53 is a major factor in preventing transformation and has a crucial role in tumor suppression in part by regulating apoptosis, a barrier to cancer (Levine and Oren, 2009). We show that low TPL2 levels lead to diminished JNK and p53 responses, reduced cell death and accelerated malignant transformation. In line with these *in vitro* findings, TPL2 ablation in mice associates with diminished p53 responses to the mutagen urethane, as determined by the impaired upregulation of two p53 target genes, bax and cdkn1a (Fig. 6F). Collectively, these data define TPL2 as a regulator of the p53 pathway and provide a mechanistic explanation for the operation of multiple pathways leading to down-regulation of TPL2 in human lung cancer (Fig.1).

However, TPL2 may have a broader role in dictating the balance between cell survival and death, thereby influencing tumorigenicity and/or the response to therapy. Indeed, an RNAi screen performed in breast cancer cells has shown that reduced TPL2 expression associates with resistance to TRAIL-induced apoptosis (Ovcharenko et al., 2007), a p53-independent process (Chinnaiyan et al., 2000). Our findings, coupled

with a recent study describing a lung tumor suppressor function for the JNK kinase MKK7 (Schramek et al., 2011) expand our appreciation of the impact of MAP3 kinases in malignancy providing a telling example of how tumor cells usurp MAP kinase pathways which lower intrinsic barriers to malignant transformation. Finally, our results suggest that re-evaluation of Tpl2 inhibitors in therapeutic regimes for chronic inflammatory diseases may be required (149), as inhibition of Tpl2 may lead to reduced p53 response and increased susceptibility to malignancy.

The rationale presented in this thesis highlights the importance of the secondary tumor suppressors (such as Tpl2 as proved here) and their regulators in carcinogenesis: When the cell senses an inappropriate proliferative signal, (as it would if its endogenous Ras gene were mutated to an oncogenic form), it responds by activating its tumor-suppressor activity. Cancer cells that have inactivated tumor suppressor responses (as in the case of Tpl2 in the lungs), outgrow inside the population of tumor cells and eventually dominate in a local tissue environment. Accordingly, multistep tumor progression can be portrayed as a succession of clonal expansions, each of which is triggered by the chance acquisition of an enabling “mutant” genotype. This selective plasticity acquired by neoplastic cells is one of the major drawbacks in the cancer’s therapeutic targeting. Most of the targeted cancer drugs developed to date have been deliberately directed toward specific molecular targets that are involved in one way or another in enabling particular capabilities (mentioned as hallmarks during the “introduction”). Such specificity of action has been considered a virtue, as it presents inhibitory activity against a target while having, in principle, relatively fewer off-target effects and thus less nonspecific toxicity. In fact, each of the core hallmark capabilities is regulated by partially redundant signaling pathways. Consequently, a targeted therapeutic agent inhibiting one key pathway in a tumor may not completely shut off a hallmark capability, allowing some cancer cells to survive with residual function until they or their progeny eventually adapt to the selective pressure imposed by the therapy being applied. Such adaptation, which can be accomplished by mutation, epigenetic reprogramming, or remodeling of the stromal microenvironment, can reestablish the functional capability, permitting renewed tumor growth and clinical relapse. Given that the number of parallel signaling path-

ways supporting a given hallmark must be limited, it may become possible to target all of these supporting pathways therapeutically, thereby preventing the development of adaptive resistance. Taking this into account, the elucidation of the molecular mechanisms regulating Tpl2 expression during lung carcinogenesis may lead us one step closer to a wiser therapeutic approach, targeting efficiently cancer-driven activation of pathway redundancy.

9. Abbreviations

Tpl2	Tumor progression locus 2
COT	Cancer Osaka Thyroid
JNK	c-Jun N-terminal Kinase
NPM	Nucleophosmin
MAPK	Mitogen Activated Protein Kinase
ERK	Extracellular signal-regulated kinase
ABIN2	A20-binding inhibitor of NFκB
NFκB	Nuclear factor κ-light-chain-enhancer of activated B cells
IκB	Inhibitor of κB
IKK	IκB Kinase
GPCR	G-protein coupled receptor
TLR	Toll like Receptor
TNF	Tumor Necrosis Factor
IL-#	Interleukin- #
MS	Microsattelite
MSI	Microsattelite Instability
LOH	Loss of Heterozygosity
TSS	Transcription Start Site
Mir370	microRNA 370
NSCLC	Non Small Cell Lung Cancer
SCLC	Small Cell Lung Cancer
MDM2	Murine double minute 2
HDM2	Human double minute 2

10.References

1. Raven, RW. The Theory and Practice of Oncology, (Parthenon, 1990).
2. Weinberg, RA. The biology of cancer, (Garland Science, 2007).
3. Hecht, S. S., Upadhyaya, P. & Wang, M. Reactions of alpha-acetoxy-N-ni troso-pyrrolidine and crotonaldehyde with DNA. IARC Sci Publ, 147-154 (1999).
4. Zhong, Y., Carmella, S. G., Upadhyaya, P., Hochalter, J. B. et al. Immediate consequences of Cigarette Smoking: Rapid Formation of Polycyclic Aromatic Hydrocarbon Diol Epoxides. Chem Res Toxicol (2011).
5. Pleasance, E. D., Cheetham, R. K., Stephens, P. J., McBride, D. J. et al. A comprehensive catalogue of somatic mutations from a human cancer genome. Nature 463, 191-196 (2010).
6. Dalgliesh, G. L., Furge, K., Greenman, C., Chen, L. et al. Systematic sequencing of renal carcinoma reveals inactivation of histone modifying genes. Nature 463, 360-363 (2010).
7. Campbell, P. J., Yachida, S., Mudie, L. J., Stephens, P. J. et al. The patterns and dynamics of genomic instability in metastatic pancreatic cancer. Nature 467, 1109-1113 (2010).
8. TheTCGA, consortium Comprehensive genomic characterization defines human glioblastoma genes and core pathways. Nature 455, 1061-1068 (2008).
9. Ding, L., Getz, G., Wheeler, D. A., Mardis, E. R. et al. Somatic mutations affect key pathways in lung adenocarcinoma. Nature 455, 1069-1075 (2008).
10. Brigham, B. A., Bunn, P. A., Jr., Minna, J. D., Cohen, M. H. et al. Growth rates of small cell bronchogenic carcinomas. Cancer 42, 2880-2886 (1978).
11. Wilke, H., Achterrath, W., Schmoll, H. J., Gunzer, U. et al. Etoposide and split-dose cisplatin in small-cell lung cancer. Am J Clin Oncol 11, 572-578 (1988).
12. Collins, L. G., Haines, C., Perkel, R. & Enck, R. E. Lung cancer: diagnosis and management. Am.Fam. Physician 75, 56-63 (2007).
13. Khuder, S. A. Effect of cigarette smoking on major histological types of lung cancer: a metaanalysis.Lung Cancer 31, 139-148 (2001).

14. Scott, W. J., Howington, J., Feigenberg, S., Movsas, B. et al. Treatment of non-small cell lung cancer stage I and stage II: ACCP evidence-based clinical practice guidelines (2nd edition).Chest 132, 234S-242S (2007).
15. Miyoshi J, Higashi T, Mukai H, Ohuchi T, Kakunaga T. Structure and transforming potential of the human cot oncogene encoding a putative protein kinase. Mol Cell Biol. 11, 4088-4096 (1993).
16. Patriotis C, Makris A, Bear SE, Tsichlis PN. Tumor progression locus 2 (Tpl-2) encodes a protein kinase involved in the progression of rodent T cell lymphomas and in T cell activation. Proc Natl Acad Sci. 90, 2251-2255 (1993).
17. Lund AH, Turner G, Trubetskoy A, et al. Genome-wide retroviral insertional tagging of genes involved in cancer in Cdkn2a-deficient mice. Nat Genet 32, 160-165 (2002).
18. Mikkers H, Allen J, Knipscheer P, et al. High throughput retroviral tagging to identify components of specific signaling pathways in cancer. Nat Genet 32, 153-159 (2002).
19. Erny KM, Peli J, Lambert JF, Muller V, Diggelmann H. Involvement of the TPL-2/COT oncogene in MMTV tumorigenesis.Oncogene 13, 2015-2020 (1996).
20. Ceci JD, Patriotis CP, Tsatsanis C, et al. Tpl-2 is an oncogenic kinase that is activated by carboxy-terminal truncation. Genes Dev 11, 688-700 (1997).
21. Julian Downward et.al. Targeting Ras signaling pathways in cancer therapy Nat Rev Cancer. 3, 11-22 (2003).
22. Increasing complexity of Ras signaling.Campbell SL, Khosravi-Far R, Rossman KL, Clark GJ, Der CJ.Oncogene. Sep 17, 17 (1998)
23. Understanding Ras: 'it ain't over 'til it's over'.Shields JM, Pruitt K, McFall A, Shaub A, Der CJ. Trends Cell Biol. 10, 147-54 (2000)
24. MET amplification leads to gefitinib resistance in lung cancer by activating ERBB3 signaling.Engelman JA, Zejnullahu K, Mitsudomi T, Song Y, Hyland C, Park JO, Lindeman N, Gale CM, Zhao X, Christensen J, Kosaka T, Holmes AJ, Rogers AM, Cappuzzo F, Mok T, Lee C, Johnson BE, Cantley LC, Jänne PA.Science. 316, 1039-43 (2007).

25. Clinical resistance to STI-571 cancer therapy caused by BCR-ABL gene mutation or amplification.Gorre ME, Mohammed M, Ellwood K, Hsu N, Paquette R, Rao PN, Sawyers CLScience. 293, 876-80 (2001).
26. Molecular correlates of imatinib resistance in gastrointestinal stromal tumors.Heinrich MC, Corless CL, Blanke CD, Demetri GD, Joensuu H, Roberts PJ, Eisenberg BL, von Mehren M, Fletcher CD, Sandau K, McDougall K, Ou WB, Chen CJ, Fletcher JA.J Clin Oncol. 24, 4764-74 (2006).
27. Mechanisms of chromosome instability in cancers.Jefford CE, Irminger-Finger I.Crit Rev Oncol Hematol. 59, 1-14 (2006).
28. Genomic instability--an evolving hallmark of cancer.Negrini S, Gorgoulis VG, Halazonetis TD.Nat Rev Mol Cell Biol. 11, 220-8 (2010).
29. Passenger mutations as a marker of clonal cell lineages in emerging neoplasia.Salk JJ, Horwitz MS.Semin Cancer Biol. 20, 294-303 (2010).
30. The DNA-damage response in human biology and disease.Jackson SP, Bartek J.Nature. 461, 1071-8 (2009).
31. DNA damage responses: mechanisms and roles in human disease.Kastan MB.Mol Cancer Res. 6, 517-24 (2008).
32. Oncogenic mutations of the p53 tumor suppressor: the demons of the guardian of the genome.Sigal A, Rotter V.Cancer Res. 60, 6788-93 (2000).
33. Cancer. p53, guardian of the genome. Lane DP. Nature. 358, 15-6 (2000).
34. Negative control elements of the cell cycle in human tumors.Adams PD, Kaelin WG Jr.Curr Opin Cell Biol. 10, 791-7 (1998).
35. Aberrant epigenetic landscape in cancer: how cellular identity goes awry.Berdasco M, Esteller M.Dev Cell. 19, 698-711 (2010).
36. Cancer epigenomics: DNA methylomes and histone-modification maps.Esteller M.Nat Rev Genet. 8, 286-98 (2007).
37. The epigenomics of cancer.Jones PA, Baylin SB.Cell. 128, 683-92 (2007).
38. DNA methylation in eukaryotes.Adams RL, Burdon RH.CRC Crit Rev Biochem.13, 349-84 (1982).
39. What is hemimethylated DNA? Adams RL, Lindsay H.FEBS Lett. 1993 Apr 12;320(3):243-5.

40. Number of CpG islands and genes in human and mouse.Antequera F, Bird A.Proc Natl Acad Sci U S A. 1993 Dec 15;90(24):11995-9.
41. Book: DNA methylation: molecular biology and biological significance. 1993 pp. 572 pp. Birkhauser Verlag, Basel (Switzerland). p. 169-85
42. CpG islands in vertebrate genomes.Gardiner-Garden M, Frommer M.J Mol Biol. 1987 Jul 20;196(2):261-82.
43. Evidence that pp42, a major tyrosine kinase target protein, is a mitogen-activated serine/threonine protein kinase.Rossomando AJ, Payne DM, Weber MJ, Sturgill TW.Proc Natl Acad Sci U S A. 1989 Sep;86(18):6940-3.
44. Organization and regulation of mitogen-activated protein kinase signaling pathways.Garrington TP, Johnson GL.Curr Opin Cell Biol. 1999 Apr;11(2):211-8. Review.
45. Cell condition-dependent regulation of ERK5 by cAMP.Pearson GW, Cobb MH.J Biol Chem. 2002 Dec 13;277(50):48094-8. Epub 2002 Sep 23.
46. Mitogen-activated protein kinase: conservation of a three-kinase module from yeast to human.Widmann C, Gibson S, Jarpe MB, Johnson GL.Physiol Rev. 1999 Jan;79(1):143-80. Review.
47. Mitogen-activated protein kinases: specific messages from ubiquitous messengers.Schaeffer HJ, Weber MJ.Mol Cell Biol. 1999 Apr;19(4):2435-44. Review
48. Frost JA, Steen H, Shapiro PS, Lewis R, Ahn J, Shaw PE, Cobb MH 1997 Cross-cascade activation of ERKs and ternary complex factors by Rho family proteins. EMBO J 16:6426–6438
49. Corbit KC, Foster DA, RosnerMR1999 Protein kinaseCd mediates neurogenic but not mitogenic activation of mitogen-activated proteinkinase in neuronal cells. Mol Cell Biol 19:4209–4218
50. Schonwasser DC, Marais RM, Marshall CJ, Parker PJ 1998 Activationof the mitogen-activated protein kinase/extracellular signalregulated kinase pathway by conventional, novel, and atypical protein kinase C isotypes. Mol Cell Biol 18:790–798

51. Robbins DJ, CobbMH1992 ERK2 autophosphorylates on a subset of peptides phosphorylated in intact cells in response to insulin and nerve growth factor: analysis by peptide mapping. Mol Biol Cell 3:299–308
52. Ferrell JE, Bhatt RR 1997 Mechanistic studies of the dual phosphorylation of mitogen-activated protein kinase. J Biol Chem 272: 19008–19016
53. Ferrell JE 1997 How responses get more switch like as you move down a protein kinase cascade. Trends Biochem Sci 22:288–289
54. Ferrell Jr JE 1999 Building a cellular switch: more lessons from a good egg. Bioessays 21:866–870
55. Mitogen-activated protein kinases: specific messages from ubiquitous messengers.Schaeffer HJ, Weber MJ.Mol Cell Biol. 1999 Apr;19(4):2435-44. Review
56. Regulation of stress-responsive mitogen-activated protein (MAP) kinase pathways by TAO2.Chen Z, Cobb MH.J Biol Chem. 2001 May 11;276(19):16070-5. Epub 2001 Mar 8.
57. Mammalian mitogen-activated protein kinase signal transduction pathways activated by stress and inflammation.Kyriakis JM, Avruch J.Physiol Rev. 2001 Apr;81(2):807-69. Review.
58. Functions of the MAPK family in vertebrate-development.Krens SF, Spaink HP, Snaar-Jagalska BE.FEBS Lett. 2006 Sep 18;580(21):4984-90. Epub 2006 Aug 28. Review.
59. Breving K, Esquela-Kerscher A: The complexities of microRNA regulation: Mirandering around the rules. Int J Biochem Cell Biol 2009, 42:1316-1329.
60. Griffiths-Jones S, Grocock RJ, van Dongen S, Bateman A, Enright AJ:miRBase: microRNA sequences, targets and gene nomenclature. NucleicAcids Res 2006, 34:D140-144.
61. Bentwich I, Avniel A, Karov Y, Aharonov R, Gilad S, Barad O, Barzilai A,Einat P, Einav U, Meiri E, Sharon E, Spector Y, Bentwich Z: Identification of hundreds of conserved and nonconserved human microRNAs. Nat Genet 2005, 37:766-770.
62. Stefani G, Slack FJ: Small non-coding RNAs in animal development. NatRev Mol Cell Biol 2008, 9:219-230.

63. Calin GA Croce CM: MicroRNA signatures in human cancers. Nat RevCancer 2006, 6:857-866.
64. Calin GA, Ferracin M, Cimmino A, Di Leva G, Shimizu M, Wojcik SE, Iorio MV, Visone R, Sever NI, Fabbri M, Iuliano R, Palumbo T, Pichiorri F, Roldo C, Garzon R, Sevignani C, Rassenti L, Alder H, Volinia S, Liu CG, Kipps TJ, Negrini M, Croce CM: A MicroRNA signature associated with prognosis and progression in chronic lymphocytic leukemia. N Engl J Med 2005, 353:1793-1801.
65. Wiemer EA: The role of microRNAs in cancer: no small matter. Eur J Cancer 2007, 43:1529-1544.
66. Zhang B, Pan X, Cobb GP, Anderson TA: microRNAs as oncogenes and tumor suppressors. Dev Biol 2007, 302:1-12.
67. Merritt WM, Lin YG, Han LY, Kamat AA, Spannuth WA, Schmandt R, Urbauer D, Pennacchio LA, Cheng JF, Nick AM, Deavers MT, Mourad- Zeidan A, Wang H, Mueller P, Lenburg ME, Gray JW, Mok S, Birrer MJ, Lopez-Berestein G, Coleman RL, Bar-Eli M, Sood AK: Dicer, Drosha, and outcomes in patients with ovarian cancer. N Engl J Med 2008, 359:2641-2650.
68. Volinia S, Calin GA, Liu CG, Ambs S, Cimmino A, Petrocca F, Visone R, Iorio M, Roldo C, Ferracin M, Prueitt RL, Yanaihara N, Lanza G, Scarpa A, Vecchione A, Negrini M, Harris CC, Croce CM: A microRNA expression signature of human solid tumors defines cancer gene targets. Proc Natl Acad Sci USA 2006, 103:2257-2261.
69. Paik S, Shak S, Tang G, Kim C, Baker J, Cronin M, Baehner FL, Walker MG, Watson D, Park T, Hiller W, Fisher ER, Wickerham DL, Bryant J, Wolmark N: A multigene assay to predict recurrence of tamoxifen-treated, nodenegative breast cancer. N Engl J Med 2004, 351:2817-2826.
70. Mattie MD, Benz CC, Bowers J, Sensinger K, Wong L, Scott GK, Fedele V, Ginzinger D, Getts R, Haqq C: Optimized high-throughput microRNA expression profiling provides novel biomarker assessment of clinical prostate and breast cancer biopsies. Mol Cancer 2006, 5:24.
71. Lu J, Getz G, Miska EA, Alvarez-Saavedra E, Lamb J, Peck D, Sweet-Cordero A, Ebert BL, Mak RH, Ferrando AA, Downing JR, Jacks T, Horvitz HR, Golub TR:

MicroRNA expression profiles classify human cancers. Nature 2005, 435:834-838.

72. Michael MZ, O'Connor SM, van Holst Pellekaan NG, Young GP, James RJ: Reduced accumulation of specific microRNAs in colorectal neoplasia. Mol Cancer Res 2003, 1:882-891.
73. Takamizawa J, Konishi H, Yanagisawa K, Tomida S, Osada H, Endoh H, Harano T, Yatabe Y, Nagino M, Nimura Y, Mitsudomi T, Takahashi T: Reduced expression of the let-7 microRNAs in human lung cancers in association with shortened postoperative survival. Cancer Res 2004,64:3753-3756.
74. Hayashita Y, Osada H, Tatematsu Y, Yamada H, Yanagisawa K, Tomida S, Yatabe Y, Kawahara K, Sekido Y, Takahashi T: A polycistronic microRNA cluster, miR-17-92, is overexpressed in human lung cancers and enhances cell proliferation. Cancer Res 2005, 65:9628-9632.
75. Chen JQ, Russo J: ERalpha-negative and triple negative breast cancer: molecular features and potential therapeutic approaches. Biochim Biophys Acta 2009, 1796:162-175.
76. Du L, Schageman JJ, Irnov , Girard L, Hammond SM, Minna JD, Gazdar AF, Pertsemlidis A: MicroRNA expression distinguishes SCLC from NSCLC lung tumor cells and suggests a possible pathological relationship between SCLCs and NSCLCs. J Exp Clin Cancer Res 2010, 29:75.
77. Raponi M, Dossey L, Jatkoe T, Wu X, Chen G, Fan H, Beer DG: MicroRNA classifiers for predicting prognosis of squamous cell lung cancer. Cancer Res 2009, 69:5776-5783.
78. Yanaihara N, Caplen N, Bowman E, Seike M, Kumamoto K, Yi M, Stephens RM, Okamoto A, Yokota J, Tanaka T, Calin GA, Liu CG, Croce CM, Harris CC: Unique microRNA molecular profiles in lung cancer diagnosis and prognosis. Cancer Cell 2006, 9:189-198.
79. Yu SL, Chen HY, Chang GC, Chen CY, Chen HW, Singh S, Cheng CL, Yu CJ, Lee YC, Chen HS, Su TJ, Chiang CC, Li HN, Hong QS, Su HY, Chen CC, Chen WJ, Liu CC, Chan WK, Chen WJ, Li KC, Chen JJ, Yang PC: MicroRNA signature predicts survival and relapse in lung cancer. Cancer Cell 2008,13:48-57.

80. Budhu A, Jia HL, Forgues M, Liu CG, Goldstein D, Lam A, Zanetti KA, Ye QH, Qin LX, Croce CM, Tang ZY, Wang XW: Identification of metastasis-related microRNAs in hepatocellular carcinoma. Hepatology 2008, 47:897-907.
81. Guo Y, Chen Z, Zhang L, Zhou F, Shi S, Feng X, Li B, Meng X, Ma X, Luo M, Shao K, Li N, Qiu B, Mitchelson K, Cheng J, He J: Distinctive microRNA profiles relating to patient survival in esophageal squamous cell carcinoma. Cancer Res 2008, 68:26-33.
82. Li X, Zhang Y, Ding J, Wu K, Fan D: Survival prediction of gastric cancer by a seven-microRNA signature. Gut 2010, 59:579-585.
83. Tong AW, Fulgham P, Jay C, Chen P, Khalil I, Liu S, Senzer N, Eklund AC, Han J, Nemunaitis J: MicroRNA profile analysis of human prostate cancers. Cancer Gene Ther 2009, 16:206-216.
84. Hu X, Schwarz JK, Lewis JS Jr, Huettner PC, Rader JS, Deasy JO, Grigsby PW, Wang X: A microRNA expression signature for cervical cancer prognosis. Cancer Res 2010, 70:1441-1448.
85. Schetter AJ, Leung SY, Sohn JJ, Zanetti KA, Bowman ED, Yanaihara N, Yuen ST, Chan TL, Kwong DL, Au K, Liu CG, Calin GA, Croce CM, Harris CC: MicroRNA expression profiles associated with prognosis and therapeutic outcome in colon adenocarcinoma. JAMA 2008, 299:425-436.
86. Boulton TG, Yancopoulos GD, Gregory JS, Slaughter C,Moomaw C, Hsu J, Cobb MH 1990 An insulin-stimulated proteinkinase similar to yeast kinases involved in cell cycle control. Science 249:64–67
87. Boulton TG, Nye SH, Robbins DJ, Ip NY, Radziejewska E, Morgenbesser SD, DePinho RA, Panayotatos N, Cobb MH, Yancopoulos GD 1991 ERKs: a family of protein-serine/threonine kinases that are activated and tyrosine phosphorylated in response to insulin and NGF. Cell 65:663–675
88. Lewis TS, Shapiro PS, Ahn NG 1998 Signal transduction through MAP kinase cascades. Adv Cancer Res 74:49–139
89. Crews C, Alessandrini A, Erikson R 1992 The primary structure of MEK, a protein kinase that phosphorylates the ERK gene product. Science 258:478–480

90. Kosako H, Gotoh Y, Matsuda S, Ishikawa M, Nishida E 1992 Xenopus MAP kinase activator is a serine/threonine/tyrosine kinase activated by threonine phosphorylation.EMBOJ 11:2903–2908
91. Wu J, Harrison JK, Vincent LA, Haystead C, Haystead TAJ, Michel H, Hunt DF, Lynch KR, Sturgill TW 1993 Molecular structure of a protein-tyrosine/threonine kinase activating p42 mitogenactivated protein (MAP) kinase: MAP kinase kinase. Proc Natl Acad Sci USA 90:173–177
92. Ahn NG, Seger R, Bratlien RL, Diltz CD, Tonks NK, Krebs EG 1991 Multiple components in an epidermal growth factor-stimulated protein kinase cascade. In vitro activation of a myelin basic protein/microtubule-associated protein 2 kinase. J Biol Chem 266: 4220–4227
93. Seger R, Ahn NG, Posada J, Munar ES, Jensen AM, Cooper JA, Cobb MH, Krebs EG 1992 Purification and characterization of mitogen-activated protein kinase activator(s) from epidermal growth factor-stimulated A431 cells. J Biol Chem 267:14373–14381
94. Zheng C-F, Guan K 1993 Dephosphorylation and inactivation of the mitogen-activated protein kinase by a mitogen-induced Thr/ Tyr protein phosphatase. J Biol Chem 268:16116–16119
95. Nakielny S, Cohen P, Wu J, Sturgill T 1992 MAP kinase activator from insulin-stimulated skeletal muscle is a protein threonine/tyrosine kinase. EMBO J 11:2123–2130
96. Zheng C-F, Guan K 1993 Cloning and characterization of two distinct human extracellular signal-regulated kinase activator kinases, MEK1 and MEK2. J Biol Chem 268:11435–11439
97. Robinson MJ, Cheng M, Khokhlatchev A, Ebert D, Ahn N, Guan K, Stein B, Goldsmith E, CobbMH1996 Contribution of the MAP kinase backbone and phosphorylation lip to MEK specificity. J Biol Chem 271:29734–29739
98. Lawler S, Fleming Y, Goedert M, Cohen P 1998 Synergistic activation of SAPK1/JNK1 by two MAP kinase kinases in vitro. Curr Biol 8:1387–1390

99. Lisnock J, Griffin P, Calaycay J, Frantz B, Parsons J, O'Keefe SJ, LoGrasso P 2000 Activation of JNK3a1 requires both MKK4 and MKK7: kinetic characterization of in vitro phosphorylated JNK3a1. Biochemistry 39:3141–3148

100. Rhodes N, Connell L, Errede B 1990 STE11 is a protein kinase required for cell-type-specific transcription and signal transduction in yeast. Genes Dev. 4:1862–1874

101. Lange-Carter CA, Pleiman CM, Gardner AM, Blumer KJ, Johnson GL 1993 A divergence in the MAP kinase regulatory network defined by MEK kinase and Raf. Science 260:315–319

102. Xu S, Robbins DJ, Christerson LB, English JM, Vanderbilt CA, Cobb MH 1996 Cloning of rat MEKK1 cDNA reveals an endogenous membrane-associated 195 kDa protein with a large regulatory domain. Proc Natl Acad Sci USA 93:5291–5295

103. Blank JL, Gerwins P, Elliott EM, Sather S, Johnson GL 1996 Molecular cloning of mitogen-activated protein/ERK kinase kinases (MEKK) 2 and 3. Regulation of sequential phosphorylation pathways involving mitogen-activated protein kinase and c-Jun kinase. J Biol Chem 271:5361–5368

104. Gerwins P, Blank JL, JohnsonGL1997 Cloning of a novel mitogenactivated protein kinase kinase kinase, MEKK4, that selectively regulates the c-Jun amino terminal kinase pathway. J Biol Chem 272:8288–8295

105. Chou MM, Hanafusa H 1995 A novel ligand for SH3 domains. The Nck adaptor protein binds to a serine/threonine kinase via an SH3 domain. J Biol Chem 270:7359–7364

106. Graves JD, Gotoh Y, Draves KE, Ambrose D, Han DK, Wright M, Chernoff J, Clark EA, Krebs EG 1998 Caspase-mediated activation and induction of apoptosis by the mammalian Ste20-like kinase Mst1. EMBO J 17:2224–2234

107. Hirai S, Katoh M, Terada M, Kyriakis JM, Zon LI, Rana A, Avruch J, Ohno S 1997 MST/MLK2, a member of the mixed lineage kinase family, directly phosphorylates and activates SEK1, an activator of c-Jun N-terminal kinase/stress-activated protein kinase. J Biol Chem 272:15167–15173

108. Rana A, Gallo K, Godowski P, Hirai S, Ohno S, Zon LI, Kyriakis JM, Avruch J 1996 The mixed lineage kinase SPRK phosphorylates and activates the stress-activated protein kinase activator, SEK-1. J Biol Chem 271:19025–19028

109. Tibbles LA, Ing YL, Kiefer F, Chan J, Iscove N, Woodgett JR, Lassam NJ 1996 MLK-3 activates the SAPK/JNK and p38/RK pathways via SEK1 and MKK3/6. EMBO J 15:7026–7035

110. Yamaguchi K, Shirakabe K, Shibuya H, Irie K, Oishi I, Ueno N, Taniguchi T, Nishida E, Matsumoto K 1995 Identification of a member of the MAPKKK family as a potential mediator of TGF-b signal transduction. Science 270:2008–2011

111. Salmeron A, Ahmad TB, Carlile GW, Pappin D, Narsimhan RP, Ley SC 1996 Activation of MEK-1 and SEK-1 by Tpl-2 protooncoprotein, a novel MAP kinase kinase kinase. EMBO J 15:817– 826

112. Ichijo H, Nishida E, Irie K, ten Dijke P, Saitoh M, Moriguchi T, Takagi M, Matsumoto K, Miyazono K, Gotoh Y 1997 Induction of apoptosis by ASK1, a mammalian MAPKKK that activates SAPK/ JNK and p38 signaling pathways. Science 275:90–94

113. Wang XS, Diener K, Jannuzzi D, Trollinger D, Tan TH, Lichenstein H, Zukowski M, Yao Z 1996 Molecular cloning and characterization of a novel protein kinase with a catalytic domain homologous to mitogen-activated protein kinase kinase kinase. J Biol Chem 271:31607–31611

114. Wang XS, Diener K, Tan TH, Yao Z 1998 MAPKKK6, a novel mitogen-activated protein kinase kinase kinase, that associates with MAPKKK5. Biochem Biophys Res Commun 253:33–37

115. Hutchison M, Berman K, Cobb MH 1998 Isolation of TAO1, a protein kinase that activates MEKs in stress-activated protein kinase cascades. J Biol Chem 273:28625–28632

116. Chen Z, Hutchison M, Cobb MH 1999 Isolation of the protein kinase TAO2 and identification of its mitogen-activated protein kinase/extracellular signal-regulated kinase kinase binding domain. J Biol Chem 274:28803–28807

117. Marinissen MJ, Chiariello M, Pallante M, Gutkind JS 1999 A network of mitogen-activated protein kinases links G proteincoupled receptors to the c-jun pro-

moter: a role for c-Jun NH2- terminal kinase, p38 s, and extracellular signal-regulated kinase 5. Mol Cell Biol 19:4289–4301

118. Chiariello M, Marinissen MJ, Gutkind JS 2000 Multiple mitogenactivated protein kinase signaling pathways connect the cot oncoprotein to the c-jun promoter and to cellular transformation. Mol Cell Biol 20:1747–1758

119. J. Cho and P. N. Tsichlis,“Phosphorylation at Thr-290 regulates Tpl2 binding to NF-kappaB1/p105 and Tpl2 activation and degradation by lipopolysaccharide, Proceedings of the National Academy of Sciences of the United States of America, vol. 102, no. 7, pp 2350-2355, 2005.].

120. Gandara ML, Lopez P, Hernando R, Castano JG, Alemany S. The COOH-terminal domain of wild-type Cot regulates its stability and kinase specific activity. Mol Cell Biol 2003; 23:7377-7390

121. Black TM, Andrews CL, Kilili G, Ivan M, Tsichlis PN, Vouros P. Characterization of phosphorylation sites on Tpl2 using IMAC enrichment and a linear ion trap mass spectrometer. J Proteome Res 2007; 6:2269-2276.

122. Cohen S, Lahav-Baratz S, Ciechanover A. Two distinct ubiquitin- dependent mechanisms are involved in NF-κB p105 proteolysis. Biochem Biophys Res Commun 2006; 345:7-13.

123. Beinke S, Deka J, Lang V, et al. NF-κB p105 negatively regulates TPL-2 MEK kinase activity. Mol Cell Biol 2003; 23:4739-4752.

124. Jia Y, Quinn CM, Bump NJ, et al. Purification and kinetic characterization of recombinant human mitogen-activated protein kinase kinase kinase COT and the complexes with its cellular partner NF-κB1 p105. Arch Biochem Biophys 2005; 441:64-74.

125. Heyninck K, Kreike MM, Beyaert R. Structure-function analysis of the A20-binding inhibitor of NF-κB activation, ABIN-1. FEBS Lett 2003; 536:135-140.

126. J. Cho, M. Melnick, G. P. Solidakis and P. N. Tsichlis,“Tpl2 (tumor progression locus 2) phosphorylation at Thr290 is induced by lipopolysaccharide via an Ikappa-B Kinase-beta-dependent pathway and is required for Tpl2 activation by external signals, The Journal of biological chemistry, vol. 280, no. 21, pp 20442-20448, 2005.

127. M. R. Waterfield, M. Zhang, L. P. Norman and S. C. Sun,“NF-kappaB1/p105 regulates lipopolysaccharide-stimulated MAP kinase signaling by governing the stability and function of the Tpl2 kinase, Molecular Cell, vol. 11, no. 3, pp 685-694, 2003.,

128. Handoyo H, Stafford MJ, McManus E, Baltzis D, Peggie M, Cohen P. IRAK1-independent pathways required for the interleukin 1-stimulated activation of the TPL-2 catalytic subunit and its dissociation from ABIN-2. Biochem J 2009; 424:109-118

129. M. J. Robinson, S. Beinke, A. Kouroumalis, P. N. Tsichlis and S. C. Ley,“Phosphorylation of TPL-2 on serine 400 is essential for lipopolysaccharide activation of extracellular signal-regulated kinase in macrophages, Molecular and cellular biology, vol. 27, no. 21, pp 7355-7364, 2007

130. Symons A, Beinke S, Ley SC. MAP kinase kinase kinases and innate immunity. Trends Immunol 2006; 27:40-48.

131. Luciano BS, Hsu S, Channavajhala PL, Lin LL, Cuozzo JW. Phoshorylation of threonine 290 in the activation loop of Tpl2/Cot is necessary but not sufficient for kinase activity. J Biol Chem 2004; 279:52117-52123.

132. Makris A, Patriotis C, Bear SE, Tsichlis PN. Genomic organization and expression of Tpl-2 in normal cells and moloney murine leukemia virus-induced rat T-cell lymphomas: activation by provirus insertion. J Virol 1993; 67:4283-4289.

133. Patriotis C, Makris A, Chernoff J, Tsichlis PN. Tpl-2 acts in concert with Ras and Raf-1 to activate mitogen-activated protein kinase. Proc Natl Acad Sci USA 1994; 91:9755-9759.

134. Tsatsanis C, Patriotis C, Bear SE, Tsichlis PN. The TPL-2 proto-oncoprotein activates the nuclear factor of activated T cells and induces interleukin 2 expression in T cell lines. Proc Natl Acad Sci USA 1998; 95:3827-3832

135. Belich MP, Salmeron A, Johnston LH, Ley SC. TPL-2 kinase regulates the proteolysis of the NF-κB inhibitory protein NF-κB1 p105. Nature 1999; 397:363-368.

136. Dumitru CD, Ceci JD, Tsatsanis C, et al. TNFα induction by LPS is regulated post-transcriptionally via a TPL2/ERKdependent pathway. Cell 2000; 103:1071-1083

137. Das S, Cho J, Lambertz I, et al. Tpl2/Cot signals activate ERK, JNK and NF-κB in a cell-type and stimulus-specific manner. J Biol Chem 2005; 280:23748-23757.

138. Beinke S, Ley SC. Functions of NF-κB1 and NF-κB2 in immune cell biology. Biochem J 2004; 382:393-409.

139. Eliopoulos AG, Wang CC, Dumitru CD, Tsichlis PN. TPL-2 transduces CD40 and TNF signals that activate ERK and regulates IgE induction by CD40. EMBO J 2003; 22:3855- 3864.

140. Kaiser F, Cook D, Papoutsopoulou S, et al. TPL-2 negatively regulates interferon-beta production in macrophages and myeloiddendritic cells. J Exp Med 2009; 206:1863-1871.

141. Mielke LA, Elkins KL, Wei L, et al. Tumor progression locus2 (Map3k8) is critical for host defense against Listeria monocytogenes and IL-1 production. J Immunol 2009; 183:7984- 7993.

142. Gringhuis SI, den Dunnen J, Litjens M, et al. Dectin-1 directs T helper cell differentiation by controlling noncanonical NF-κB activation through Raf-1 and Syk. Nat Immunol 2009; 10:203-213.

143. Lin X, Cunningham ET, Mu Y, Geleziunas R, Greene WC. The proto-oncogene Cot kinase participates in CD3/CD28 induction of NF-κB acting through the NF-κB-inducing kinase and IκB kinases. Immunity 1999; 10:271-280.

144. Tsatsanis C, Patriotis C, Tsichlis PN. Tpl-2 induces IL-2 expression in T-cell lines by triggering multiple signaling pathways that activate NFAT and NF-κB. Oncogene 1998; 17:2609-2618.

145. Babu G, Waterfield M, Chang M, Wu X, Sun SC. Deregulated activation of oncoprotein kinase Tpl2/Cot in HTLV-1- transformed T cells. J Biol Chem 2006; 281:14041-14047.

146. Sanchez-Valdepenas C, Punzon C, San-Antonio B, Martin AG, Fresno M. Differential regulation of p65 and c-Rel NF- κB transactivating activity by Cot, protein kinase C ζ and NIK protein kinases in CD3/CD28 activated T cells. Cell Signal 2007; 19:528-537.

147. Karin M, Ben-Neriah Y. Phosphorylation meets ubiquitination: the control of NF-κB activity. Annu Rev Immunol 2000; 18:621-663

148. DeCicco-Skinner KL, Trovato EL, Simmons JK, Lepage PK, Wiest JS. Loss of tumor progression locus 2 (tpl2) enhances tumorgenesis and inflammation in two-stage skin carcinogenesis. Oncogene 11 October 2010; doi: 10.1038/onc.2010.447.

149. George, D. & Salmeron, A. Cot/Tpl-2 protein kinase as a target for the treatment of inflammatory disease. Curr Top Med Chem 9, 611-22 (2009

150. Shivdasani R. A. MicroRNAs: regulators of gene expression and cell differentiation Blood. 2006 December 1; 108(12): 3646–3653

151. Lee Y, Kim M, Han J, et al. MicroRNA genes are transcribed by RNA polymerase II. EMBO J. 2004;23:4051-4060

152. Lee Y, Ahn C, Han J, et al. The nuclear RNase III Drosha initiates microRNA processing. Nature. 2003;425:415-419

153. Zeng Y, Cullen BR. Sequence requirements for micro RNA processing and function in human cells. RNA. 2003 Jan;9(1):112-23.

154. Yi R, Qin Y, Macara IG, Cullen BR. Exportin-5 mediates the nuclear export of pre-microRNAs and short hairpin RNAs. Genes Dev. 2003;17: 3011-3016.

155. Bohnsack MT et.al. Exportin 5 is a RanGTP-dependent dsRNA-binding protein that mediates nuclear export of pre-miRNAs. RNA. 2004 Feb;10(2):185-91.

156. Lund E, Guttinger S, Calado A, Dahlberg JE, Kutay U. Nuclear export of microRNA precursors. Science. 2004;303:95-98.

157. Grishok A, Pasquinelli AE, Conte D, et al. Genes and mechanisms related to RNA interference regulate expression of the small temporal RNAs that control C. elegans developmental timing. Cell. 2001;106:23-34.

158. Hutvagner G, McLachlan J, Pasquinelli AE, Balint E, Tuschl T, Zamore PD. A cellular function for the RNA-interference enzyme Dicer in the maturation of the let-7 small temporal RNA. Science. 2001; 293:834-838.

159. Hammond SM, Boettcher S, Caudy AA, Kobayashi R, Hannon GJ. Argonaute2, a link between genetic and biochemical analyses of RNAi. Science. 2001 Aug 10;293(5532):1146-50.

160. Martinez J, Patkaniowska A, Urlaub H, Lührmann R, Tuschl T. Single-stranded antisense siRNAs guide target RNA cleavage in RNAi. Cell. 2002 Sep 6;110(5):563-74.

161. Schwarz DS, Zamore PD. Why do miRNAs live in the miRNP? Genes Dev. 2002 May 1;16(9):1025-31.

162. Yoon S, Seger R. The extracellular signal-regulated kinase: multiple substrates regulate diverse cellular functions. Growth Factors. 2006 Mar;24(1):21-44.

163. Dunn KL, Espino PS, Drobic B, He S, Davie JR. The Ras-MAPK signal transduction pathway, cancer and chromatin remodeling. Biochem Cell Biol. 2005 Feb;83(1):1-14.

164. Weston CR, Davis RJ. The JNK signal transduction pathway. Curr Opin Genet Dev. 2002 Feb;12(1):14-21.

165. Adler V, Polotskaya A, Wagner F, Kraft AS. Affinity-purified c-Jun amino-terminal protein kinase requires serine/threonine phosphorylation for activity. J Biol Chem. 1992 Aug 25;267(24):17001-5.

166. Wu GS. The functional interactions between the p53 and MAPK signaling pathways Cancer Biol Ther. 2004 Feb;3(2):156-61.

167. Buschmann T, Adler V, Matusevich E, Fuchs SY, Ronai Z. p53 phosphorylation and association with murine double minute 2, c-Jun NH2-terminal kinase, p14ARF, and p300/CBP during the cell cycle and after exposure to ultraviolet ir-radiation. Cancer Res. 2000 Feb 15;60(4):896-900.

168. Buschmann T, Potapova O, Bar-Shira A et.al. Jun NH2-terminal kinase phos-phorylation of p53 on Thr-81 is important for p53 stabilization and transcrip-tional activities in response to stress. Mol Cell Biol. 2001 Apr;21(8):2743-54.

169. She QB, Ma WY, Dong Z. Role of MAP kinases in UVB-induced phosphorylation of p53 at serine 20. Oncogene. 2002 Feb 28;21(10):1580-9.

170. Cheng HL, Mostoslavsky R, Saito S, et.al. Developmental defects and p53 hyperacetylation in Sir2 homolog (SIRT1)-deficient mice. Proc Natl Acad Sci U S A. 2003 Sep 16;100(19):10794-9.

171. Fuchs SY, Adler V, Buschmann T, et.al. JNK targets p53 ubiquitination and deg-radation in nonstressed cells. Genes Dev. 1998 Sep 1;12(17):2658-63.

172. Kumar S, Boehm J, Lee JC. p38 MAP kinases: key signalling molecules as therapeutic targets for inflammatory diseases. Nat Rev Drug Discov. 2003 Sep;2(9):717-26.
173. Zarubin T, Han J. Activation and signaling of the p38 MAP kinase pathway. Cell Res. 2005 Jan;15(1):11-8.
174. Kyriakis JM, Avruch J. Mammalian mitogen-activated protein kinase signal transduction pathways activated by stress and inflammation. Physiol Rev. 2001 Apr;81(2):807-69.
175. Giancotti FG, Ruoslahti E. Integrin signaling. Science. 1999 Aug 13;285(5430):1028-32.
176. Ovcharenko D, Kelnar K, Johnson et.al., Genome-scale microRNA and small interfering RNA screens identify small RNA modulators of TRAIL-induced apoptosis pathway. Cancer Res. 2007 Nov 15;67(22):10782-8.